DISS. ETH NO. 27577

SIMULATIONS OF ELECTRIC VEHICLE USAGE BASED ON A COMPREHENSIVE CHARACTERISATION OF PASSENGER CAR MOBILITY

A thesis submitted to attain the degree of
DOCTOR OF SCIENCES of ETH ZURICH
(Dr. sc. ETH Zurich)

presented by

Giacomo Pareschi

MSc ETH EST, ETH Zurich
born on 12.11.1991
citizen of Italy

accepted on the recommendation of

Prof. Konstantinos Boulouchos, examiner
Prof. Tobias Schmidt, co-examiner
Dr. Gil Georges, co-examiner

2021

Giacomo Pareschi
giacomo.pareschi@alumni.ethz.ch

Dedicata a mio nonno Mario

A rationalist is simply someone for whom it is more important to learn than to be proved right
Karl R. Popper

Acknowledgements

First and foremost I would like to thank Prof. Boulouchos for giving me the opportunity to perform this Ph.D. and for providing constant guidance along this important journey of my life. Our regular discussions were a source of research inspiration where I learnt to combine a broader vision of the field with nonetheless meticulous scientific approaches. I am also extremely grateful for the encouragement given me in the demanding phases of the doctorate.

My sincere gratitude goes to Prof. Schmidt for the helpful exchanges in the closing stage of this doctorate and for providing valuable insights from a more policy-oriented perspective.

Many thanks go to Gil Georges for the manifold discussions and exchanges both in and outside the office. His modelling expertise and comprehensive knowledge of the field have been extremely valuable for carrying out this work; but I am also grateful for the exciting and dynamic discussions which we had on practically any topic.

My deep gratitude goes to all my colleagues, especially the ones I had the luck to share the office with. They created an environment that went beyond professional teamwork and allowed for an authentic and enjoyable sharing of everyday life. A special mention goes to my (student)-colleagues-flatmates-friends Emir and Lukas for all the professional, manufacturing, leisure, enlightening as well as miserable moments shared together. Companions of trips and memorable (sometimes with the help of B12) nights, they have profoundly enriched my life in these years. Many thanks go also to my co-workers and friends Max and Moritz, who have been outstanding teammates both in research and in office "entertainment"; they have also been a fundamental source of encouragement and optimism in the final stages of this doctorate, despite the difficulties posed by the pandemic. I would also like to explicitly thank Olga and Michele for their valuable contributions to my research experience and personal growth.

I would then like to thank all my friends for their constant presence and support in all phases of the doctorate. I am grateful for all the enjoyment and colour that they bring in my life even when living far away.

Fundamentally important has also been the role of my family along the entire doctorate and all stages of my life. The unconditional support and encouragements that they have perseveringly provided have been crucial

for all my achievements.
Last but definitely not least, huge thanks go to my girlfriend Noemi for her invaluable support, unlimited patience and unconditional affection. With her closeness she has decisively contributed to every step of this journey. Grazie davvero.

Zürich, March 2021

Giacomo Pareschi

Abstract

Electric vehicles (EV) are a key ingredient in the process of decarbonising the transportation sector and mitigating the rate of climate change. After a halting start, their introduction has taken off in many developed countries mostly thanks to public support. Nevertheless, EVs entail a set of new challenges and potential hindrances that can hamper or severely slow down their diffusion. Examples range from the possibly critical impact on local electric grids to the discouragement caused by the limited driving range.

Confronting these aspects requires investigations in complementary specialised fields but a common fundamental prerequisite is a deep understanding of EVs mobility patterns. On one side, EVs interact with the energy sector at an unprecedented timescale for road transport, and assessing potential risks necessitates meticulous modelling of intra-day movements of passenger cars. On the other side, the range limitation of EVs calls for a comprehension of the varying range requirements of drivers along the year in order to quantify the actual amount of discomfort to be borne.

This thesis presents a comprehensive model to flexibly simulate EV mobility at any opportune timescale. The starting point are household travel surveys collected by national statistical offices due to their generally adequate resolution of intra-day mobility and their representative sample size. After a characterisation of the car patterns captured by these surveys, few solutions to some of the typical limitations of these datasets are presented. The modelling effort is then dedicated to the adaptation of these patterns to the simulation of EVs, with a special focus on the charging behaviour of EV drivers. Finally, a methodology to construct plausible annual profiles from the short-term data available in travel surveys is provided.

Both the simulation of intra-day EV mobility and the construction of annual profiles compare favourably with empirical reference data. Regarding the former, uncontrolled charging loads detected in four EV field tests are used as validation proxy due to their pivotal role as an interface between EVs and the energy sector. The validation particularly highlights that a

simple stochastic function, where the decision to charge depends on the EV state of charge, can capture the charging behaviour observed in different contexts. Annual driving profiles are instead assessed in terms of the resulting annual mileage distribution and its conformity with the empirically observed curves. The most accurate annual profiles are constructed by clustering the raw mobility information into 5–10 groups according to the self-reported car annual mileages and by then sampling from each group about 4–12 distinctive weeks of mobility (repeated to form one year).
Illustrative applications of the model are then provided with a special focus on the electrification potential of EVs considering different charging scenarios and the variety of usage profiles in the fleet. Increasing the range of BEVs to 350 km clearly supports the replacement of conventional cars. But further range increases achieve only mild results. Effective measures to unlock more potential include either installing charging stations at any location where the car may get parked or, more decisively, providing BEV drivers with alternatives for the few very long trips of the year. These alternatives could be fast *en-route* chargers, the rental of hybrid vehicles or the usage of public modes of transport.
Finally, given the recent surge in alternative mobility models, the benefits of integrating EVs with car-sharing schemes are also assessed. The analysis shows that the bigger the car-sharing community, the larger the reductions in the number of vehicles and total battery capacity. Urban environments are thus the most suitable thanks to their high population density. However, the largest benefits are unlocked if only the least driving people in the surrounding area give up their private cars and join the EV-sharing community. Additionally, the remarkable decrease in required battery capacity indicates that EVs benefit from car-sharing to a greater extent than conventional cars.

Sintesi

Le automobili elettriche sono una componente fondamentale del processo di decarbonizzazione del settore dei trasporti e di mitigazione del cambiamento climatico. Dopo un inizio incerto, la diffusione di questa tipologia di veicolo è decollata in molti paesi industrializzati soprattutto grazie a supporti a livello statale. Ciononostante le auto elettriche comportano una serie di nuove sfide e difficoltà che possono ostacolare o severamente rallentare la loro diffusione. Tali difficoltà spaziano dal potenziale impatto critico sulle reti locali di distribuzione elettrica allo scoraggiamento dovuto alla limitata autonomia dei veicoli elettrici.

Affrontare queste tematiche richiede indagini in campi specialistici complementari, anche se un prerequisito comune fondamentale è una profonda comprensione delle modalità di utilizzo delle auto elettriche. Da un lato i veicoli elettrici interagiscono col settore energetico con una istantaneità inedita per il trasporto su gomma: valutarne potenziali rischi richiede una meticolosa modellazione dei singoli movimenti giornalieri delle automobili. Dall'altro, la ridotta autonomia delle auto elettriche richiede una comprensione del variabile fabbisogno degli automobilisti durante l'anno così da stimare l'effettivo disagio causato da tale limitazione.

Il presente elaborato propone un modello articolato atto a simulare la mobilità delle auto elettriche in qualunque richiesta scala temporale. Il punto di partenza è costituito dalle indagini sulla mobilità dei cittadini effettuate da uffici statistici nazionali, scelte in funzione della loro adeguata risoluzione dei movimenti giornalieri e delle significative dimensioni dei campioni di popolazione. Dopo una prima caratterizzazione della mobilità osservata in queste indagini, si è proceduto a proporre soluzioni a tipiche problematiche ad esse relative. Successivamente la ricerca si è diretta ad adattare e organizzare le informazioni emerse da queste indagini al fine di simulare la mobilità di veicoli elettrici, dando particolare attenzione alla frequenza con cui gli automobilisti effettuano le ricariche.

Sia la simulazione dei movimenti giornalieri che la costruzione di profi-

li annuali rispecchiano fedelmente le rilevazioni empiriche. I movimenti giornalieri sono validati da un confronto della domanda incontrollata di elettricità delle auto elettriche con le misurazioni ottenute da quattro test sul campo; la domanda di elettricità è stata scelta in quanto cruciale interfaccia tra le auto elettriche e il settore energetico. La validazione mostra in particolare che una semplice funzione stocastica, dove la decisione di ricaricare l'auto dipende dal livello di carica, permette di catturare le attitudini di ricarica osservate in contesti diversi. I profili di mobilità annuali sono stati invece validati sulla base della risultante distribuzione di chilometraggio e della conformità di quest'ultima con le distribuzioni osservate empiricamente. I profili annuali più accurati sono ottenuti dividendo i dati originali sulla mobilità in 5–10 gruppi secondo il chilometraggio annuo riportato dagli utenti e successivamente estraendo da ogni gruppo circa 4–12 settimane distinte di mobilità (da ripetere fino a formare un anno).
Vengono successivamente presentate alcune applicazioni del modello, rivolgendo particolare attenzione all'idoneità dei veicoli elettrici a soddisfare le necessità degli automobilisti e considerando vari scenari di infrastruttura di ricarica e gli eterogenei casi d'uso delle auto. Aumentare l'autonomia delle auto elettriche fino a 350 km porta a chiari vantaggi in termini di sostituzione delle auto tradizionali. Ulteriori incrementi dell'autonomia portano però solo a lievi benefici. Misure efficaci per raggiungere più fasce della popolazione includono l'installazione di colonnine di ricarica presso ogni possibile parcheggio o, ancora meglio, la disponibilità per gli autisti di alternative alle auto elettriche per i pochi viaggi lunghi dell'anno. Alcune alternative potrebbero essere l'accesso a ricariche rapide lungo il tragitto, il noleggio di auto ibride o l'utilizzo dei trasporti pubblici.
Infine, vista la recente diffusione di sistemi di mobilità alternativa, si considerano anche i possibili benefici nell'adottare auto elettriche in servizi di *car-sharing*. L'analisi dimostra che più grande è la comunità di *car-sharing*, maggiori possono essere le riduzioni del numero di veicoli e del fabbisogno di batterie. I contesti urbani sono quindi i più favorevoli grazie alla loro alta densità di popolazione. Tuttavia, i maggiori benefici si ottengono se solamente le persone che guidano di meno rinunciano all'auto privata per iscriversi al servizio di *car-sharing*. In aggiunta, la notevole riduzione nel fabbisogno di batterie indica che le auto elettriche beneficiano del *car-sharing* in maniera maggiore delle auto tradizionali.

Contents

Chapter 1

Introduction

1.1 Motivation

The battle against climate change is pressing, and countermeasures must be deployed at a higher rate than ever before. CO_2 emissions are the main contributor to the problem and only recently they seem to have stabilised [1]. Nevertheless, annual emissions in line with the 2018–2020 period would exhaust by 2028 the global carbon budget required not to exceed 1.5°C above pre-industrial levels with a 66% probability [2]. These estimates include the 7% drop in CO_2 emissions projected for 2020 due to the COVID-19 pandemic [3].

CO_2 emissions mostly stem from the combustion of fossil fuels in the energy sector. The detailed breakdown of Fig. 1.1 shows that all economic sectors contribute to these emissions and thus must put forward drastic mitigation strategies.

Passenger cars lead the transport sector with 11% of total CO_2 emissions and have long been a target of decarbonisation measures. These include technological advancements such as hybridisation and lightweighting or behavioural adjustments like mode shift and car sharing. But the most relied-upon solution are electric light-duty vehicles (EVs): this technology combines high maturity levels with the possibility to entirely abate local pollutants and CO_2 emissions [4, 5]. CO_2 may still be emitted at electricity generation sites, but the very high powertrain efficiency of EVs can compensate even mildly dirty electricity mixes. Fig. 1.2 shows that pure battery electric vehicles (BEV) entail the lowest well-to-wheel (WTW) CO_2 emissions for grid CO_2 intensities lower than 500 gCO_2/kWh [6][1]. How-

[1]For distances shorter than 50 km plug-in hybrid electric vehicles (PHEV) can run entirely on elec-

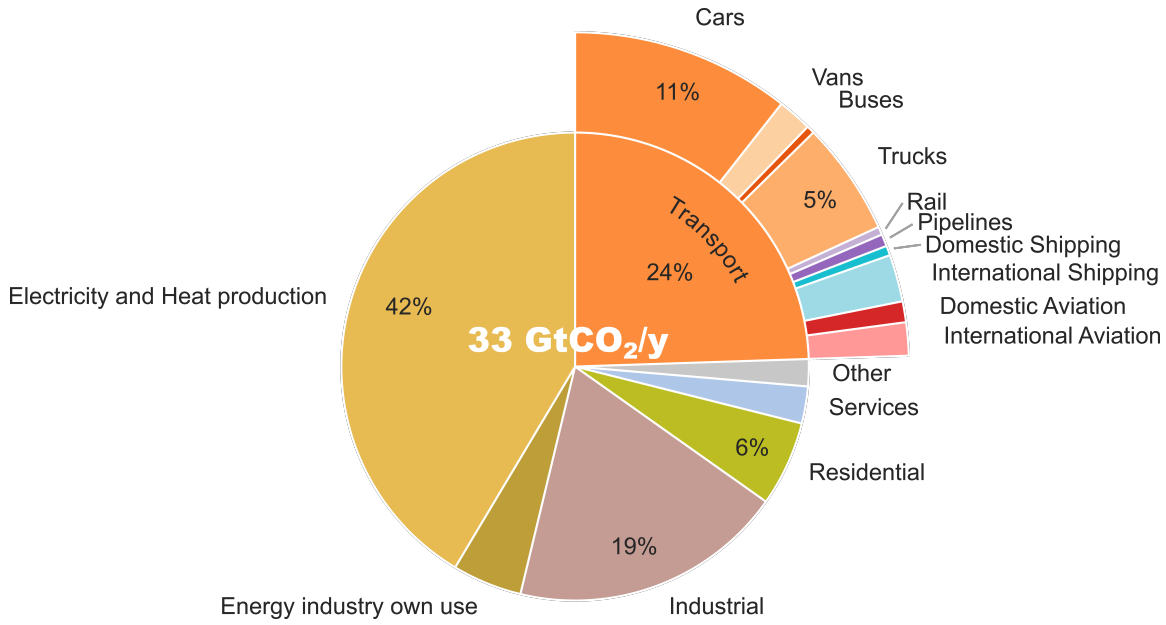

Figure 1.1: Distribution by sector of global CO_2 emissions from fossil fuel combustion in 2017.

ever, BEVs suffer also from range limitations and Fig. 1.2 shows that current battery technology does not allow to fit into cars batteries that cover distances larger than 370 km. The lateral histograms show that most European electricity is generated below the 500 gCO_2/kWh tipping point and that daily trips extremely rarely exceed the driving range of BEVs. From a techno-environmental point of view, BEVs and PHEVs seem to be the best option to decarbonise private passenger transportation.

This is why EVs have increasingly received both private and public financial support and today they are one of the few mitigation strategies which are judged on track to meet the 1.5°C target from the Paris Agreement [7]. This progress is also confirmed by the substantial penetration of EV models in some developed countries [8].

Yet, this recent success has long been delayed and keeps being threatened by some technical and cultural hindrances. First, EVs introduce an interaction with the energy sector at a timescale that is unprecedented for road transportation. Contrary to conventional cars, EVs require their "fuel" to be instantaneously generated and transported over long distances as soon as it is demanded. Only trains entail a similar phenomenon, but their scheduled and coordinated movements make the electricity demand

tricity and manage to outperform BEVs thanks to their lighter weight. In a nutshell, direct electrification is the best solution for any distance shorter than 370 km.

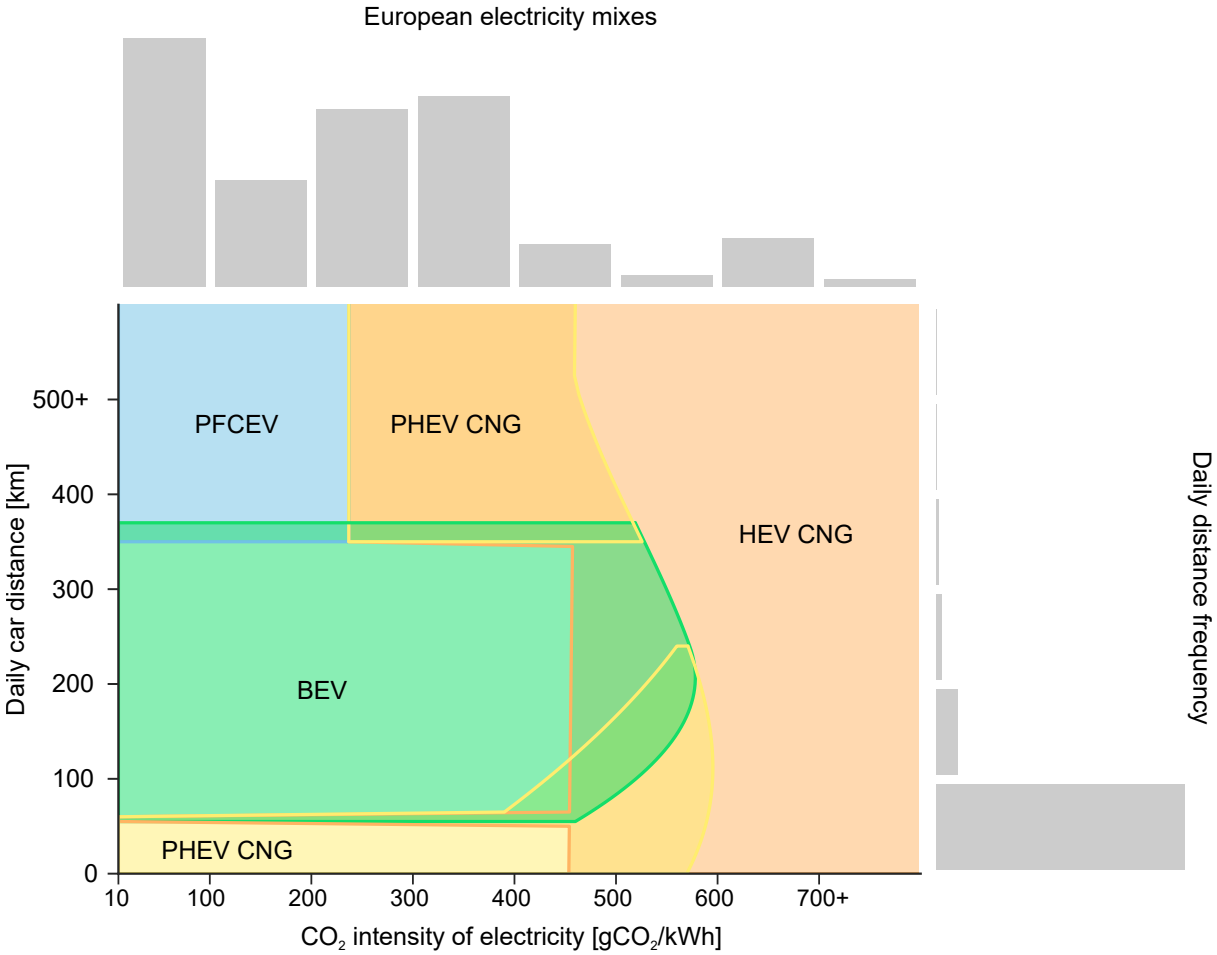

Figure 1.2: Powertrain technology that minimises the specific well-to-wheel (WTW) CO_2 emissions [gCO_2/km] for a given daily distance (y-axis) and CO_2 intensity of the grid (x-axis) without *en-route* charging [6]. The histogram at the top depicts the distribution of European electricity mixes (weighted with the total generated electricity) [9]; the histogram on the right shows the distribution of daily car distances recorded in Switzerland [10] and Great Britain [11] (weighted with the respective populations). See nomenclature for a description of the acronyms.

much more predictable. The uncontrolled demand for electricity from EVs may damage the local distribution grid or compete with other consumption sectors for the limited transmission capacity. Furthermore, this additional electricity may be supplied by only a part of the generation assets connected to the grid. That is, the actual x-coordinate of Fig. 1.2 to be used for environmental assessment may differ from the national average and can even depend on the time of charging. To address these points a detailed knowledge of EV usage is required, where the timing and energy flows involved with every movement or charging event are adequately known.

Accurate description of car mobility can help addressing another criti-

cism commonly made to BEVs, that is their relatively short driving range. The horizontal histogram of Fig. 1.2 already suggests that users rarely drive distances unfulfillable by averagely sized BEVs. However, on one side single-day performances may overlook the long-term mobility needs of drivers and misrepresent the battery preferences of potential buyers. On the other side, opportunity charging during the day could soften the battery requirements of BEV drivers. These uncertainties call for a comprehensive description of EV mobility that can capture both intra-day details and multi-day fluctuations.

Other important criticisms made to EVs involve their high upfront price and the controversial sustainability of the battery manufacturing process. While these subjects deserve dedicated analyses and are already being successfully tackled [12, 13, 14, 15], detailed knowledge on car mobility can provide further useful insights. This is particularly the case when entirely different mobility concepts, such as car-sharing, are introduced as partial solutions to those problems [16, 17].

All these needs for a detailed picture of EV mobility conflict with their relatively low diffusion in worldwide fleets. The current standard way for governments and institutions to acquire reliable knowledge regarding people's mobility is through household travel surveys (HTS), inquiries regularly carried out by many countries on the mobility patterns of their citizens. Until EVs have profoundly entered some national fleet stocks, these HTSs will essentially describe the usage of internal combustion engine vehicles (ICEV). This travelling information, albeit abundant and statistically representative, might thus misrepresent the future usage of EVs.

Accurate information on EV mobility can be obtained from EV trials, i.e. field tests where participants are given EVs and all their movements and charging events are thoroughly tracked. The drawback of EV trials is that they are usually limited in size and are necessarily bound to the socio-geographic context where they take place.

A way out of the impasse can come from a comparison of the results obtained from an EV simulation platform based on HTSs and the empirical measurements of EV trials. This thesis fulfils this objective by using as benchmark the hourly electricity demand triggered by charging EVs. Such a validated model can then be employed to confidently address some of the aforementioned drawbacks of EVs.

1.2 Thesis structure

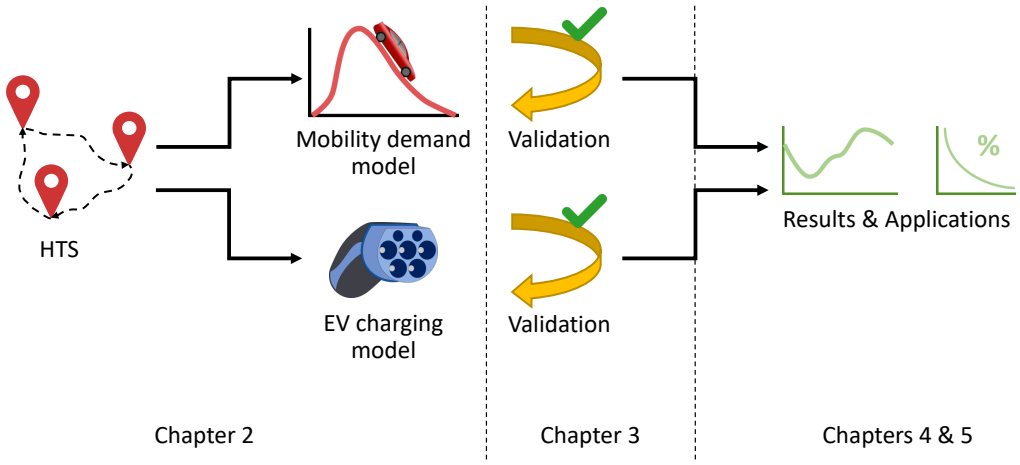

Figure 1.3: Schematic organisation of this thesis.

The thesis is organised as depicted in Fig. 1.3. Chapter 2 presents the methodology used to build an EV simulation platform based on traditional HTSs. On one side, this includes the understanding and cleaning of the information included in HTSs; on the other, it requires the modelling of multi-day mobility and of EV energy flows, from charging to propulsion.
Chapter 3 then presents the validation of the two main introduced models. The multi-day model is used to build annual mobility profiles and the resulting distribution of yearly mileages is compared against empirical observations. The EV charging model is employed to construct hourly load profiles from charging EVs and these are compared against the loads measured in EV field tests. The chosen basis for comparison allows the assessment of the whole simulation chain, from the timing of cars usage to the energy consumption of EVs. The favourable outcome of the validation conclusively proves that even traditional HTSs can adequately capture the mobility behaviour of EVs.
The model so validated is then employed in Chapter 4 to address some of the aforementioned EV hindrances. Particular focus is given to the electrification potential of BEVs when accounting for the variety of mobility needs of individual drivers on a yearly timescale. A brief discussion on the actual CO_2 content of the electricity fed to BEVs is also proposed, in order to assess whether future mixes won't exceed the tipping point shown in Fig. 1.2.

Given the recent uptake of alternative mobility models such as car-sharing and autonomous driving, it is important to assess how these disruptions would interact with the parallel expansion of EVs. Therefore, chapter 5 proposes an exploratory investigation of the benefits of EV-sharing systems. The results suggest that such mobility models could effectively contribute to addressing issues such as the economical access to EV mobility or the demand for large quantities of battery storage.
This thesis aims to demonstrate the adequacy of HTS-based EV models and hence corroborate the pivotal role of EVs in decarbonising private mobility. It further aspires to provide useful insights for future research on the most recent developments of EVs and passenger transportation.

Chapter 2

Methodology

This chapter introduces the approaches used to describe the mobility of passenger cars in general and of EVs in particular. Private mobility arises from the balance of multiple necessities, which confront the utility of reaching the destination against the time, cost and discomfort of travelling. The creation of entirely synthetic mobility data has thus been seldom attempted [18] and the vast majority of research relies on some form of recorded movements.

Household travel surveys (HTS) are among the datasets most commonly used thanks to their favourable characteristics. They are surveys regularly carried out in many countries worldwide which track every movement of a large sample of the population for one or multiple days. The samples are statistically significant and the surveys allow to draw conclusions for both the entire country and specific socio-demographic groups. These data are also usually accessible by research institutes, since they are generally collected by governmental institutions for the public interest.

HTSs are relatively accurate pictures of *today*'s mobility, but lack any flexibility or specificity. HTSs do not inform about the specific usage of EVs or the utilisation factor of shared cars. These phenomena might take place in the survey but do not reach the significance threshold necessary to elaborate useful conclusions. Scientists thus employ modelling techniques to shape HTSs for their specific needs.

Section 2.1 provides an overview of the typologies and applications of HTS-based models in literature. The chapter then describes the approaches employed in this thesis to characterize firstly the demand for passenger car mobility (Section 2.2) and then the specific energy demand from EVs (Section 2.3).

2.1 HTS-based EV models in literature

HTSs have been extensively employed to investigate potential challenges posed by the quick introduction of EVs. The following literature focuses on studies that have employed HTS to model charging profiles (CP), that is the hourly load demand generated by one or multiple EVs being charged. CPs play the important role of interface between EVs and the energy sector. Depending on the system scale, CPs may impact the performance of the local distribution grid, as well as the national transmission grid or the generation of electricity. The goal of EV modellers is to estimate realistic CPs so that downstream simulations can evaluate the impact of EVs on any relevant asset.

CPs from raw HTS

[19, 20] build CPs from the American HTS and compare the load shape for different socio-spatial groups. [21] derives CPs from the Swiss HTS and then proceeds to assess their impact on the distribution grid substations. [22, 23] provide more comparative analyses by building CPs from different European HTSs and conclude that, although some differences between countries exist, the biggest impact comes from assumptions on charging opportunity and behaviour. These aspects are thoroughly investigated in Section 3.1.4 while testing the model developed in this thesis.

Modelling mobility behaviour

Several researchers choose to describe the variable nature of private mobility through a stochastic formulation of their models. [24] derives CPs from the American HTS and then randomly samples some of those CPs from a selected pool of drivers. But the majority of works incorporates stochasticity by firstly deconstructing the HTS into its elementary variables — such as travelling times or mileage driven — and then restructuring the gathered information to obtain CPs. [25, 26] extract univariate distributions of driven distances and parking times and sample from these the individual charging events. [27, 28] recognise the importance of maintaining the interdependent structure linking those quantities and build charging events by conditionally sampling the necessary variables. [29, 30] model the multivariate nature of mobility by employing copula functions: [29]

then performs a Monte Carlo simulation to reproduce individual driving, and consequently charging, events; [30] additionally shows the effectiveness of using queueing theory to model the lag between arrival time distribution and CPs. [31] preserves the interdependency between travelling times and trip lengths by training artificial neural networks on the American HTS. The trained model is then used by a local aggregator to forecast EV travel behaviour and minimize the total cost of charging. Finally, some studies use the disaggregated information of HTSs to build new synthetic daily schedules before computing the CPs; to account for the interdependence of the fundamental variables [32] employs a Naive Bayes while [33, 34, 35] opt for Markov-chain simulations.

Modelling charging behaviour

The derivation of CPs from a daily driving schedule — synthetic or extracted from a HTS — requires modelling the charging decision process of EV drivers. Most studies impose a constant number of recharges per day [36] or assume that EVs will be charged at every possible opportunity [37]. A more elaborate approach is proposed in [24, 22], where a time-dependent probability to charge is introduced. Similarly, [38] uses the journey number of the day as proxy for the location of the vehicle, hence of its probability to charge. Other studies model charging behaviour as a function of the battery's state of charge (SOC): [29, 36, 39, 40] use fixed thresholds of SOC below which drivers always decide to charge their EVs, while [33] designs a charging probability that follows a logistic function over the car SOC. Finally, [41] proposes an advanced charging decision scheme that combines some of the above criteria with the cost of charging and the maximum rechargeable energy.

Validation of simulated CPs

Simulation models require a validation of their outputs to gain legitimacy. Most literature has focused on synthesising stochastic driving patterns and has accordingly prioritized validating the resulting travel behaviour against the original HTSs [30, 32, 33, 38]. While this verification is important, there is evidence that charging behaviour of EVs is as big a source of uncertainty as the mobility behaviour itself [42]. Since CPs result from both phenomena, they are a suitable candidate to validate the entire modelling

procedure. However, few works effectively present a comparison between CPs measured in a public EV trial and CPs built from a HTS.
In [25] CPs measured in a large British EV trial [43] are compared with CPs built either from the raw data of the trial itself or from the British HTS. The comparison predictably favours the CPs built from the trial itself, but also the HTS performs well, for instance by returning the same peak demand. However, the authors' focus on the trial did not allow for a refined modelling of the HTS, and few adaptations would have improved the HTS's score. [24] validates CPs obtained from the American HTS against a small demonstration project in Austin, Texas. The quality of the comparison is remarkable although they employ normalised CPs and thus cannot assess the peak demand accuracy.

Research gap

Any model aiming at describing EV mobility should undergo a validation that captures both the simulation of car movements and the modelling of EV characteristics. While CPs can serve this purpose, no thorough validation process of HTS-based CPs has been performed in literature. In Chapter 3 CPs generated from HTSs are compared against the empirical loads measured in 4 different EV trials.
The advantage of assessing the whole EV driving and charging chain is that the validated model can be employed for purposes other than the construction of CPs. Chapters 4 and 5 include illustrative applications such as the sizing of BEV battery capacities.

2.2 Mobility demand

This first methodological section details the construction of car usage profiles from raw HTSs. The outcome of this process solely reflects the mobility demand of drivers and disregards any characteristic of the cars such as weight or powertrain. These factors will be considered in the energy calculations of Section 2.3.
Nevertheless, grounding the car mobility demand on existing HTSs implies assuming a conventional powertrain on most vehicles, as entailed by the current composition of worldwide fleets. Whether the derived demand properly reflects also the usage of EVs is one of the fundamental objec-

tions to all HTS-based EV models. While some studies observe that range anxiety may impact the driving routine of EV users [44, 45, 46, 47], others find this alteration not to be particularly significant, especially after longer driving experience [48, 49, 50, 51]. The successful validation of Chapter 3 decisively endorses the legitimacy of HTS-based EV models, especially when the objective is the construction of CPs.
In this thesis HTSs are taken as is and no disassembling-resampling of their information is performed: the quality and abundance of their data is usually satisfactory without the need to synthesize artificial trips. The modelling efforts of this thesis thus focus on attenuating peculiar shortcomings of HTSs:

- the bias and inaccuracies introduced by respondents when filling out the surveys (in Section 2.2.2);
- the potential misrepresentation of car mobility when tracking personal movements (in Section 2.2.3);
- the lack of multi-day mobility: the vast majority of HTSs track a single day, with the important exception of the UK [52] (in Section 2.2.4).

Before discussing these steps, the next section briefly introduces the HTSs used in this thesis.

2.2.1 Household travel surveys

Two HTSs are used as a basis for this thesis:

- the *Mikrozensus Mobilität und Verkehr* (MZMV) from Switzerland [10];
- the National Travel Survey (NTS) from the UK [11].

The Swiss HTS: MZMV

The Swiss HTS has primarily been chosen due to the multiple collaborations with Swiss stakeholders during the development of this thesis. This comes from the intrinsic interfacial nature of CPs, which should ideally be generated from a HTS that is consistent with the context of the downstream simulations they are applied to.

Additionally, MZMV is a highly detailed HTS with rich intra-day travelling information and a large sample of participants. MZMV is carried out every 5 years and this thesis employs the results from the latest survey in 2015, which tracked the movements of 57,090 people, i.e. about 0.7% of the Swiss population [53]. Each person is drawn from a different household. The dataset assigns to each participant a calibrated weighting factor that allows to draw statistically significant conclusions not only for the entire country but also for specific socio-geographic groups [54]. Temporal information comes with a 1-minute resolution, which is valuable to model the dynamic CPs from various EV patterns.
According to [52], any HTS that aims at accurately investigating EVs-infrastructure interactions should possess the following features:

- data collected as trip diaries;
- data disaggregation to the individual level (not household or community);
- survey of a full week;
- details on socio-economic identity of individuals;
- details on duration and place of parking;
- details on size and age of vehicles;
- segmentation in rural and urban areas;
- geographic coverage of the entire country.

MZMV fulfils most of the above requirements with the sole drawback of missing weekly travelling information. The value of this knowledge and potential remedies for its absence are discussed in Section 2.2.4.

The British HTS: NTS

NTS is the only HTS analysed by [52] which fulfils all the above requirements, including tracking the movements of participants for an entire week. The sample size is smaller than MZMV, about 7500 households per edition, but every member of the household is interviewed and the survey is carried out every year. NTS included the whole Great Britain until 2012 and then

focused only on England. Nevertheless, methodology and weights of NTS are adjusted so that multiple editions can legitimately be employed in the same analysis.
Although all years 2002–2017 were available, only the editions from 2009 were finally employed in this work. This choice is justified by the observed decrease in average mileages of household cars [55], which makes older surveys obsolete for modelling current and future usage of vehicles. The reduction is particularly steep until 2009, when it mildly attenuates.
NTS distinguishes between households that provide only general information about members and vehicles owned (interview sample) and households that supply a fully detailed travelling schedule (diary sample, subset of the former). Given the objective to construct intra-day car usage profiles, only the data reported in the diary sample were considered[1].

2.2.2 HTS entries corrections

Most of the fields in HTSs are directly filled in with the respondents' answers and as such may be altered by human perception and forgetfulness. Particularly critical for the technical analyses are the reported times and distances.

Reported times

Participants tend to round travelling times to the hour, half hour and quarter hour. Only few authors have acknowledged the problem and have proposed solutions to offset this distortion [24, 56, 57]. A simple approach to realistically disperse these times is proposed in Algorithm 1.
GCD computes the greatest common divisor and $t_{i,dep}$, $t_{i,arr}$ are the vectors of departure and arrival times for the i^{th} daily car trip. The method assumes that every respondent has an inner time resolution and thus reports travelling times rounded to that resolution (line 2 in Algorithm 1). The share of participants with a given time resolution for the case of MZMV is plotted with $\times$ in Fig. 2.1. Departure and arrival times are shown separately since the latter come with much finer precision. The likely reason for this behaviour is that respondents think more in terms of trip duration and tend to add this to the departure time to estimate the arrival time.

[1]The diary sample includes on average 90% of all interviewed households.

Algorithm 1 Shift of departure and arrival times.

1: **for** i **in** trips **do**
2: $\text{resolution}_{\text{raw}} = \text{GCD}\,(t_{i,dep})$
3: **for** k **in** $[60, 30, 15, 10, 5, 1]$ **do**
4: **if** $\text{resolution}_{\text{raw}} \bmod k = 0$ **then**
5: $\text{resolution} = k$
6: **exit for loop**
7: **end if**
8: **end for**
9: $\text{shift}_{\max} = \min\left(t_{i,dep}[1 : \text{end}] - t_{i,arr}[0 : \text{end} - 1]\right)$
10: $\text{shift}_{\max} = \min\left(\text{shift}_{\max},\ \text{resolution}/2\right)$
11: sample $X \sim \mathcal{U}\,(-1, 1)$
12: $\text{shift} = \text{truncate}\,(X \cdot \text{shift}_{\max})$
13: $\left(t^{new}_{i,dep},\ t^{new}_{i,arr}\right) = (t_{i,dep},\ t_{i,arr}) + \text{shift}$
14: **end for**

Overall, about 80% of respondents report departure times with a resolution of 5 minutes or coarser. According to this approach, the actual trips may have occurred at any moment falling within the respondents' time resolution around the reported times. More diversity can thus be introduced by randomly shifting travelling times within their time resolution (lines 11, 12). It is also reasonable to assume that respondents tend to round only to 5, 10, 15, 30 and 60 minutes and the set of possible resolutions is accordingly reduced (e.g. trips with apparent resolutions of 20 or 90 minutes are assigned resolutions of 10 or 30 minutes respectively; lines $3 - 8$). In order to maintain the original logistic structure of the trips, all daily movements of each trip are shifted by the same amount (line 13) and no shifted stage should overlap with the non-shifted neighbouring stages (lines 9, 10). The resulting time resolutions of trips are depicted with $\bullet$ in Fig. 2.1. Both distributions steadily improve, and arrival times exhibit time resolutions finer than 6 minutes for more than 80% of trips. This is crucially important to obtain sparse parking times, hence smoother CPs.

Reported distances

Since the correct estimation of travelling distances is of paramount importance for taking any meaningful action, most statistical offices have taken

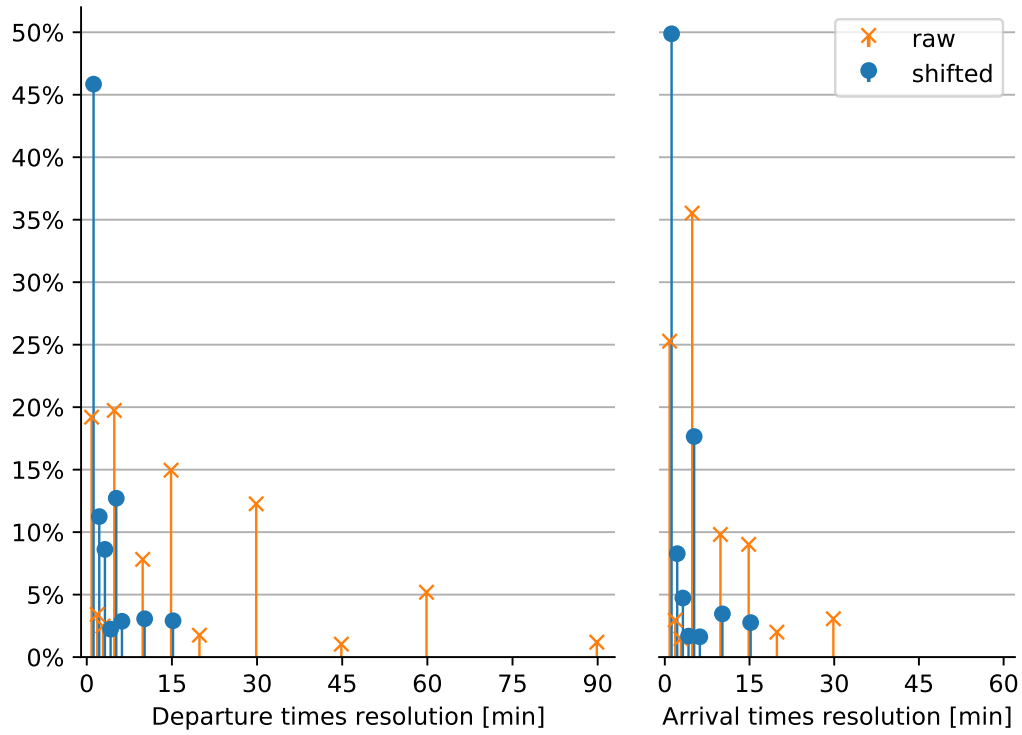

Figure 2.1: Probability mass function of the time resolutions used by respondents while reporting travelling times. Time resolutions belonging to less than 1% of respondents are not shown for clarity. Clear peaks at 1, 5, 15 and 30 minutes are visible for both departure and arrival times.

countermeasures. Regarding the two analysed countries:

- since 2010 MZMV performs a routing process that maps each respondent's movement to the plausible itinerary on the Swiss transportation network [58];
- NTS provides, beyond the manually reported daily movements:
  - the total weekly mileage of each household-owned vehicle as indicated by the on-board odometer;
  - a weighting factor *W5xhh* to offset the observed reduction of trips reported along the surveyed week, regardless of the weekday on which it began [59][2].

While MZMV directly provides the corrected distances, NTS does not make a presumptive use of the additional information, letting the end user apply

[2] *W5xhh* is so labelled since it represents the trip weight *W5 excluding* the *household* weight (either *W2* or *W3* depending on the sample under consideration). In other words, it is the general weight of trips during any surveyed week irrespective of the interviewed household.

the appropriate corrections.
Therefore, in this work NTS is preprocessed by firstly applying *W5xhh* to adjust the distances recorded on each day within a reported week, increasing the average mileage by 5%. The resulting weekly distances come still short of the values measured by the odometer, due to the omissions of car stages that may not or should not be reported to NTS, such as when the car is driven by a non-household member, when transporting goods in course of work, or when commercially escorting passengers [59]. The average gap amounts to 7.4% and a second uniform scaling factor of 1.074 is thus applied to all recorded movements.

2.2.3 Car mobility characterisation

Both HTSs asked participants to list all vehicles available to the household (regardless of the ownership) and to indicate for every driving stage which car has effectively been used. With this car identifier, it is possible to link together all stages performed by the same vehicle and to obtain the daily driving schedule from the car's point of view.
The procedure is straightforward but the accuracy of the resulting schedule depends on a HTS feature overlooked by [52]: whether all household members have taken part in the survey. Cars are often shared by members of the same household and interviewing a single person does not ensure an accurate picture of the cars' usage. This aspect does not fundamentally impede the generation of CPs and that is why [52] has not included it in their indispensable list. Nor are the aggregated statistics on car mobility significantly impacted. The simple example of Fig. 2.2 better illustrates the impact of interviewing a single member per household.
Fig. 2.2 presents the mobility patterns of 6 households (HH): on the y-axis are the cars owned, on the x-axis the household members (all adults with a driving license) and in the cells are the km driven on a day by the x-person with the y-car (− if none). Any movements with other means of transport are neglected for simplicity. Let's assume that the 6 households represent the entire population. Household members surveyed are circled in green, together with their mobility. To make sure that the sampling procedure is correct and representative, HHs 4–6 are copies of HHs 1–3, with the other person being selected for the HTS.
Firstly, the personal mobility by car is evaluated. The *real* average daily

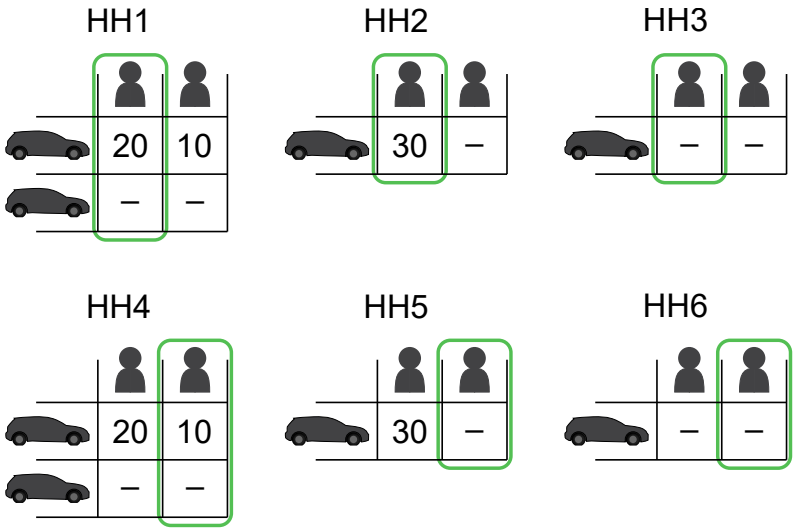

Figure 2.2: Imaginary community of 6 households, each depicted by a table with a column per member (all adults with driving license) and a row per car owned. The cells of the table indicate the daily distance driven by the x-person with the y-car. The people surveyed in the HTS are circled in green.

distance by car per person d_{person} and the *estimate* $\hat{d}_{\text{person}}$ by the HTS are:

$$d_{\text{person}} = \frac{20 + 10 + 30 + 20 + 10 + 30}{12} = 10 \text{ km/p} \tag{2.1}$$

$$\hat{d}_{\text{person}} = \frac{20 + 10 + 30}{6} = 10 \text{ km/p} \tag{2.2}$$

Therefore, if the sampling procedure is correct, the estimated personal mobility matches the actual one. Let's now consider car mobility. The *real* average daily distance per car d_{car} is:

$$d_{\text{car}} = \frac{30 + 30 + 30 + 30}{8} = 15 \text{ km/car} \tag{2.3}$$

However, the survey has never tracked cars, but only people. To *estimate* the average car distance researchers can either rely on all detected cars or on only the used ones:

$$\hat{d}_{\text{car all}} = \frac{20 + 30 + 10}{8} = 7.5 \text{ km/car} \tag{2.4}$$

$$\hat{d}_{\text{car used}} = \frac{20 + 30 + 10}{3} = 20 \text{ km/car} \tag{2.5}$$

These estimates are wrong as they miss both the actual distance of cars when driven ($d_{\text{car used}} = 30$ km/car) and the relative frequency f_{used} of

driving days ($f_{\text{used}} = 1/2$, $\hat{f}_{\text{used}} = 3/8$). Both these estimates should be corrected to improve the description of mobility from the car's point of view.

A HTS like the British NTS that interviews all household members does not face these issues as all car movements are necessarily tracked. Such a HTS might still miss stages where the car is driven by a non-household member, but these situations are significantly limited. In the case of NTS at least the distances of these and other exceptions can be accounted for with the reported car weekly mileages and the correction factor of 1.074.

The next sections provide steps to refine the estimates of $\hat{d}_{\text{car used}}$ and $\hat{f}_{\text{used}}$ in HTSs that do not interview all household members, such as in MZMV.

Improve distance of cars when driven

An excellent solution to account for stages where the car is driven by a person other than the HTS respondent is provided in [60]. The authors use socio-demographic information about the other driving-license-holders of the same household to sample new car stages entirely. This approach still requires a wealth of information about the other household members — albeit not a travelling schedule — and this may not be possible for most HTS, as in the case of MZMV.

However, MZMV reports also all the stages where the interviewed household member was a car passenger. If that car was also driven by the surveyed person on the same day, these passenger stages can be added to the overall car movements of the day. This approach can offset some of the cars performance of HHs 1 and 4 in Fig. 2.2 missed by the survey, thus increasing $\hat{d}_{\text{car used}}$ towards $d_{\text{car used}}$.

The distribution of daily distances of active cars recorded in MZMV is shown in Fig. 2.3. The histogram exhibits, on a logarithmic scale, the typical quasi-log-normal distribution of car mileages observed in literature [61, 62, 63]. The inclusion of passenger stages to the cars' mileage slightly shifts the distribution to the right, i.e. towards longer trips. Specifically, both the median and average daily distances increase by 4%, resulting in $\hat{d}_{\text{car used}} = 48.7$ km.

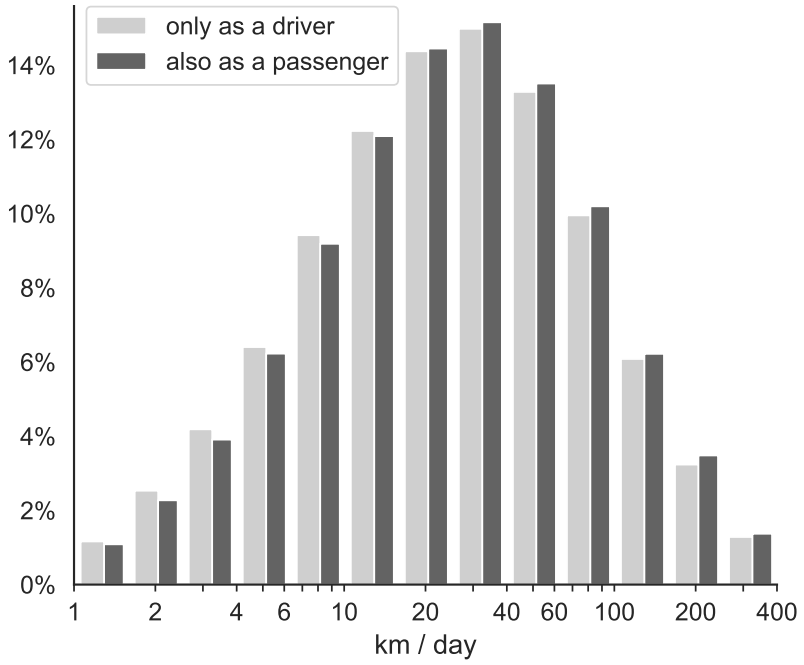

Figure 2.3: PDF of daily distances driven by car. The logarithmic scale on the x-axis makes the distributions look approximately Gaussian given their quasi-log-normal natural shape.

Improve frequency of driving days

Even from a HTS with a single household member surveyed it is possible to estimate the average car distance $\hat{d}_{\text{car}}$ if the total number of adults and cars in the population is known. In the example of Fig. 2.2 this means:

$$\hat{d}_{\text{car}} = 10 \text{ km/car} \cdot \frac{12 \text{ people}}{8 \text{ cars}} = 15 \text{ km/car} \tag{2.6}$$

which matches the actual value from Eq. 2.3. This approach relies on a key difference between the HTS sample and the entire population: while the former is an open system where the detected cars may be driven by individuals outside the sample, the whole country can be reasonably considered a close system where the mobility by car of all residents has to be performed by all the cars registered in that country. Scaling the mobility performance to the national level enables the change of point of view from people to cars that at the sample level is impossible.

For the case of Switzerland the Federal Statistical Office recommends to use the number of adults for scaling from MZMV to the entire population

[64]. The figures for Switzerland thus become:

$$\hat{d}_{\text{adult}} = 22.1 \text{ km/adult} \tag{2.7}$$

$$\hat{d}_{\text{car}} = 22.1 \text{ km/adult} \cdot \frac{6{,}755{,}656 \text{ adults}}{4{,}458{,}069 \text{ cars}} = 33.4 \text{ km/car} \tag{2.8}$$

With $\hat{d}_{\text{car}}$ and $\hat{d}_{\text{car used}}$ it is possible to estimate the average driving frequency $\hat{f}_{\text{used}}$:

$$\hat{f}_{\text{used}} = \frac{\hat{d}_{\text{car}}}{\hat{d}_{\text{car used}}} = \frac{33.4}{48.7} = 68.6\% \tag{2.9}$$

This means that on any given day approximately a car every three is not driven or, equivalently, an average car is not driven every three days.

Summary car mobility statistics

The key statistics for car mobility in Great Britain directly stem from NTS as preprocessed in Section 2.2.2. The final figures for Switzerland and Great Britain are provided in Table 2.1.

		MZMV (CH)	NTS (GB)
Average daily distance [km]...			
...per person by car as a driver	$\hat{d}_{\text{person}}$	19.4	15.6
...per adult by car as a driver	$\hat{d}_{\text{adult}}$	22.1	19.7
...per car	$\hat{d}_{\text{car}}$	33.4	31.9
...per car when driven	$\hat{d}_{\text{car used}}$	48.7	48.4
Average car usage frequency	$\hat{f}_{\text{used}}$	68.6%	65.8%

Table 2.1: Key car mobility statistics extracted from MZMV for Switzerland and from NTS for Great Britain.

Beyond these aggregated statistics, the above preprocessing steps return the detailed intra-day schedule of driven cars. Fig. 2.4 shows the distribution of Swiss active cars between locations and road on an average day of the year. The distributions for different days of the week are available in Section A.1 of the appendix.

The portion of actively mobile cars is depicted by the Road and Highway shares and is almost always lower than 10%: EVs have in principle plenty of time to charge while being parked. The human bias in the reported departure times is still slightly visible in the Road segment, but

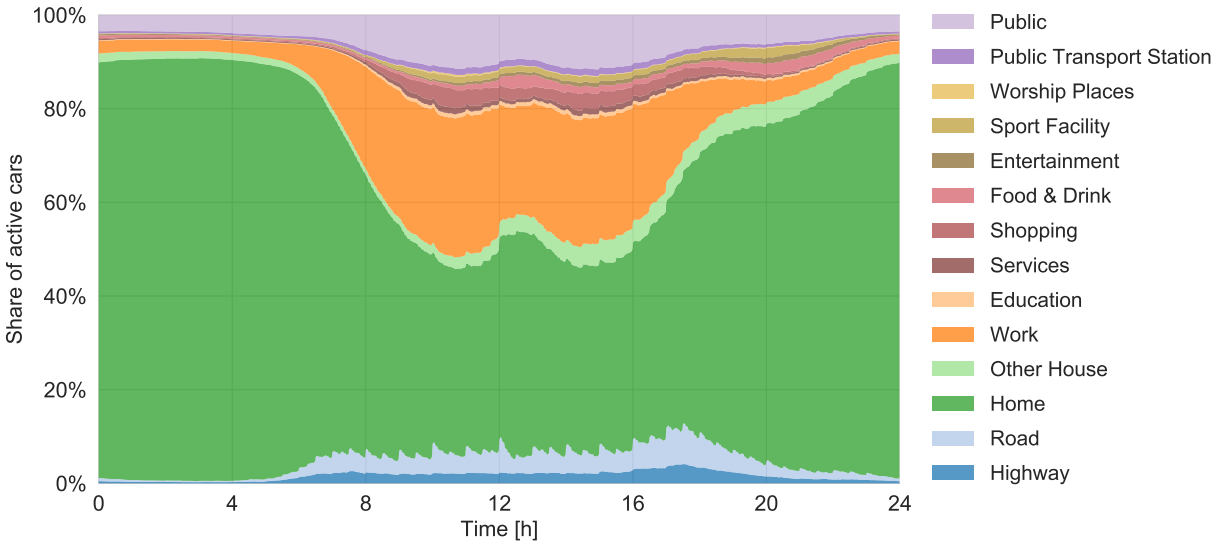

Figure 2.4: Locations and activities of cars in Switzerland during an average day of the year. Only cars which are used at least once during the day are shown.

more aggressive shifting procedures of Section 2.2.2 would jeopardize the original information; moreover, the CPs-relevant arrival times exhibit an adequately smooth behaviour.
Rush hour is reached at the end of the working schedule, between 5 p.m. and 6 p.m., and it is followed by a quick increase of vehicles parked at Home: these concurrent events might trigger a considerable demand for electricity at home. The other major opportunity for EV charging is at Work, where the share of vehicles parked in the mornings and afternoons reaches 40% on working days (see Section A.1). However, the morning commute to work exhibits even more synchronised behaviour than the afternoon one and it could trigger, when not managed, an increasingly demanding load. The Public share clusters together all undefined locations, while the Public Transport Station portion represents the times when the driver transfers from car to public transport. Finally, opportunity charging at leisure sites like Food & Drink and Sport Facility may be helpful, but might not dramatically affect EVs' range requirements or their impact on the grid.

2.2.4 Multi-day mobility

This section deals with the construction of car usage profiles lasting multiple days. Most HTSs provide single mobility days but, depending on the application, there might be a need for weekly or even annual profiles. The-

oretically, multiple single days could be randomly concatenated to obtain the desired time range. Despite the simplicity, this approach can already deliver acceptable results under certain conditions. The reason comes from the characteristic PDFs of car mobility depicted in Fig. 2.5.

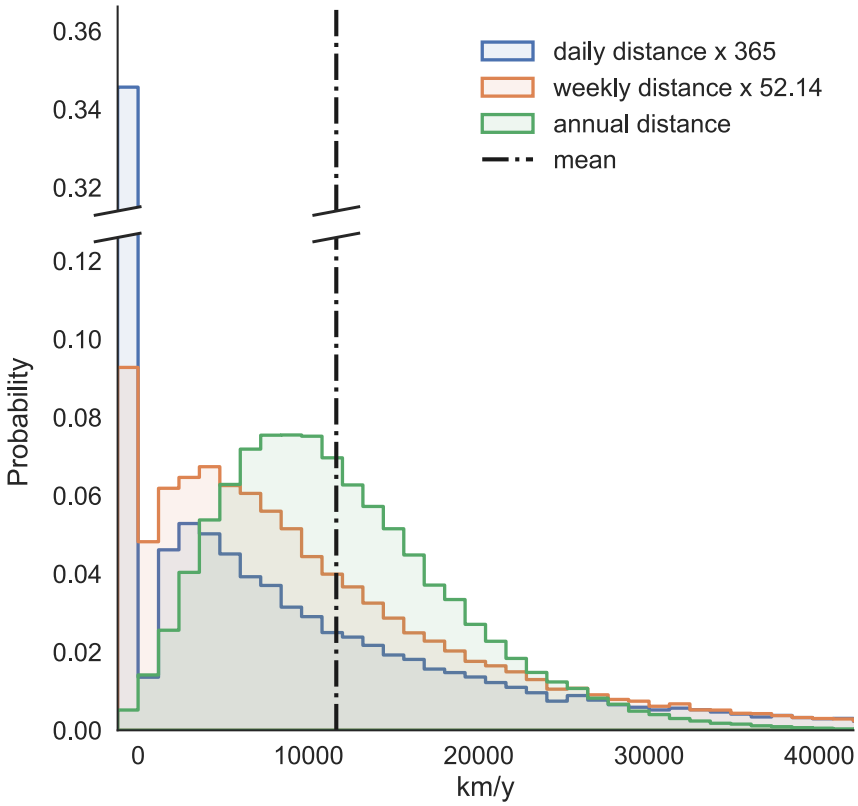

Figure 2.5: PDF of distances driven by a British car on an average day (blue), week (orange), and year (green). All distances have been annualised to allow for comparison. The high bars at 0 indicate the share of cars which do not travel on a given time frame.

The three histograms show the PDFs of daily, weekly and yearly mileage for GB, all *annualised* so to be plotted on the same x-axis. Daily and weekly PDFs come from NTS while the annual data come from the "Motoring and vehicle Ownership Trends in the UK" project (MOT) [65, 66], which analysed the mileage readings from about 28 million cars collected during annual inspections that all British vehicles must undertake.

The high bars at 0 indicate the share of cars which do not drive in the given time period. As observed in Table 2.1, about 34.2% of British cars are not used on any given day, but the share drops to 9.3% when considering an entire week. Very rarely are cars not driven for a whole year.

Importantly, the three annualised PDFs share the same mean of 11640

km/y.[3] This follows naturally from the construction of the PDFs, but implies that, with a sample large enough, any concatenation criterion would return the correct average of the target time period. For instance, when sampling multiple single days to obtain one full year the two extreme cases are 1) no random selection but reproduction of the same mobility day for 365 days or 2) purely random selection from the entire pool of one-day profiles. When repeating many times, technique 1) would exactly return the blue PDF of *annualised* daily profiles, while approach 2) would produce an extremely tight distribution around the mean. Neither PDF would be realistic or close to the target green distribution, but both distributions would have the correct mean. If the target application is strongly focused on mean values, these artificial and inaccurate annual profiles may be adequate. The same reasoning applies to any concatenation between different time spans.

The most obvious application of this simplified technique is the derivation of the total annual car performance of a country. Researchers aggregate the one-day results from the local HTS, scale it up to the entire population and multiply the final result with 365 [64]. The final figure is assumed to correctly describe the national annual car performance, which is in fact only a central value. Exactly because this is one of the main purposes of HTSs, these are designed so that the mean of *annualised* recorded one-day data closely aligns with the unknown annual mean. This explains the need of HTSs to take place on multiple days of the year: a HTS recorded on a single day might still be representative for the population, but would not be representative (i.e. match the mean) for the distribution of annual profiles.

An accurate PDF of weekly or annual profiles is required when the application uses the variance of the data, beyond the central value. This is particularly the case when each car usage profile interacts with other elements of the system before any aggregation occurs.

When a realistic PDF is required, the concatenation of single mobility days (or weeks) must adhere to some conformity criteria. On one side mobility varies on a day-to-day basis following the temporal patterns of human activities. On the other side car usage heavily depends on the driver profile. Coherent mobility profiles can thus be constructed by firstly

[3]The annual mileages from the MOT project return a mean 2% higher than NTS. This is acceptable considering the different sources, years and selection criteria of the studies.

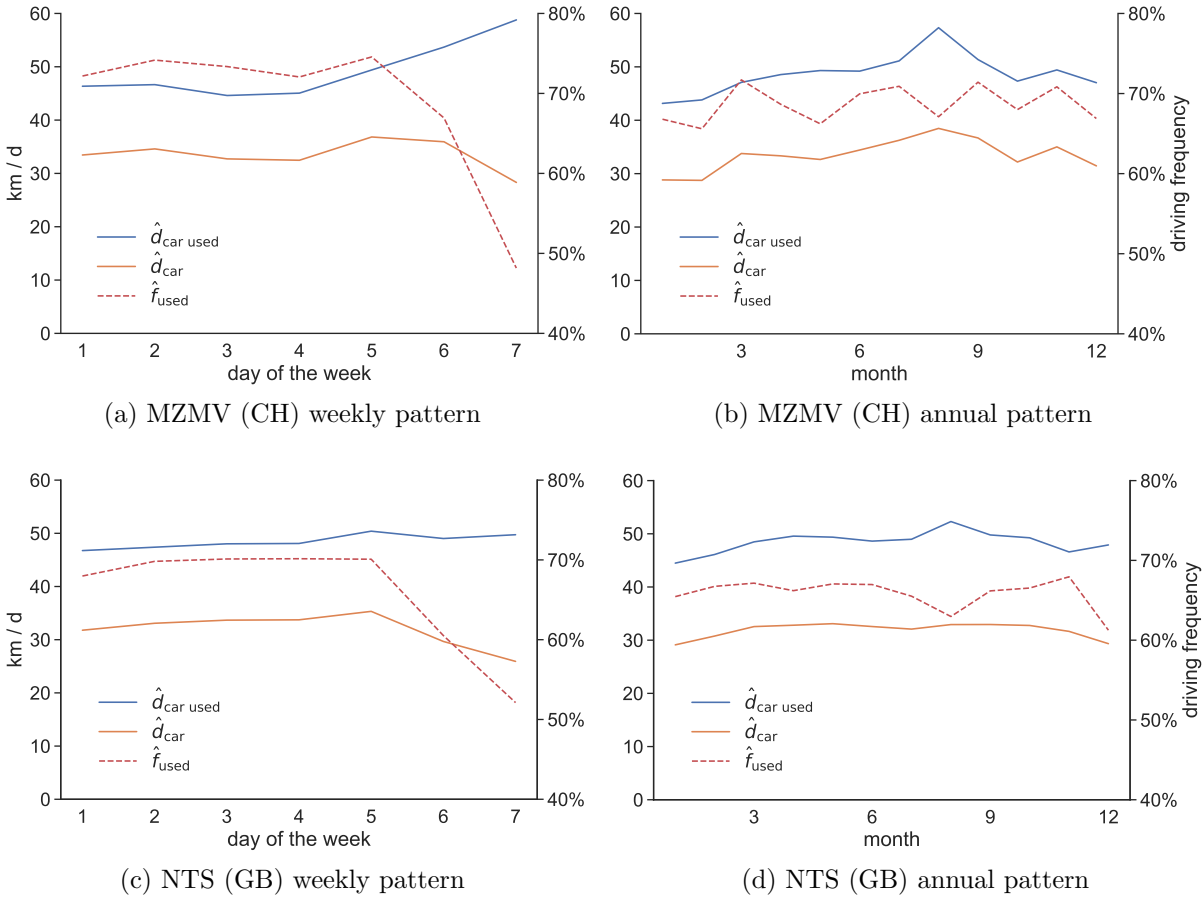

(a) MZMV (CH) weekly pattern

(b) MZMV (CH) annual pattern

(c) NTS (GB) weekly pattern

(d) NTS (GB) annual pattern

Figure 2.6: Average daily car distance on any ($\hat{d}_{\text{car}}$) or on an active day ($\hat{d}_{\text{car used}}$) and average car usage frequency ($\hat{f}_{\text{used}}$) by day of the week (a, c) or month of the year (b, d).

clustering HTS records into homogeneous groups and then by sampling multiple days (or weeks) from the same group.

Clustering: temporal characterisation of mobility

Human activities are organized around two main time frames: the week and the year. To assess the impact of these structures Fig. 2.6 presents the key car mobility statistics of Table 2.1 ($\hat{d}_{\text{car}}$, $\hat{d}_{\text{car used}}$, $\hat{f}_{\text{used}}$) for different days of the week and different months of the year.
The two countries display very similar patterns. On an average week, all key statistics stay approximately constant on weekdays (Monday to Friday) but the car usage frequency markedly drops on the weekend. This results in a slight decrease in average car distance in both countries, despite longer journeys in CH. In both nations Friday exhibits the highest average distance, probably due to the combination of professional and leisure mobility.

Annual mobility displays less distinctive patterns. Winter statistics are marginally lower than in Summer and August is characterized by fewer longer journeys. Nevertheless, the overall "signal-to-noise" ratio is less pronounced than the weekly case.
These observations agree with common research findings on weekly characterisation of car usage [67, 68, 69, 70]. Therefore, only weekly variability is taken into account to construct multi-day profiles. This modelling choice implies that:

- the one-day records of MZMV (or other single-day HTSs) are firstly grouped by the day of the week the survey took place; the concatenation then considers, beyond other socio-economical criteria from the next section, the logical sequence of days in the week.

- The already weekly records of NTS are kept consolidated; since annual variability is disregarded, the sampling of multi-day profiles from NTS does not require any temporal grouping.

Clustering: socio-economical characterisation of mobility

Separate categories of society use the car in different ways but each person will likely maintain a consistent mobility behaviour in the target time frame. There is a multitude of criteria that can be employed to cluster HTS data and the final selection necessarily depends on the features available in the HTS and in the purpose of the concatenated profiles. The only general requirement is ensuring a representative size of the groups, as individual records may suffer from sampling errors. For instance, MZMV authors warn about the reliability of estimates based on fewer than 50 observations. Considering that records are split within each group by day of the week, the minimum group size becomes about $50 \times 7 = 350$ HTS records. Since no optimal grouping strategy exists, in the following only the most relevant and exemplary grouping approaches are described.
1. The simplest approach excludes any form of grouping beyond the day of the week. Analogously to the initial discussion of the section, this straightforward method is useful when the application is only concerned with central values but wants to retain the differences between days of the week. When weekly profiles are already available as in NTS, this method implies no grouping of any kind.

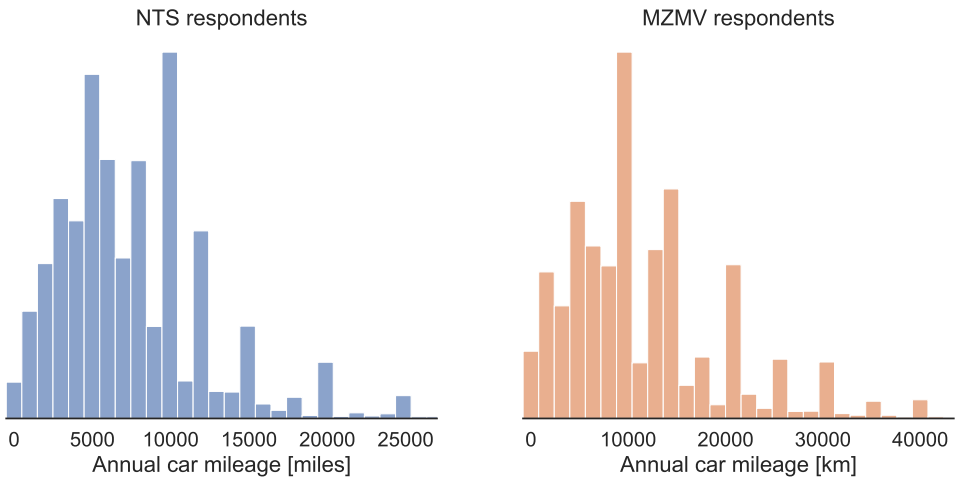

Figure 2.7: PDF of annual car mileage reported by respondents of MZMV and NTS. Despite the different units, both x-axes span the same mileage interval. A tendency to round to multiples of 2000 or 5000 can be observed in both surveys, regardless of the distance unit employed.

2. A typical application of EV models is the design of optimal charging strategies. If a study focuses on the allocation of charge between home and workplace, a reasonable consistency in commuting distances is desirable. In this case a suitable grouping strategy should consider the working status of drivers and their average home-to-workplace distance.

3. If the goal is the reproduction of the annual mileage PDF of Fig. 2.5, the best grouping variable is the cars' annual mileage itself as reported by HTS participants. This variable is usually very approximately estimated by participant and is subject to large rounding errors. The PDFs of self-reported annual mileages for MZMV and NTS are shown in Fig. 2.7 and are quite dissimilar from the empirical PDF of Fig. 2.5. Despite the discrepancy, self-reported annual mileages can create very homogeneous groups and the subsequent sampling allows the closest approximation to Fig. 2.5 (see Section 3.1.3).

4. While approach **2.** overlooks the annual PDF, method **3.** may lump together inconsistent daily (or weekly) profiles. For a more universal approach it could be recommended to employ a hybrid technique, e.g. by grouping HTS records by working status and reported annual car mileage (see Section 4.1).

5. Another frequent application is the generation of mobility data for a synthetic population. In these cases daily and annual car usages are to be estimated solely based on socio-economical characteristics of the popula-

tion. Beyond the driver's working status, also sex and age are shown to play an important role in characterizing the mobility behaviour.

HTS clustering cheat sheet. Tables 2.2 and 2.3 list the effect size between the reported annual car mileages and various features of MZMV and NTS. Effect size generally indicates any measure of the correlation or association between variables. Since some features are numerical and other nominal two different measures have been adopted. The Pearson correlation coefficient r is used to measure the *linear correlation* between annual mileage and any numerical feature. It ranges from 0 (no correlation) to 1 (perfect correlation) and comes with a sign indicating the direction of the correlation. The coefficient ratio η measures the *association* between annual mileage and any nominal (i.e. categorical) variable. It ranges from 0 (no difference between categories) to 1 (no difference within each category) and has no sign since nominal variables cannot be ordered.

The two measures can be cautiously compared since they share many traits:

- both squares r^2 and η^2 indicate the share of variance in annual mileage explained by the independent variable;
- η equals the $|r|$ between the mean annual mileages of every category and the raw annual mileages;
- binary variables can be treated in either way and give the same score.

These measures provide a first-order approximation of the statistical power of some typical variables to explain the annual mileage of cars. They do not consider causality, cross-correlations or the complex structures linking the data. The selection of clustering variables requires more sophisticated analyses and tools suited to the available data, e.g. Cramer's V for nominal variables and decision tree classifier for numerical ones [71]. Additionally, the scores are based on samples of the population and the reported annual mileage is quite imprecise. Nevertheless, Tables 2.2 and 2.3 can serve as first point of contact before undertaking more thorough investigations. For interpretation, in social sciences the strength of the relationship is considered low for $|r| = 0.1$, medium for $|r| = 0.3$ and large for $|r| = 0.5$ [72].

The results predictably show a strong correlation between performance variables. In Table 2.3 the weekly mileage outperforms the daily distance, substantiating the more informative contribution of weekly surveys. From

	Variable type	Effect size	Variable category
annual mileage	numerical	+1.000	performance
working status	nominal	0.218	driver
distance to workplace (if working)*	numerical	+0.216	household
car age	numerical	−0.214	car
maximum permissible weight*	numerical	+0.212	location
fuel type	nominal	0.211	
job type (if working)	nominal	0.211	
employment type (if working)	nominal	0.204	
daily distance (if driven)	numerical	+0.204	
kerb weight*	numerical	+0.199	
driver age (binned)	nominal	0.187	
market segment	nominal	0.169	
driver age	numerical	−0.165	
driver sex	nominal	0.148	
engine displacement (binned)	nominal	0.143	
household income	numerical	+0.121	
engine power*	numerical	+0.117	
highest qualification	nominal	0.108	
canton of residence	nominal	0.102	
marital status	nominal	0.102	
household structure	nominal	0.093	
household size*	numerical	+0.085	
urban/rural area	nominal	0.082	
population density*	numerical	−0.079	
commune typology/purpose*	nominal	0.075	
public transport quality*	nominal	0.072	
settlement size class	nominal	0.071	
engine displacement	numerical	+0.060	
driver nationality	nominal	0.046	
tenancy type	nominal	0.045	
CO_2 emissions	numerical	−0.041	

Table 2.2: Effect size between annual car mileage and key features of MZMV (CH). Effect size is measured with Pearson correlation coefficient r for numerical variables and with correlation ratio η for nominal variables. Features with * are not available in NTS (GB).

the general ranking of variable categories it can be inferred that mobility is primarily induced by the driver's needs and specifically by their profession[4]. In order to fulfil these mobility requirements, the driver then purchases a suitable car. This last decision seems particularly rational and pondered, since car-related variables display the highest correlation with the driving

[4] *Working status* indicates whether the person is employed, unemployed or permanently inactive; *job type* specifies whether the occupation is managerial, clerical, routine, etc. [73, 74]; *employment type* details whether the person is an employer, an employee or a freelancer, and whether they have subordinates.

	Variable type	Effect size
annual mileage	numerical	+1.000
weekly mileage*	numerical	+0.528
daily distance (if driven)	numerical	+0.336
privately/company owned*	nominal	0.333
fuel type	nominal	0.300
working status	nominal	0.299
car age	numerical	−0.243
driver age (binned)	nominal	0.226
engine displacement (binned)	nominal	0.215
household income	numerical	+0.194
driver age	numerical	−0.187
job type (if working)	nominal	0.180
engine displacement	numerical	+0.135
settlement size class	nominal	0.130
household structure	nominal	0.128
employment type (if working)	nominal	0.128
driver sex	nominal	0.127
marital status	nominal	0.120
urban/rural area	nominal	0.117
region of residence	nominal	0.097
highest qualification	nominal	0.092
accommodation/property type*	nominal	0.055
market segment (2 segments)	nominal	0.041
CO_2 emissions	numerical	−0.040
survey year*	numerical	−0.034
country of residence*	nominal	0.032
driver nationality	nominal	0.026
tenancy type	nominal	0.020

Variable category
performance
driver
household
car
location
survey year

Table 2.3: Effect size between annual car mileage and key features of NTS (GB). Effect size is measured with Pearson correlation coefficient r for numerical variables and with correlation ratio η for nominal variables. Features with * are not available in MZMV (CH).

performance.

Geographical and household variables seem to play a minor role, with the exception of the household income, which is however likely correlated with the driver's occupation. Interestingly, *survey year* exhibits a mild negative correlation with the annual mileage reported in NTS, confirming that car mileages have been slowly dropping in recent years.

All numerical variables have also been tested in a "binned" version, to check whether a nominal association can capture patterns hidden to the linear correlation. The only features displaying a significant difference are *driver age* and *engine displacement* since in both cases the annual mileage

picks in the middle of the range and drops on the far ends.

Sampling

The procedure finally features the random sampling of the clustered days (or weeks) until the desired time span is achieved. When the usage of cars is perfectly known as in the NTS case the sampling pool includes the days when the car is not driven. Annual profiles built from randomly sampling NTS weeks would thus automatically include inactive days.
This is not the case for MZMV and other HTSs which do not track the full usage of cars. Distances and activities recorded on driven days (eventually corrected as in Section 2.2.3) can be used but no information is available on actual non-usage of individual cars. The sampling procedure thus employs the mean driving frequency derived in Section 2.2.3. Given the weekly pattern of mobility, the driving frequencies displayed in Fig. 2.6a for every day of the week are specifically used. Therefore, in the sampling procedure a random number is firstly drawn to determine whether the car is used on a specific day; then, if successful, a random daily profile from the corresponding day-of-week and socio-economical group is drawn and added to the concatenated profile.
A further refinement may consider the varying driving frequency between socio-economical categories. The approach employed in Section 2.2.3 to derive Fig. 2.6a cannot be applied in this case, since the national number of cars belonging to a specific socio-economical category is unlikely known and the average car distance $\hat{d}_{\text{car}}$ cannot be estimated with Eq. 2.8. Alternatively, the individual daily driven distances $\hat{d}_{\text{car used}}$ can be compared to the reported annual mileage to estimate the car usage frequency. While this method is weak at an individual level (as suggested by the modest Pearson's r in Table 2.2), it gains robustness when applied to large socio-economical categories. Driving frequencies so obtained can then be crossed with the weekly frequencies of Fig. 2.6a to obtain the specific likelihood of a car belonging to a definite group to be driven on a given day. Tests have shown that this driving frequency refinement can be successfully employed with few socio-economical categories (e.g. up to 5 groups defined by average mileage or working status) but it becomes rather unstable with an increasing number of categories.
Finally, the sampling procedure must take into account the weighting factors reported in the HTSs, so that each entry is drawn with a probability

proportional to its actual frequency in society (as estimated by the national statistical offices).

2.3 Energy module

This second part of the methodology converts the car usage patterns developed in the former section into energy demand profiles. While the car pattern may apply to any powertrain, the following discussion focuses on EVs, comprising both pure battery-electric vehicles (BEV) and plug-in hybrid electric vehicles (PHEV). The derivation of grid electricity demand requires two sequential steps:

1. computation of the specific electricity consumption at the battery outlet of EVs [kWh/km] (Section 2.3.1);

2. modelling the charging strategy of EVs, including energy losses (Section 2.3.2).

These two aspects as well as the car usage behaviour are three separate components which can be modelled and employed independently of one another. This thesis proposes a model for each aspect, but their lean interfaces allow for an easy integration of individual components within alternative frameworks.
Regarding the car energy consumption this work heavily relies on the model developed by Lukas Küng in his dissertation [75]. Section 2.3.1 summarizes the main features used in this thesis and few additional adaptations. The charging behaviour of EVs is developed in Section 2.3.2 with the main focus on plug-and-charge schemes.

2.3.1 Energy consumption

The electricity consumption at the battery outlet per unit distance c_{batt} is computed in [75] based on the physical properties of the car and of the journey performed. The calculation unfolds in the following steps.
Wheel energy demand. First, the specific wheel energy demand c_{wheel} is obtained by integrating the force equation along the velocity and altitude profiles undertaken by the vehicle. This estimation is affected by the car weight, its rolling and aerodynamic resistances, and the detailed slope of

the road. The resulting c_{wheel} accurately captures the wheel energy demand for that specific car usage. Unfortunately this calculation requires a wealth of data often unavailable.

Additionally, in [75] a reduced model to estimate c_{wheel} starting from fewer inputs is provided. In this second approach the force equation is integrated along the Worldwide harmonized Light-duty vehicles Test Cycle (WLTC) Class 3 to obtain a nominal $c_{\text{wheel}}^{\text{WLTC}}$. Only weight and resistances of the car still play a role in this calculation. The real-world c_{wheel} is then obtained by applying two amplification factors based on mean velocity and mean slope of the specific journey [76].

Electricity consumption at the battery. The specific electricity consumption at the battery outlet c_{batt} is obtained from c_{wheel} by accounting for the powertrain efficiency. L. Küng modelled the conversion losses of every powertrain with empirically-derived Willans-lines, which linearly relate the mean wheel energy demand to the mean fuel (or electricity) consumption [6]. Additionally, c_{batt} is affected by the non-propulsive loads due to thermal management of car and other auxiliary loads. In the case of EVs, the power demand from non-propulsive loads is modelled as a function of the mean journey temperature and is directly added to the outputs of the Willans-lines.

The overall procedure returns a car- and journey-specific c_{batt} from the mean temperature, slope and velocity of the journey. Yet, also this information might be not readily available or the involved level of detail might exceed the requirements of the application. Therefore, L. Küng finally provides a lumped real-world factor based on the average temperatures, slopes and velocities observed in MZMV 2015 [76]. This factor embodies the various impacts of actual journeys and can be applied to derive from a car-specific nominal $c_{\text{batt}}^{\text{WLTC}}$ the corresponding car-specific real-world c_{batt}. This lumped real-world factor is found to be 1.28 for both BEVs and PHEVs in charge depleting mode [76].

All three levels of complexity can be coupled with the upstream car usage profiles and the downstream EV-charging model. However, the simplest lumped approach allows to focus on the impact of car properties such as the weight rather than on the actual characteristics of every individual journey. Since the main purposes of this thesis include sizing BEV batteries, it is considered relevant to detail the feedback of the battery weight on the energy consumption. The resolution of the above-derived car usage profiles

in terms of plain distances between stops is thus considered sufficient and no further characterisation of each journey is required. In short, this thesis employs the single factor approach, with the specific electricity consumption c_{batt} obtained from the car-specific $c_{\text{batt}}^{\text{WLTC}}$ and a constant real-world factor of 1.28.

Impact of car weight on energy consumption

Fig. 2.8 shows the specific electricity consumption c_{batt} returned by the model for a BEV with varying battery size and kerb weight[5]. All other car parameters are kept constant and equal to the default values suggested in [6][6].

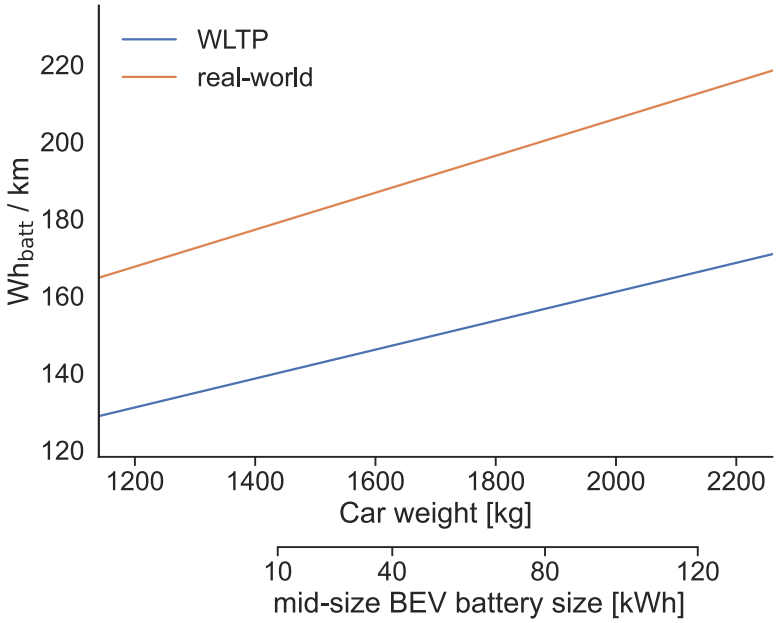

Figure 2.8: Specific electricity consumption c_{batt} at the battery outlet of a BEV with varying weight. For a given vehicle class, different battery sizes entail different weights, hence energy consumptions. Location of bottom x-axis refers to a mid-size BEV pinned at 1628 kg – 40 kWh. Future higher energy densities of EV batteries will shift the bottom x-axis towards the left, with everything else staying constant.

The relationship between weight and battery size depicted on the x-axis is exactly linear and is determined by the following battery properties:

- battery cell energy density: 0.225 $\text{kWh}_{\text{batt}}/\text{kg}_{\text{cell}}$ [6]

[5]Kerb weight defined according to the EU standard, hence including the driver.

[6]These default values are calibrated around the average Swiss vehicle and lie between the compact and mid-size segments.

- battery cell mass share: 0.7 kg_{cell}/kg_{batt} [6]

The reference point used in Fig. 2.8 to pin this relation is a mid-size BEV with 40 kWh and a weight of 1628 kg[7]. Compact or large BEVs would entail a different weight — hence energy consumption — for the same battery size. Depending on the application, the characteristic distribution of vehicles sizes in the fleet can be taken into account and used to accurately model the energy consumption of the fleet. For instance, this is considered in the computation of the charging profiles in Section 3.1.
The relationship between energy consumption and weight also turns out to be approximately linear, with the constant real-world factor proportionally scaling the electricity consumption. Depending on the battery installed, the electricity consumption of the same vehicle model may vary by ±15%.
The above specifications of EV batteries reflect the technological state of the art at the time of writing. However, the increasing sales of EVs and the large investments in battery manufacturing and research are rapidly improving the technical properties of EV batteries. Section A.2 presents an overview of current and future estimates of battery energy densities, with the remarkable growth foreseen in the next decades. This means that the same energy content will be provided by smaller batteries and that BEVs in the same market segment and with the same battery capacity will weigh less. Therefore, while the c_{batt}–kerb weight relation won't be affected by this progress, the c_{batt}–battery capacity relationship will. In other words, future lighter batteries will shift the bottom x-axis on battery sizes of Fig. 2.8 to the left, with everything else staying constant.
There are technological innovations that may directly affect the c_{batt}–kerb weight relation, such as improvements on energy recuperation technologies or the management of non-propulsive loads. However, there is general agreement that battery innovation will be the most dramatic evolution and the key technological enabler to widespread adoption of EVs [77].
The energy consumption values obtained by the model for a given vehicle type and battery size are suitable for forward simulations, where the mobility and charging behaviour of pre-designed BEVs are simulated during one or multiple days (see Section 2.4). If the objective is to design a BEV that can fulfil a certain range, the feedback of the battery weight on the

[7]The estimate comes from applying the "intervention" approach developed in [6] to convert the mid-size average Swiss vehicle to its equivalent BEV. The resulting weight – battery size couple aligns well with the current mid-size BEV market, including VW e-Golf and Tesla Model 3.

BEV consumption has to be taken into account.

Feedback of battery size on EV consumption

The battery capacity E_{batt} that satisfies a range r is:

$$E_{\text{batt}} = \frac{r \cdot c_{\text{batt}}}{DoD} \tag{2.10}$$

where DoD is the depth of discharge, i.e. the usable share of the battery capacity, and is assumed constant at 0.8 [6, 12].
However, Fig. 2.8 shows that E_{batt} through its weight affects the energy consumption c_{batt}. The linear relationship exhibited by the plot can be written as:

$$c_{\text{batt}} = c^0_{\text{batt}} + \left(E_{\text{batt}} - E^0_{\text{batt}}\right) \cdot \frac{\partial c_{\text{batt}}}{\partial E_{\text{batt}}} \tag{2.11}$$

where E^0_{batt} and c^0_{batt} refer to the reference vehicle used to pin the weight – battery size relation.
Combining Eqs. 2.10 and 2.11 provides a general expression to determine the gross battery capacity E_{batt} needed to cover the full distance r without *en-route* charging:

$$E_{\text{batt}} = \frac{c^0_{\text{batt}} - E^0_{\text{batt}} \cdot \frac{\partial c_{\text{batt}}}{\partial E_{\text{batt}}}}{\frac{DoD}{r} - \frac{\partial c_{\text{batt}}}{\partial E_{\text{batt}}}} \tag{2.12}$$

For the mid-size reference BEV used in Fig. 2.8 the key parameters are:

$$\begin{aligned} E^0_{\text{batt}} &= 40 \text{ kWh} \\ c^0_{\text{batt}} &= 188 \text{ Wh/km} \\ \frac{\partial c_{\text{batt}}}{\partial E_{\text{batt}}} &= 0.3046 \ \frac{\text{Wh/km}}{\text{kWh}_{\text{batt}}} \end{aligned}$$

and Eq. 2.12 becomes:

$$E_{\text{batt}}\,[\text{kWh}] = \frac{0.1759}{\frac{0.8}{r[\text{km}]} - 0.3046 \cdot 10^{-3}} \tag{2.13}$$

2.3.2 EV charging

For most applications there is a need to model not only the usage of EVs but also their charging behaviour. This is particularly the case for the

construction of CPs which are employed in Chapter 3 to validate HTS-based EV models. There are two general typologies of charging processes:

- uncontrolled or plug-and-charge, where the EV starts charging as soon as the EV is plugged in to a connector;
- managed or smart charging, where the charging process is externally controlled by user settings, a local utility or a local aggregator to maximise a certain utility function.

On one hand, there are "unlimited" ways to manage the charging process, depending on the application and the point of view of the simulation. The analyses and benefits of different management options are beyond the scope of this thesis. Nevertheless, the EV driving and consumption profiles generated in the previous sections can be integrated in smart charging models to pursue the desired research question. Examples of such applications are presented in Chapter 4. The underlying assumption is that the charging strategy does not affect the driving behaviour. Chapter 3 shows that this assumption seems to hold for uncontrolled charging and smarter schemes might also prove the same: the assurance not to experience mobility disruptions — e.g. finding the BEV battery totally depleted before a trip — is a likely prerequisite for drivers to allow an external operator to control the SOC of their EVs [48].
On the other hand, uncontrolled charging is more uniquely definable. It is mostly a function of the EV's SOC, the availability of charging stations, and the risk propensity of drivers. This makes uncontrolled charging particularly reproducible and the resulting CPs easily comparable. Most of the charging data currently available also comes from plug-and-charge schemes [24, 25, 30, 38, 78]. Uncontrolled charging is thus the most suitable candidate for the validation of HTS-based EV models and its modelling is presented in the following.

Uncontrolled charging modelling

Plug-and-charge events are determined by the availability of charging stations on one side and by the decision to plug in the EV on the other. Charging stations can be modelled with two parameters:

- their density, defined as the probability of finding an available charging point (also called Electric Vehicle Supply Equipment - EVSE)

once the EV gets to a certain location. These probabilities can range from 100% (where it is always possible to charge) to 0% (where there are no connectors).

- the charging rate, i.e. the nominal charging power (kW), of potential EVSEs at each location. This rate should also take into account the limitations of the employed EVs, whose on-board charger may constitute the actual bottle-neck of the charging process.

If a charging stations is available at the parking location, the decision to charge is then up to the driver. For this two criteria are used:

- the stop must last long enough to make the charging seem sensible; i.e. a minimum time threshold is set under which the driver would not plug in the EV. This constraint is appropriate for modelling opportunity charging, where EVs park at their intended destinations regardless of the availability of EVSEs. To model *en-route* fast charging this constraint should be removed, but also the driving routine of EV users would slightly change as a result. For the purpose of the validation, only opportunity charging at the intended destinations is considered and the minimum parking duration threshold is set at 1 hour (values in literature range from 0 to 120 minutes [20, 33, 79]).

- the decision to charge then depends on the SOC of the vehicle. This thesis employs a stochastic method which makes charging more likely, albeit not necessary, for lower SOC. For PHEVs, a random number is sampled from a normal distribution ($X \sim \mathcal{N}(\mu, \sigma)$) and is compared to the SOC of the vehicle; if $\mathrm{SOC}_{\mathrm{PHEV}} < X$ then the driver decides to plug in and charge. A similar decision process applies to BEVs, although the normal distribution is truncated on the lower tail so that fully depleted BEVs are always charged. The difference between the two cases is illustrated in Fig. 2.9. The normal distribution parameters μ, σ are derived from empirical EV demonstrators in the next section.

While these thresholds are conceived and calibrated for uncontrolled situations, they could be regarded as plugging-in decision criteria in smart charging environments, determining whether the EV is actually connected to the grid and can participate in management schemes.

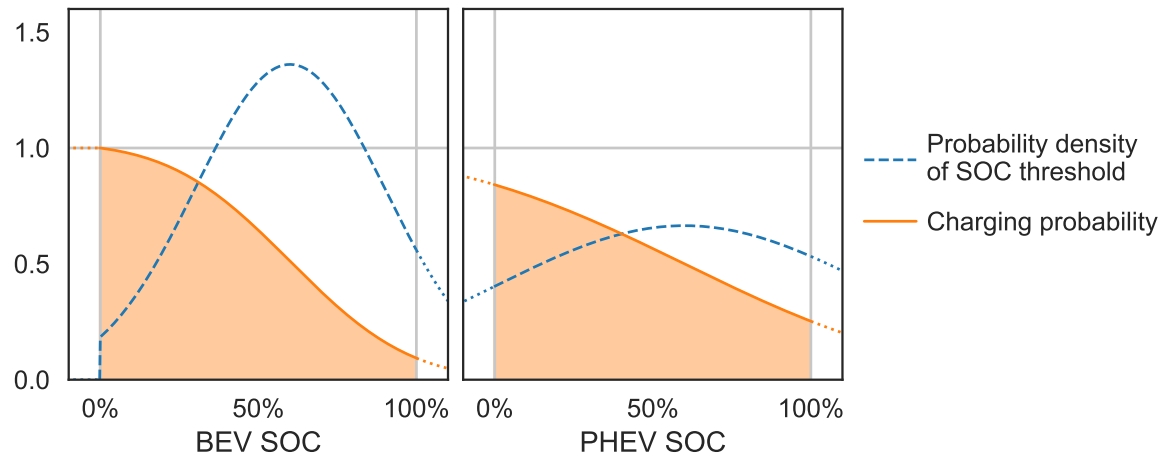

Figure 2.9: With blue dashes, PDFs of sampled SOC during the charging decision process. With orange solid lines, the reverses of the cumulative distribution functions, i.e. survival functions, which represent the probability of charging of an EV reaching the station with a certain SOC. The BEV distribution on the left is truncated on the lower tail so that the survival function starts from 1 and forces drivers to always charge a fully depleted BEV. To the right, the survival function of PHEVs is non-truncated and starts from a fraction of 1, allowing the possibility not to charge even when fully depleted. The examples shown are computed for: $\mathrm{SOC}_{\mathrm{BEV}} \sim \mathcal{N}(0.6, 0.3)$ truncated between $[0, +\infty]$ and $\mathrm{SOC}_{\mathrm{PHEV}} \sim \mathcal{N}(0.6, 0.6)$.

In plug-and-charge situations once the driver decides to plug in the EV the charging process starts immediately at the power rate of the station; the recharge terminates either when the car leaves the place or when the battery is fully charged. Charging losses are modelled according to the empirical Willans-line correlation found in [6]. The energy E_{station} supplied by the station relates to the change in energy content of the battery $\Delta\mathrm{SOC}$ through the following linear equation:

$$E_{\mathrm{station}}\,[\mathrm{kWh}] = 1.1992 \cdot \Delta\mathrm{SOC}\,[\mathrm{kWh}] + 0.1896$$

Finally, pure uncontrolled charging assumes that no criticality is reached neither in the local grid nor on the generation side. If this were not the case, some form of control mechanism would likely occur. The EV demonstrators used for comparison in Chapter 3 always present low EV penetration levels, which are not a threat for existing distribution grids and do not necessitate a control of the charging processes [21, 34, 80].

Charging behaviour calibration

This section provides a detailed procedure to derive from empirical data the normal distribution parameters μ, σ which characterise the charging decision process. The estimates obtained from different EV trials compare favourably with each other, providing credibility to the methodology and results here proposed. The same procedure can in principle apply to both BEVs and PHEVs, but BEVs are first addressed since PHEVs require additional considerations.

BEV. The charging probability survival function can be derived with Algorithm 2 and the graphical aid of Fig. 2.10. Provided the access to the PDF of SOC before a charging event (line 1) and the PDF of SOC at any charging opportunity (line 2), the charging probability function can be obtained as the ratio between the two PDFs (line 4). The ratio is then normalised to the peak (line 5) and set to 1 for all low SOCs (line 6) since the maximum charging probability for a BEV is 100% and occurs at low SOCs. The resulting function resembles an S curve, which can be parametrised by fitting the survival function of a truncated normal distribution (lines 7, 8).

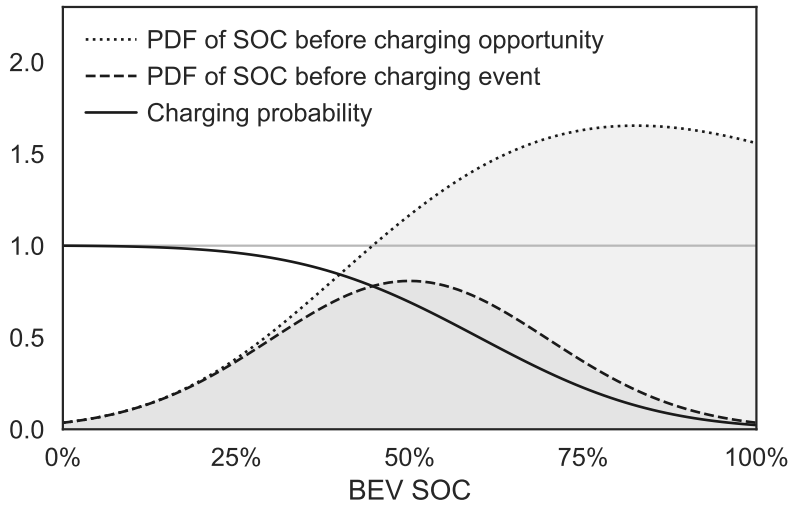

Figure 2.10: Relation between characteristic PDFs and charging behaviour. The probability of charging at a given SOC (solid line) is the ratio between the times the BEV is plugged in starting from that SOC (dashed line) and all the times the BEV has a charging opportunity at that SOC (dotted line). The PDF of the latter is rescaled in the figure to better visualise the ratio between the two SOC curves: thus its area is lower than 1.

The procedure is short, but the two input PDFs require fully detailed records of SOCs at every charger-equipped stop, with or without a sub-

Algorithm 2 Estimation of charging probability function from characteristic PDFs of SOC.

1: get empirical PDF of SOC before charge, c
2: get [empirical] PDF of SOC at charging opportunity (if unavailable, at any stop), s
3: smooth c by fitting a normal PDF
4: get charging probability $p = c/s$
5: normalise $p = p/\max(p)$
6: set p for $\mathrm{SOC} < \mathrm{SOC}_{\max(p)} = 1$
7: fit p with survival function of truncated normal distribution
8: get μ, σ of resulting truncated normal distribution

sequent charge. While a simulation can provide this full insight, physical trials may lack some information. The majority of EV trials only reports the PDF of SOC at the beginning of a charge [42, 70, 81, 82]. The closest examples in literature come from 2 Danish demonstrators carried out in the framework of the Green eMotion project [83]. The report on consumers' use of EVs [84] publishes, for the demo regions DK1 and DK2, both the PDFs of SOC before charge and the PDFs of SOC after a trip event, i.e. at any stop. The latter may differ from the SOC PDF at any charging opportunity, hence affecting the estimation of the charging threshold. In addition, demo region DK2 involves a captive fleet composed by only 4 BEVs, while demo region DK1 employs 10 BEVs whose use case is unknown. The resulting estimates of charging behaviour are thus approximative and may not properly reflect the attitude of private BEV users. The parameters obtained when applying Algorithm 2 to these trials are indicated with □ in Fig. 2.11 and average $\mu = 0.69,\ \sigma = 0.15$.

Algorithm 3 Iterative approach to derive charging behaviour function from EV simulations.

1: set $\mu_{\mathrm{in}} = 0.69,\ \sigma_{\mathrm{in}} = 0.15$
2: **for** i **in** [1 : N] **do**
3: run EV simulation with inputs $\mu_{\mathrm{in}},\ \sigma_{\mathrm{in}}$
4: extract PDF of SOC at charging opportunity s
5: run **Algorithm 2** to get $\mu_{\mathrm{out}},\ \sigma_{\mathrm{out}}$
6: set $\mu_{\mathrm{in}} = \mu_{\mathrm{out}},\ \sigma_{\mathrm{in}} = \sigma_{\mathrm{out}}$
7: **end for**

To refine the estimation some of the trials introduced in Section 3.1.1

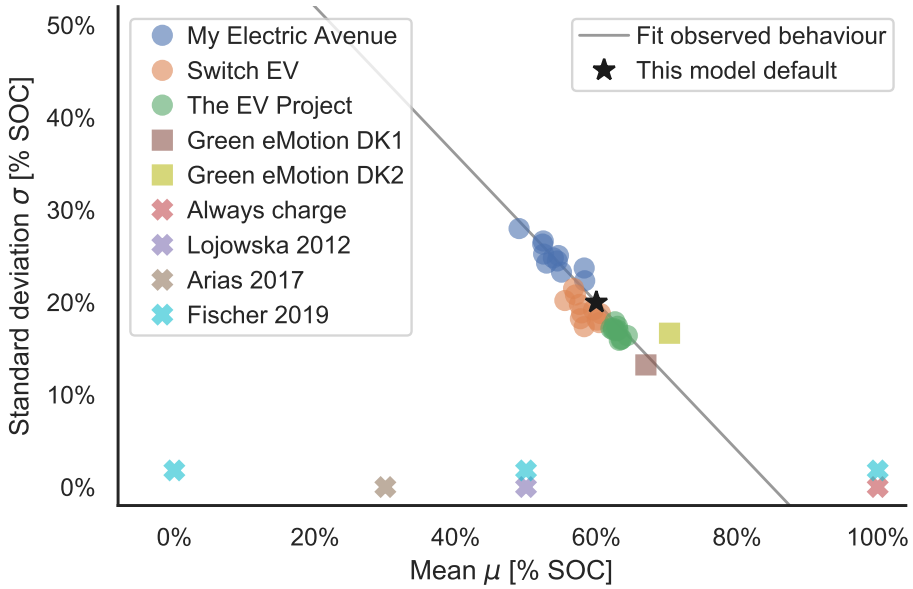

Figure 2.11: Mean μ and standard deviation σ of the threshold SOC below which drivers connect their BEVs to the charger: approximations used in literature ($\times$) and obtained from the trials via Algorithms 2 and 3 ($\bigcirc$, $\square$). The weighted average of the trials thresholds is chosen as default behaviour ($\bigstar$).

are employed[8]. These demonstrators tracked the SOC before a charging event [70, 81, 82], but not at every charging opportunity[9]. However, the latter information can be extracted from a simulation of those trials. The details involved in the numerical reproduction of the EV trails are discussed in Section 3.1.1. The only missing input to the simulation of the trials would be the charging behaviour itself. The μ, σ parameters are thus initiated with the Green eMotion estimates and then Algorithm 2 is applied iteratively. The overall procedure is summarised in Algorithm 3.

After the first three iterations, the behavioural parameters for each trial start converging towards similar values. The resulting μ and σ for every iteration of each trial are shown with $\bigcirc$ in Fig. 2.11. The three simulated EV trials exhibit lower charging thresholds than the Green eMotion

[8] Although the same trials are used for the calibration of charging behaviour and the validation of CPs, the overall methodology does not become a self-fulfilling process. The information exchanged in the two phases is entirely different: the calibration of charging behaviour employs the PDF of SOC before charging events; the validation uses the measured charging loads. The two quantities are linked, but would not be derivable from one another without a fully functional simulation model. Notably, CPs require timing information that is missing from the PDF of SOC. Moreover, during the modelling the PDF of SOC is reduced to a simple probability function before being used in the simulations. Nevertheless, the link between charging behaviours and CPs of each trial is visible in the sensitivity analyses of Section 3.1.4, where adjusting μ and σ towards the trial-specific values leads to better fitting CPs.

[9] The "Pecan Street" project does not provide information regarding the before-charge SOC PDF either and could not be employed for the charging behaviour estimation.

demonstrators (lower μ). The trials also predictably show more variable behaviour (higher σ) since they involve private mobility, in contrast to the captive fleets used in DK2 and probably in DK1. Overall, the 5 demonstrators exhibit a linear trend between μ and σ, where lower mean thresholds correspond to more scattered behaviours. This joint shift of μ and σ indicates that the trials present more similar charging probabilities for loaded batteries than for depleted ones. Fig. A.4 in the appendix confirms this impression, as it shows that the S-curved charging probabilities of the different trials look more alike at high SOCs. This pattern may be due to the different attitudes of people towards range anxiety, attitudes that emerge especially for lower SOCs. Moreover, BEVs are more likely to stop with a high SOC (trend of the dotted line in Fig. 2.10): this imbalance in the amount of information between low and high SOCs can cause the higher spread of charging probabilities for low SOCs. This empirical correlation between μ and σ is exploited in the sensitivity analysis in Section 3.1.4 (see Fig. 3.6).

Fig. 2.11 also includes examples of BEV charging behaviours used in literature. All studies that employ a fixed charging threshold essentially assume no behavioural variability, i.e. $\sigma = 0$. On the other hand, a purely random charging threshold would entail $\sigma \to +\infty$ (out of scale in Fig. 2.11). While the results of this methodology still manifest a little volatility, these also prove that the introduced behavioural model can capture the charging attitude of BEV drivers from different contexts and that their behaviours converge towards similar values. A weighted average that considers the higher trustworthiness of the simulated EV trials returns:

$$\mu_{\text{BEV}} = 0.6 \quad \sigma_{\text{BEV}} = 0.2$$

These two values, depicted with ★ in Fig. 2.11, are set as default BEV charging behaviour for forward simulations aimed at building CPs, including the validations of all trials in Chapter 3.

It is possible that future charging behaviour will differ from the ones observed in the trials of Fig. 2.11. Two phenomena are likely to occur: BEV will have larger batteries and drivers will have higher confidence about the charging network and the range of their BEVs. The latter effect will probably lead to a "rationalization" of charging decisions, leading simultaneously to lower μ and lower σ. The impact of larger BEV batteries is harder to predict: if drivers react by maintain the same safety margin as

of today (e.g. 5 kWh) the average charge will occur at lower relative SOC, i.e. μ will drop; if drivers react by keeping a regular charging schedule at the end of their trips (e.g. when returning home after work) the average charge will occur at higher relative SOC, i.e. μ will increase.

PHEV. Charging behaviour of PHEVs could be estimated in a similar way, but their hybrid operation introduces an additional degree of freedom. Specifically, steps 5 and 6 of Algorithm 2 assume that a BEV driver would always charge for depleted batteries; this does not hold true for PHEV users, who can drive on liquid fuels after depletion of the battery. In other words, while BEVs owners necessarily charge all the electricity they consume, PHEVs drivers may indefinitely postpone charging while relying on conventional propulsion. This additional degree of freedom can be fixed by considering the utility factor (UF) of PHEVs or their average number of recharges per day. However, the complexity of the resulting procedure and the shortage of SOC distributions for PHEVs induce to the provisional adoption of the same behavioural parameters as BEVs, hence:

$$\mu_{\text{PHEV}} = 0.6 \quad \sigma_{\text{PHEV}} = 0.2$$

These parameters are not supported by empirical evidence and serve mostly to simulate PHEV charging behaviour in the few EV trials of Chapter 3 that have PHEVs in their fleets. This assumption is acceptable mostly because those PHEVs have battery capacities comparable to the BEVs used in the calibration of charging behaviour (see Table 3.1).

SOC initialisation

A common issue faced when modelling EV usage is the initialisation of SOC at the beginning of the simulation. The chosen SOCs artificially affect the charging behaviour of the first simulation days. If the overall simulation covers a long time span (more than 10 days[10]) the impact of SOC initialisation is inconsequential. But for shorter simulations countermeasures must be taken.

Particularly critical is the conservation of energy, meaning that the total energy stored in batteries at the beginning and at the end of the simula-

[10]The sensitivity analysis in Section 3.1.4 shows that 4 random simulation days are enough to mitigate the SOC initialisation bias. If a week is to be simulated, starting 3 days before the beginning of the week is enough to ensure undisturbed charging behaviour from the first day of the week.

tion should be comparable, otherwise the detected charging loads do not account for all the electricity consumed by EVs. Researchers in [20] resolve this issue by imposing the same SOC at the beginning and at the end of the simulated day, but this strongly constrains the model.
The simplest alternative is the simulation of few auxiliary days before the actual start of the simulation [29, 32, 38]. In section 3.1 this technique is employed to simulate a single mobility day; the subsequent sensitivity analysis shows that three preceding auxiliary days are sufficient to remove the SOC initialisation bias.

2.4 Overarching simulation

The models presented in the previous sections can be combined to simulate various EV situations and to answer different research questions. The typical application in this thesis is to perform *forward* (or exploratory) simulations as depicted in Fig. 2.12.

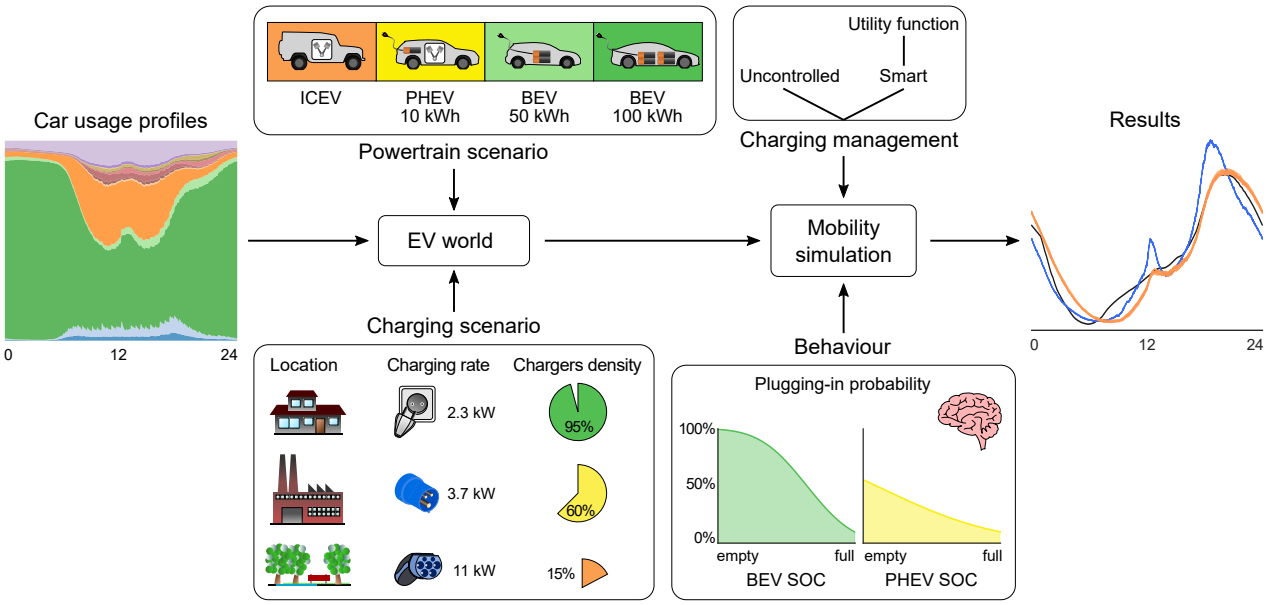

Figure 2.12: Combination of the technological and behavioural models to perform forward EV simulations. The design of EVs and charging stations is fixed and descriptive information on their usage and interaction (such as CPs) can be extracted. The numbers in the boxes are just provided as examples.

The car usage profiles derived in Section 2.2 are applied to an "EV world" where cars are mostly electric and locations offer the possibility to charge EVs. The fleet can be composed of different vehicles types and powertrains

and the collective specifications form the *powertrain scenario*. Parking locations can be equipped at a varying degree (density) with charging connectors with different power rates and the collective assumptions constitute the *charging scenario*.
Then one or multiple mobility days can be simulated taking into account charging management schemes and the plugging-in propensity of EV drivers. The results extractable from forward simulations are descriptive and illustrate what happens in the system: the share of BEVs which can fulfil the assigned mobility demand (Section 4.1), the UF of PHEVs, the electric load borne by certain locations (Section 3.1), etc.
The same individual models can be employed for *backward* (or normative) simulations, where a certain result or performance indicator is fixed and the powertrain or charging setups that can achieve that result are sought. This approach can serve to size the batteries required to fulfil a certain share of mobility demand or to quantify the need for *en-route* charging.

Chapter 3

Validation

This chapter presents a validation of the two most innovative features of the proposed methodology. On one side the reliability of traditional HTSs to describe the micro-mobility of EVs is questioned. Section 3.1 thus presents a comparison of the hourly charging loads derived from the constructed model against the empirical loads measured in four different EV trials. Section 3.2 then compares the annual mileage distributions obtained with different clustering and sampling criteria against the distributions observed in reality.

3.1 Uncontrolled charging loads

This validation used the simulation framework of Fig. 2.12 in a forward fashion: all parameters settings are fixed, the simulation is run and the charging profile are a-posteriori extracted and compared to the empirical loads. This investigations unfolds in the following steps:

- section 3.1.1 introduces the real-world trials that form the basis of the subsequent investigations;
- section 3.1.2 presents few methodological adaptations specific to the trials to be simulated;
- section 3.1.3 performs a qualitative comparison between the simulated and the empirical CPs;
- section 3.1.4 finally provides a quantitative sensitivity analysis of the model's parameters.

3.1.1 EV trials

Four public EV trials are used for the validation:

- The "My Electric Avenue" Project (UK, 2013-15) [43, 25];
- The North East's "Switch EV" electric vehicle trial (UK, 2010-15) [85, 81];
- "The EV Project" from Nashville region (US, 2011-13) [86];
- The "Pecan Street" Smart Grid Demonstration Project (US, 2011-13) [24].

The My Electric Avenue and Pecan Street trials have been chosen since they constitute the bases for the few validation attempts found in literature [24, 25]. The EV Project and Switch EV trials are included because they report CPs by different location type (home, workplace, etc.) and can be used for a finer and disaggregated validation of the model.
The original trial conditions are recreated in the simulation by solely operating on the charging and powertrain scenarios of Fig. 2.12; all other model settings are kept constant between trials. Table 3.1 summarises the original trial information used to set up the simulation and the resulting parameters settings. However, all the trials represent open systems, where tracked EVs may charge at untracked charging points and vice versa. This lack of control on the investigated system is one of the main reasons that discourage researchers from pursuing this kind of validations. Nevertheless, important conclusions can still be drawn even with these uncertainties.
In order to have access to fully post-processed analyses, only trials that had published their results before this thesis' evaluations could be considered. This is why all introduced demonstrators were carried out before 2016. This explains the rather small EV batteries and low charging rates that characterise all trials. The proposed validation strictly applies only to the tested conditions and the gathered insights may not apply to situations with larger batteries or faster chargers. Nevertheless, the proposed analysis offers a first assessments of HTS employment for the development of CPs and establishes a methodology to perform further analyses with more up-to-date specifications. In addition, primary focus of these analyses is opportunity charging at home or workplace, where longer parking times are likely to make faster charging rates unnecessary for their cost.

	Trial EV fleet	Powertrain scenario
My Electric Avenue [25]	221 Nissan Leaf with 24 kWh battery	100% BEVs with 25 kWh battery
Switch EV [87]	15 Nissan Leaf with 24 kWh battery 20 Peugeot iOn with 16 kWh battery 9 other	43% BEVs with 25 kWh battery 57% BEVs with 18 kWh battery
The EV Project [88]	656 Nissan Leaf with 24 kWh battery 54 Chevrolet Volt with 16 kWh battery	93.5% BEVs with 25 kWh battery 6.5% PHEVs with 13 kWh battery
Pecan Street [24]	8 BEVs 25 PHEVs (primarily Chevrolet Volt)	30% BEVs with 25 kWh battery 70% PHEVs with 13 kWh battery

	Trial charging outlets installed	Charging scenario[0]
My Electric Avenue [25, 70]	88 home charging outlets at 3.6 kW 13 work charging outlets at 3.6 kW	100% stations at home at 3.6 kW 43% stations at work at 3.6 kW 0% stations anywhere else
Switch EV [78, 80, 81]	91 home charging outlets at 2 kW 268 public/work charging outlets at 2 kW 8 public/work charging outlets at 50 kW	100% stations at home at 2 kW 83% stations anywhere else at 2 kW
The EV Project [69, 89, 90]	596 home charging outlets at 3.76 kW 241 public charging outlets at 3.76 kW	100% stations at home at 3.76 kW 11% stations anywhere else at 3.76 kW
Pecan Street [24]	monitored home charging outlets at 3.3 kW limited work/public charging infrastructure	100% stations at home at 3.3 kW 0% stations anywhere else

Table 3.1: Configuration settings of EV trials.

[0]The percentages refer to the charging stations densities at each location and the sum may exceed 100%. The densities take into account the relative frequency of different locations in the MZMV (home:work:non-home = 1:0.35:1.42) and are adjusted in order to obtain the same station shares as in the trial. For public stations, 2.58 charging outlets per charging site are assumed [91, 92].

The gradual introduction of faster chargers plays a crucial role in the deployment and utilisation of fast *en-route* charging stations during long trips, but it has smaller influence on everyday mobility, which combined covers the most kilometres and hence constitutes the bulk of CPs.

3.1.2 Methodological adaptations

The trials involve mixed powertrain fleets characterised by rather small batteries. The model has been thus adapted in order to accommodate mixed fleets and to remove unlikely driving profiles. Fig. 3.1 shows how this is accomplished during the execution of the simulation.

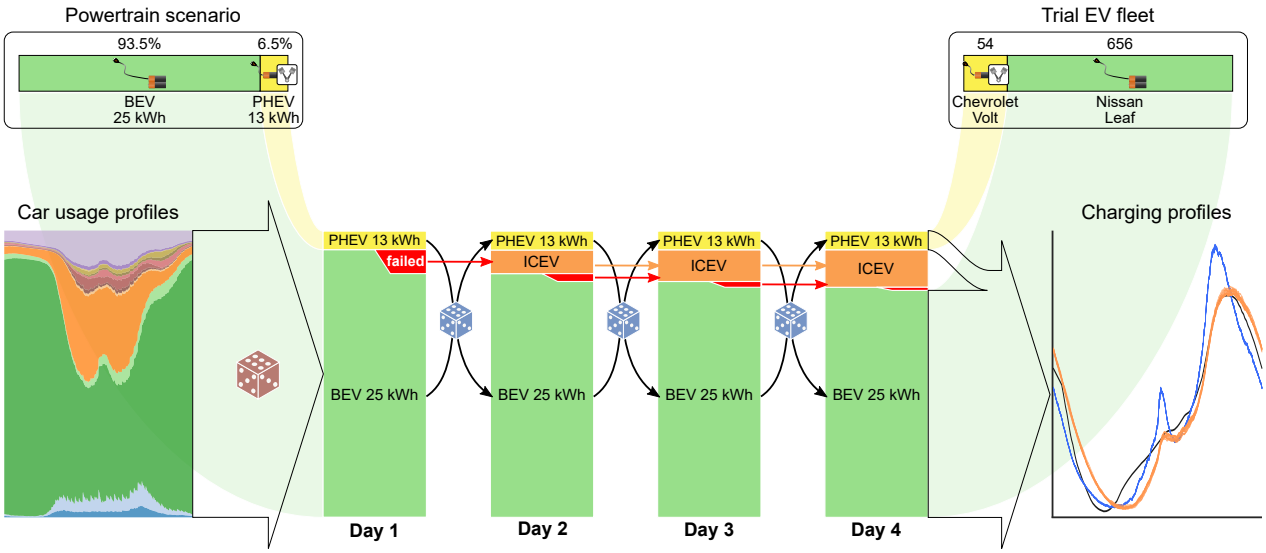

Figure 3.1: Evolution of the powertrain mix from the input powertrain scenario to the final distribution which is post-processed. The example shown results from the simulation of The EV Project with default settings. The two types of random assignments are marked by dice: the initial allocation in copper, and the iterative shuffling in cerulean.

Since all EV trials report only average CPs, there is no need for a dedicated construction of multi-day profiles. The single-day profiles available in MZMV are directly used as mobility basis in order to give a more general applicability to the validation, since the weekly profiles from NTS are rather an exception.

Firstly, the powertrains are randomly assigned to daily trips in proportion to the shares specified in the powertrain scenario in Table 3.1. The first simulation day starts with all EVs (BEVs and PHEVs) fully charged. At the end of the first day (**Day 1**) all trips that could not be completed with BEVs due to the limited range are removed from the EV simulation

and are virtually assigned an ICEV for the next days. All completed trips are instead assigned a new successful {powertrain, SOC_{end}} pair from the previous day: since the two sets have the same length this allocation is a purely random sampling without replacement. A new mobility day is then simulated and the whole process is repeated two more times. The fourth simulated day (**Day 4**) is finally used for evaluation and analyses.
This process allows on one side to erase the SOC initialisation bias and on the other to robustly remove all trips which might be unfeasible or implausible considering BEV ranges, charging behaviour, and morning SOC.
The last simulation day is used for analyses and validation, but the powertrain mix on that day differs from the powertrain scenario due to all BEVs that have been removed by the above selective algorithm. The powertrain scenario should thus overestimate the BEV share compared to the target EV trial if the last day is supposed to emulate the demonstrator's fleet. This explains the slightly larger BEVs shares in the powertrain scenarios of Table 3.1 with respect to the trial EV fleets.

3.1.3 Qualitative comparison

This section presents for each trial the CPs obtained from the model, the reference CPs observed in the field and, whenever possible, other simulated CPs from literature. For each trial the y-axis unit indicating the load "magnitude" follows the unit used to report the reference empirical CP. Unfortunately, the 4 EV demonstrators publish their CPs in different units (e.g. in kW or dimensionless) meaning that comparisons *between* trials cannot be confidently made. The following discussion provides also suggestions on the most adequate units to present numerical and empirical CPs as a guideline for future research. CPs from multiple simulation runs are shown so that the randomness built in the model can be appreciated.
My Electric Avenue (UK). Fig. 3.2 shows the CPs for the My Electric Avenue demonstrator. Both reference profiles come from [25] with the numerical CP obtained through Gaussian mixture models (GMM). The reference profiles are reported in absolute power demand [kW] per EV, but a deeper analysis of the original study suggests that EVs not charging during a day are neglected from the analysis[1]. Therefore, all CPs plotted

[1] [25] does not report any non-charging EV in Fig. 1 and states that monitored EVs on average consumed 12.63 kWh/day: this translates to about 60 km/day, that is almost twice the average daily mileage of cars in England (see Table 2.1 and [93]).

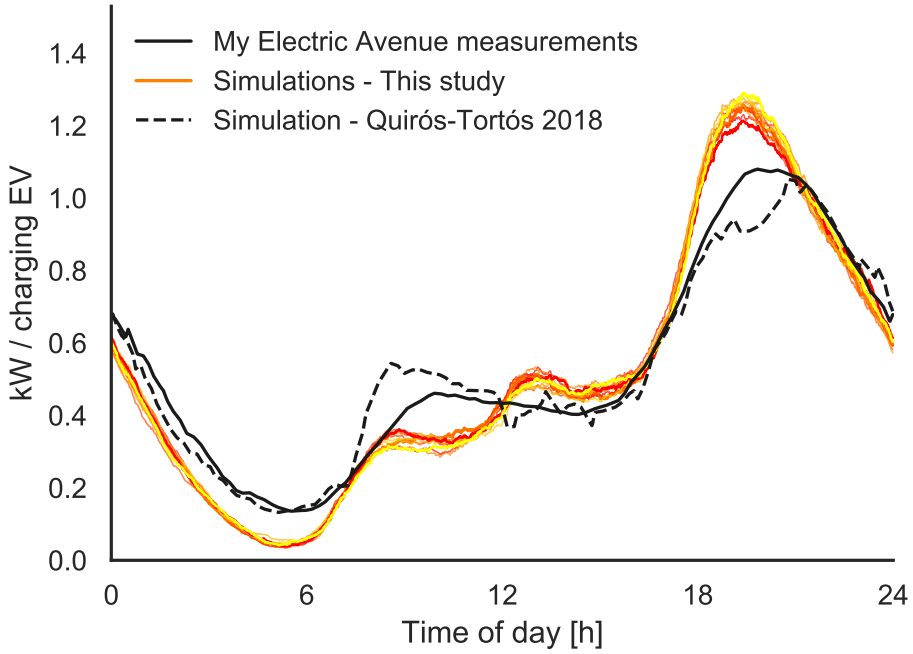

Figure 3.2: CPs for the My Electric Avenue trial. The CPs represent the average power demand on a weekday for an EV that charges at least once.

in Fig. 3.2 represent the average power demand for a *charging* EV, i.e. an EV that charges at least once during the day. All CPs are restricted to working days (Monday–Friday), but may originate at any location (in the default case, at home and workplace).

The CPs resulting from the proposed methodology slightly overshoot the reference peak load, but they capture the general trend during the day. The accuracy of these MZMV-based CPs is notably comparable to the numerical CPs proposed by [25], which are however based on tracking data of the same EVs that generated the empirical profiles. The local maximum around 1 p.m. is caused by Swiss residents returning home for lunch break or working part-time in the mornings (see Fig. 2.4). This can be explained by the higher share of part-time workers in Switzerland compared to most countries [94].

The stochasticity built in the model generates a multitude of slightly different CPs, which are depicted with various shades of orange in Fig. 3.2. The gradual transition from red to yellow in the evening peak has opposite direction compared to the morning local maximum (∼8 a.m.), revealing that charging more at work helps to relieve the peak load at home (case of the red CP). The tendency of the colours actually suggests that the density of station at workplaces has been underestimated in the simulation

and this illustrates the difficulty in translating the trials conditions into the model. The consequent overestimation of the peak load may impact the design of a local distribution grid with many EVs, but only if the total electricity demand (including non-EV applications) is also increased.

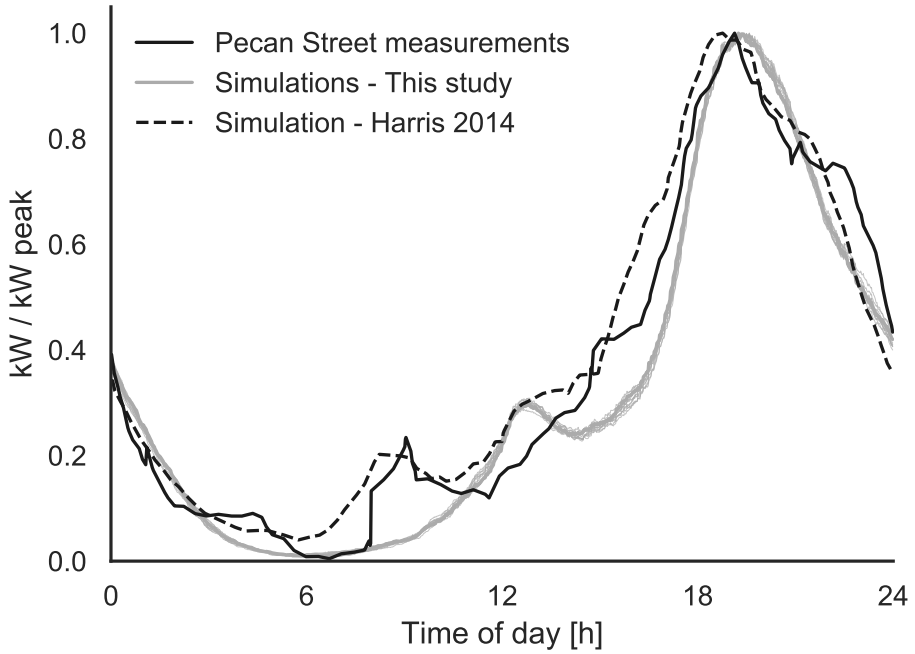

Figure 3.3: CPs for the Pecan Street trial. The CPs represent the normalised power demand on a weekday for an EV charging at home.

Pecan Street (US). Fig. 3.3 presents the CPs for the Pecan Street project. Also for this example both an empirical and a numerical reference CP are available from [24]. All CPs consider only working days and home chargers. The authors of [24] propose a validation based on CPs normalised to the peak. The result is that all CPs follow a close pattern and distinguishing accurate simulations from deficient ones becomes a harder task. The CPs here derived exhibit a local maximum at noon, which is also mildly shown by the numerical profile of [24], but fail to capture the morning peak exhibited by both reference CPs. The empirical profile especially manifests a sharp increase around 8 a.m., which is quite unexpected from home chargers and may be due to some sort of control strategy. Such phenomena cannot be recreated with plain plug-and-charge strategies, but this small mismatch is not relevant for the goal of the validation. Finally, the CP variability of the stochastic model is also reduced by the normalisation process.

Switch EV (UK). Fig. 3.4 displays the CPs for the Switch EV trial for

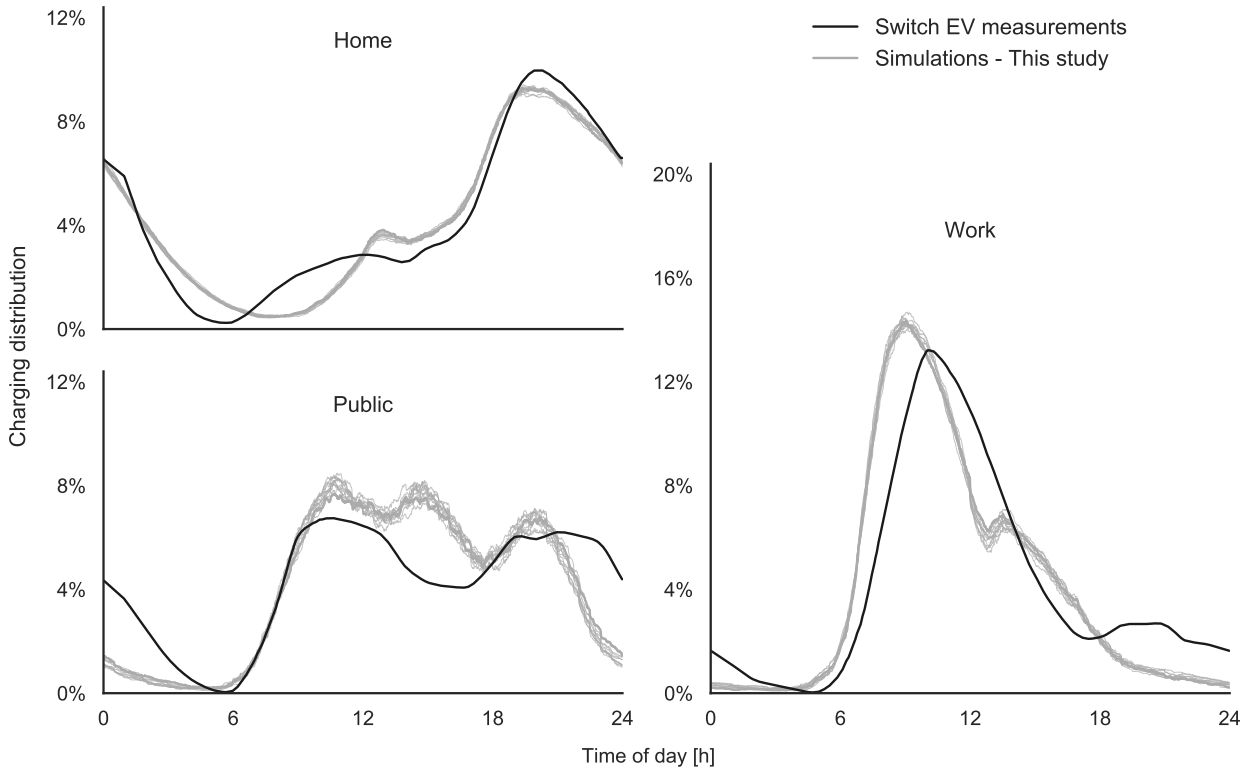

Figure 3.4: CPs for the Switch EV trial at three different locations. All profiles are normalised by total daily energy and they thus represent the probability of charging at each hour. All CPs apply to an average day of the week.

three different charging locations: home, workplace and public spaces. The empirical EV trials come from [78] and represent the charging distribution during an average day, i.e. the probability that a car is being charged at any hour. In other words, all CPs are normalised to the area beneath the curves. Since MZMV deals mostly with individual mobility, the empirical CPs triggered by individual users of the Switch EV trial are adopted for the validation (Fig. 6–8 in [78]).

The comparison shows that the presented model manages to replicate all empirical CPs, capturing the specific charging features of each location. Home charging manifests the usual evening peak load already seen in My Electric Avenue and Pecan Street trials. Switch EV's peak is however smoother since the less synchronised weekend patterns are also included. On the other hand, work charging shows the highest *relative* peak load due to the high simultaneity characterising morning commuters. Finally, public chargers exhibit rather steady behaviour during all active hours. Overall, the CPs generated by the present model slightly miss the reference peak

loads, but the normalisation of the profiles impedes further evaluations. Public CPs from the model manifest the biggest gaps from the reference profile, especially during the night (9 p.m.–5 a.m.), but the higher noise displayed also indicates the larger uncertainty surrounding this estimate. In addition, starting from 11 p.m. the reference public CP displays a slow night decay which resembles the domestic CP. This observation matches the findings of [78] that some Switch EV participants had used public stations also for night charging.

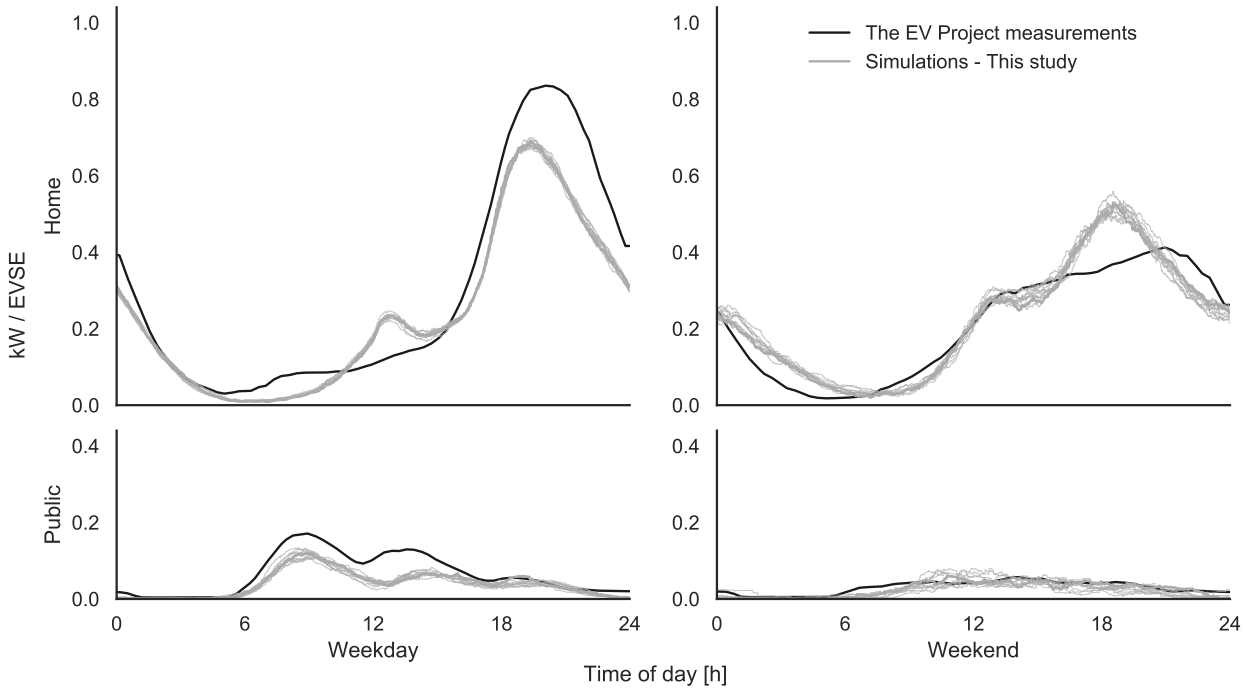

Figure 3.5: CPs for The EV Project. All profiles illustrate the average daily power supplied by a single EVSE (i.e. charging unit). Top plots refer to private home chargers, while bottom ones to publicly accessible EVSEs (both at work or other locations). The left CPs apply to working days and the right ones to the weekend.

The EV Project (US). Fig. 3.5 shows the CPs from The EV Project for private homes and public spaces, while also differentiating weekdays from weekends [88][2]. CPs are presented in terms of average power demand per charging unit[3].

Public charging stations are more rarely used than domestic ones, and

[2]The EV Project involved many American cities and states; the profiles here used come from the 2013 results from the Nashville region.

[3]The empirical CPs are available from [88] as aggregated electricity demand through all charging stations of the same type; with the number of charging units, i.e. EVSE, by type of Table 3.1 the average empirical CP per charging unit could be derived.

their average power demand is significantly smaller. This is confirmed by the lower utilisation rate of public charging units compared to residential ones reported in [69]. The simulated CPs reflect the general trends of the reference profiles, although some differences exist. The peak loads at residential EVSEs are particularly divergent, but the differences have opposite sign on weekdays and weekends, signalling that these are not due to a calibration error. Comparing the American HTSs [95] to MZMV reveals that Swiss residents tend to drive shorter distances than Americans on weekdays, but longer ones at weekends, as foreseeable from Fig. 2.6a. This means that daily electricity demand of Swiss EVs is lower (and higher) than American EVs on weekdays (on weekends). This fully explains the opposite shifts observed for home charging, but also reveals the importance of checking the comparability of different data sources before attempting a validation. The investigations in [22, 23] endorse the comparability between European countries, but this last comparison suggests that the same may not hold true for combinations of more diverse regions.

The numerically simulated public CPs for weekdays nicely manifest the same three local maxima as the reference CP, while the net scaling mismatch points to a possible calibration error. As already mentioned, the adjustment of the charging station density in public spaces is particularly difficult for open systems like EV trials. Finally, the simulated public CPs for the weekend match reasonably well the empirical profile from The EV Project.

Summary

Overall, the qualitative validation is satisfactory as the general charging trends in distinct locations and days are always well captured by the model. Small differences arise, but they can mostly be explained by the usage of different datasets or cumbersome reporting units.

3.1.4 Sensitivity analysis

This section explores how the simulation responds to changes in the input parameters and how a departure from the trial conditions negatively impacts the performance of the model.

Metrics and nomenclature

To quantify both the magnitude of model adjustments and the discrepancy from the empirical profiles, the coefficient of determination R^2 is employed. R^2 assesses the accuracy of the numerical CP during the whole day while still penalising a potential vertical mismatch in peak load.
Two types of parametric analyses are performed for each EV trial:

- a raw sensitivity analysis, where any quantitative input is adjusted by $\pm 10\%$;
- a set of exploratory scenarios, where particularly uncertain or evolving parameters are modified more considerably.

The former helps to identify which parameters influence the output the most while the latter investigates quantities characterised by higher uncertainty. For instance, vehicles energy consumption is slowly and measurably improving, but the density of public stations is rarely well-known and is evolving quickly in many countries [8].
The newly introduced charging behaviour is particularly uncharted and deserves a deeper analysis. Fig. 3.6 summarises all explored scenarios in terms of mean μ and standard deviation σ of the Gaussian SOC threshold. In the raw sensitivity μ and σ are individually adjusted by $\pm 10\%$. For the exploratory scenarios the linear behavioural pattern observed in Fig. 2.11 is utilised. Specifically, a distinction is made between an "empirical behaviour" that fits the thresholds observed in the trials, and an "alternative behaviour" opposed to it. Conceptually, the empirical behaviour assumes that charging at high SOCs is well understood (as observed in the trials) and it spans the possible charging attitudes at low SOCs. On the other hand, the alternative behaviour assumes good agreement for low SOCs (which was not observed in the trials) and explores different charging reactions at high SOCs. For each trend four diffrent points are tested (1–4 with empirical behaviour, A–D with alternative behaviour). The case where EV drivers always charge regardless of the SOC is also included. The specific charging probabilities for all these scenarios are presented in detail in Section A.3.2.
Fig. 3.7 and 3.9 show the R^2 results for both parametric analyses for all trials. The red bars and lines indicate the scores of the default simulation settings, while all other colours refer to a change in a single input setting

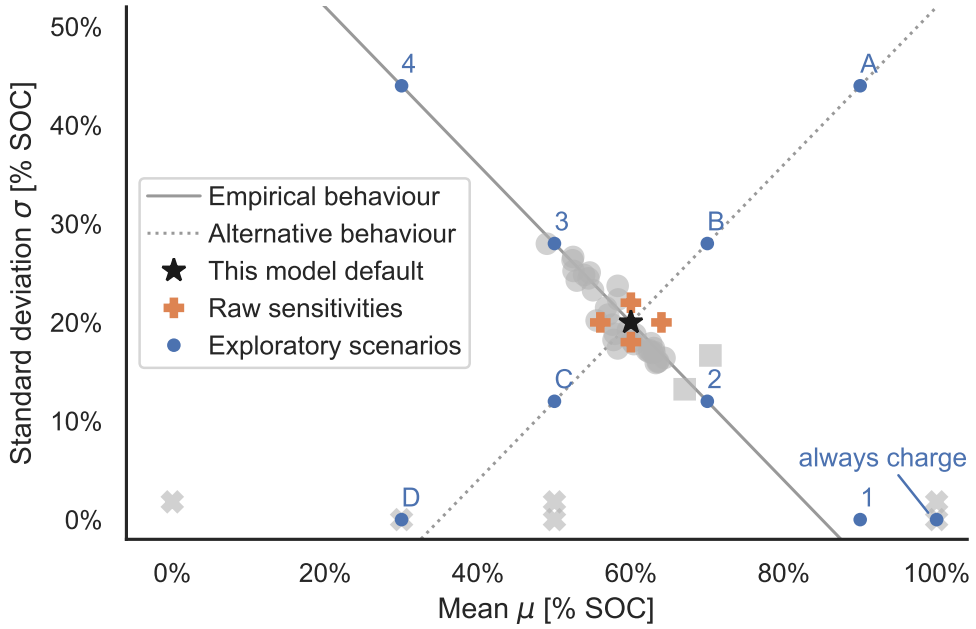

Figure 3.6: Mean μ and standard deviation σ of the tested charging thresholds: default case (★), variations of the single parameters by ±10% (✚) and exploratory scenarios (•). These scenarios are either based on the observed behaviour (points 1–4 on the solid line) or on a hypothetical alternative behaviour antithetical to the former (points A–D on the dotted line). The "always charge" scenario is also tested. The points' labels link the sensitivities in Fig. 3.7 and 3.9 to the different behaviours. The grey background depicts the thresholds observed in trials or used in literature introduced in Fig. 2.11. More details are available in Section A.3.2

at a time. The grey bars depict the R^2 scores of previous validation attempts available in literature. Since The EV Project and the Switch EV demonstrator comprise CPs computed at different locations, their final R^2 coefficient is computed as a weighted average of the single scores at each location[4].

Results of the sensitivity analysis

My Electric Avenue & The EV Project. Fig. 3.7 presents the R^2 results for the My Electric Avenue and The EV Project trials as both are tested on CPs expressed in absolute power. In both demonstrators the CPs produced with the default settings rank among the best cases, meaning that an uncalibrated setup already allows for a very accurate reproduction of the empirical profiles. The raw sensitivities only marginally impact the

[4]The number of charging events per location detected during the trials is used as weighting factor [69, 78].

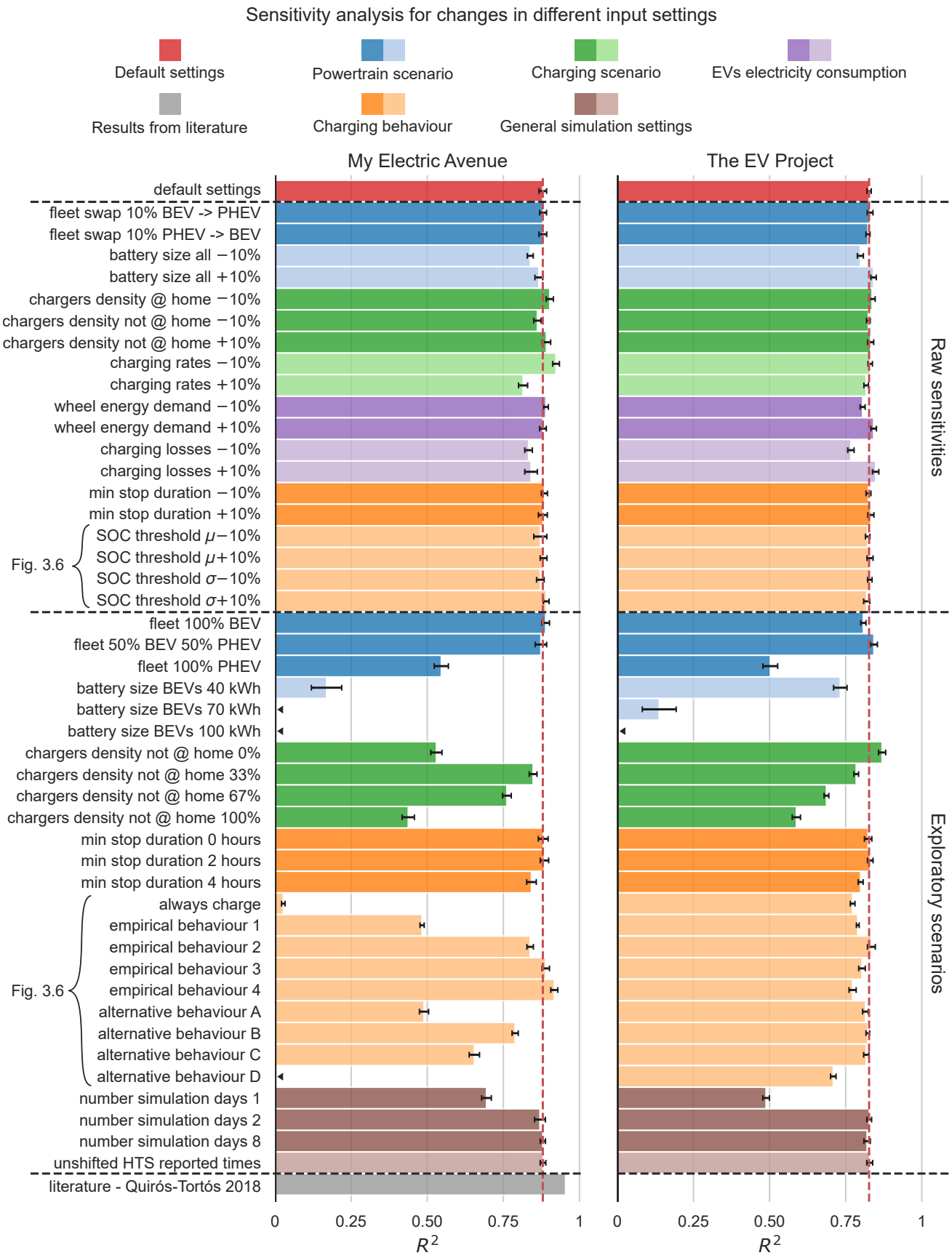

Figure 3.7: Sensitivity analyses for the simulations of My Electric Avenue and The EV Project trials. The bars use the coefficient of determination R^2 to show the closeness of the simulated CPs to the empirical ones from the trials. The R^2 values shown for The EV Project are an average of the coefficients computed at each location, weighted with the number of charging events. Note that in few cases the R^2 score is negative.

quality of the results, with charging rate and losses playing a greater role as they directly impact the CPs without feeding anything back to the driving pattern. The delicate role of charging rate and losses observed means that modellers must pay particular attention to these parameters when their goal is the derivation of CPs. This also justifies the choice not to investigate further the sensitivities of these parameters in the exploratory scenarios.

As expected, the exploratory scenarios heavily curtail the R^2 achieved by the model, because they span a much wider parametric space. The most significant impact is caused by variations in the powertrain fleet, as these changes drastically affect the total electricity consumption of EVs. The small BEVs used with default settings can thus only fulfil the shortest assigned trips. When replacing these BEVs with PHEVs with the same battery capacity, all previously unfeasible trips become possible as the driver would just switch to charge sustaining mode once the battery is drained. All trips that were deemed unfeasible with BEVs are now performed with PHEVs that finish the day with fully discharged batteries. Therefore, each new trip added to the analysis entails a total electricity consumption higher than the average trip previously attainable by BEVs. The average daily electricity consumption per EV thus increases together with the daily electricity to be supplied by EVSEs. This causes longer and more frequent charges that negatively impact the R^2 of The EV Project. The same phenomenon is magnified in the My Electric Avenue trial, where days without charges are excluded from the analysis. The higher electricity consumption that accumulates on every driven day causes much longer charges on the few days the PHEV is plugged in, extending the simulated CPs and penalising R^2. This effect can be appreciated in Fig. 3.8, where the blue CPs represent the case where all cars are PHEVs. The same argument explains also the deterioration of R^2 when larger battery sizes are supplied to BEVs. The effect in this case is even stronger as the larger, heavier, batteries also entail a higher wheel energy demand.

Changing the density of work and public stations also negatively impacts the predictive power of the model since it adds charging patterns that were absent in the trials. The EV Project case with no public stations is the only scenario with an improvement of the score. This is due to two factors: firstly, the bad R^2 scores of the public CPs are excluded from the average, leaving it to the more accurate residential CPs. Secondly, the

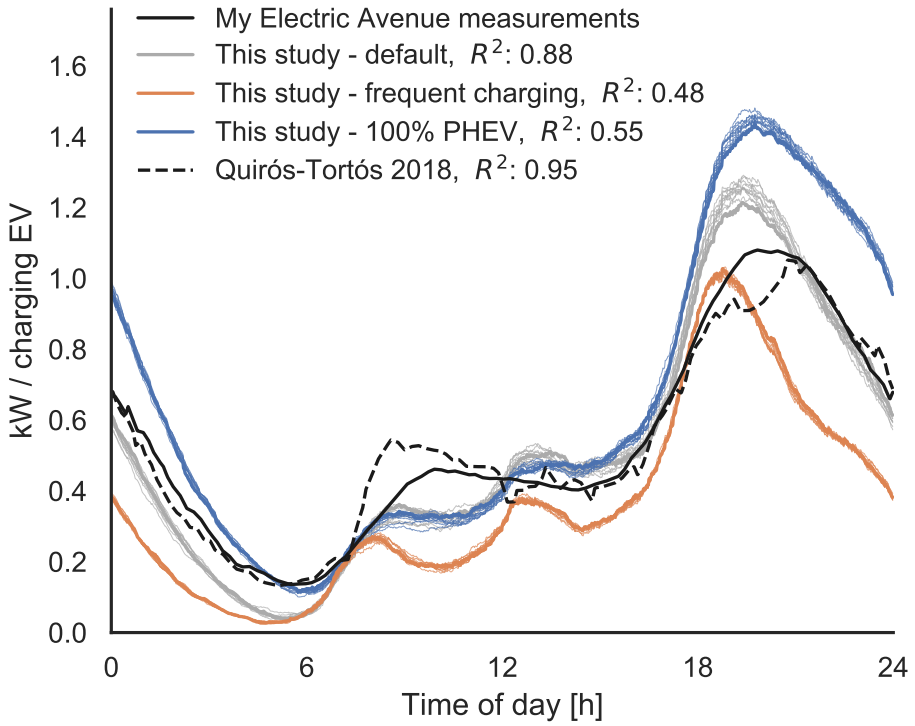

Figure 3.8: Examples of My Electric Avenue CPs obtained with different settings. In blue the case with all cars being PHEVs with the original battery size; in orange the case with empirical behaviour 1 from Fig. 3.6, i.e. with more frequent charging.

lack of public stations forces EV drivers to charge more often at home, increasing the peak load especially during weekdays and reducing the gap with the reference profile.

Behavioural variations affect the results for the two demonstrators very differently. The major repercussion of behavioural tuning is a change in charging frequency, but the average energy to be supplied over time is only mildly impacted. The profiles reported for The EV Project depict the average daily electricity to be provided by each EVSE and are thus only marginally impacted by a change in behaviour. On the other hand, the profiles of My Electric Avenue consider only days where the EV is charged and a change in charging frequency causes a similar but opposite change in CPs magnitude. For instance, empirical behaviour 1 from Fig. 3.6 leads drivers to charge their EVs any time the SOC goes below 90%, causing more frequent and shorter charges. This effect is captured by the orange CPs in Fig. 3.8.

In My Electric Avenue, the scenarios implementing an empirical behaviour expectedly show better alignment with the reference profile than the alternative ones. Notably, case 4 improves the R^2 score compared to the

default model, suggesting that the charging threshold for My Electric Avenue should have been fixed at lower μ and higher σ. Fig. 2.11 and 3.6 show that this is exactly the direction where the empirical SOC thresholds from My Electric Avenue are located with respect to the point chosen as default behaviour.

In both trials the default charging behaviour outperforms most other behavioural settings. This is particularly remarkable considering that, albeit the same trials are used, no information is exchanged between the estimation of the charging thresholds and the computation of the CPs. Namely no empirical distribution of SOC is used to compute the numerical CPs, and no empirical CP is used to derive the SOC thresholds in Section 2.3.2. This good agreement is a strong argument in favour of the charging behaviour model proposed in this work and of the methodology used to calibrate it.

The sensitivity analysis of the number of simulation days per run confirms that four days are more than sufficient to reach convergence also in terms of CPs. Finally, the employment of the original time series as reported in MZMV does not affect the general CPs patterns and leaves R^2 untouched. The impact is however appreciable at smaller scale where CPs exhibit a serrated behaviour with a frequency of about 5 minutes, consistently with Fig. 2.1.

For My Electric Avenue also the R^2 score of the numerical CP proposed in [25] and depicted in Fig. 3.2 and 3.8 is given. The profile performs better than any CP proposed by this work, mostly because it does not overshoot the peak load. However, that CP is computed with data extracted from the same My Electric Avenue trial used as reference, while the present model employs MZMV as input. Most importantly, the improvement of [25] with respect to the CP generated with default settings is small when compared to other possible modelling imprecisions such as the ones investigated in the parametric analysis.

Pecan Street & Switch EV. Fig. 3.9 reports R^2 scores for Pecan Street and Switch EV projects since all their CPs undergo some kind of normalisation. The peak load normalisation applied to CPs from Pecan Street particularly helps any numerical CP to closely approach the empirical profile, often resulting in R^2 greater than 0.90. To appreciate the different R^2 scores of the parametric analysis the x-axis scale of the Pecan Street demonstrator is thus magnified. The simulations involving a change in the powertrain scenario are the only ones which exhibit lower R^2. As explained

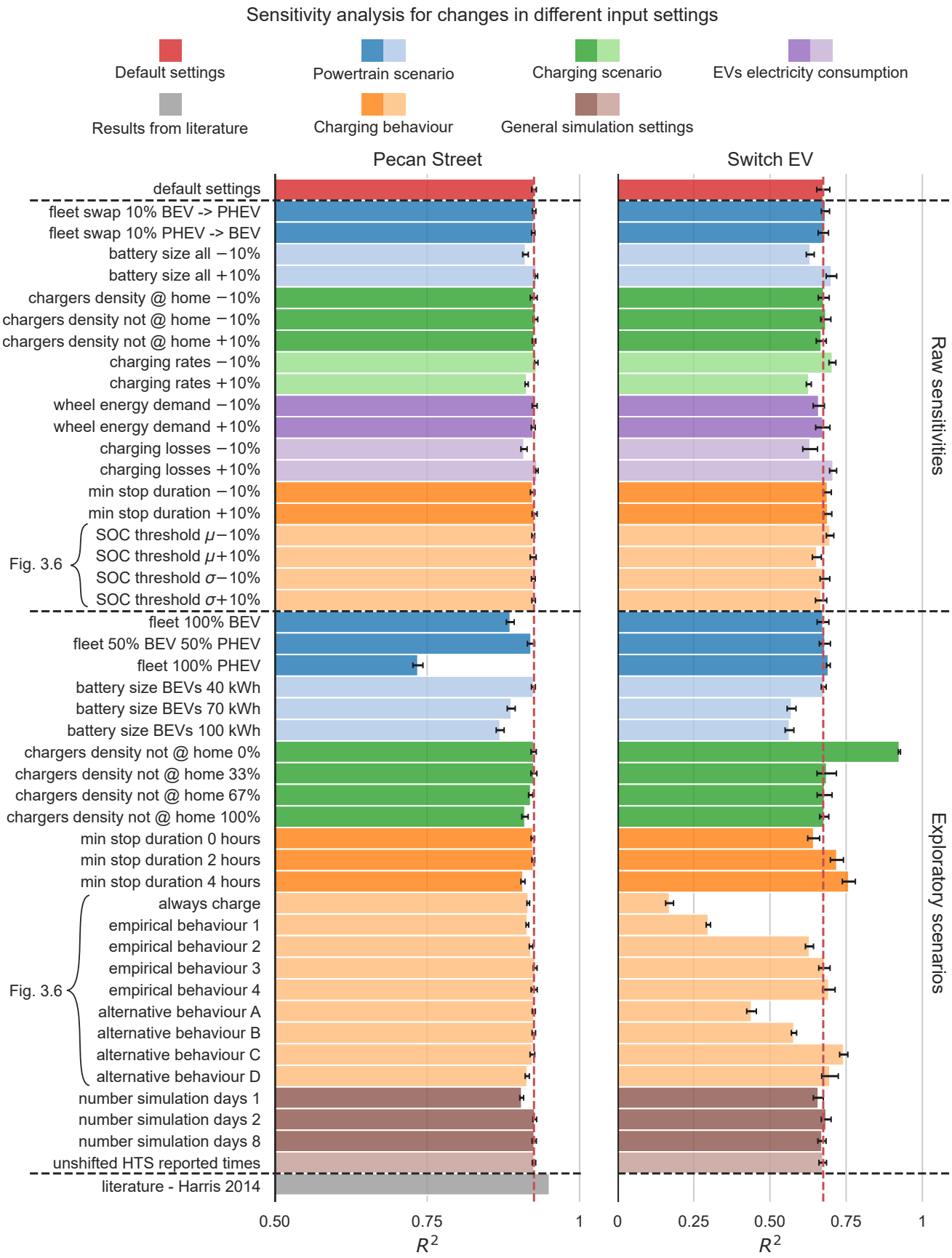

Figure 3.9: Sensitivity analyses for the simulations of Pecan Street and Switch EV trials. The bars use the coefficient of determination R^2 to show the closeness of the simulated CPs to the empirical ones. The R^2 values shown for Switch EV are an average of the coefficients computed at each location, weighted with the number of charging events. Note the different x-axis scale used for the Pecan Street demonstrator.

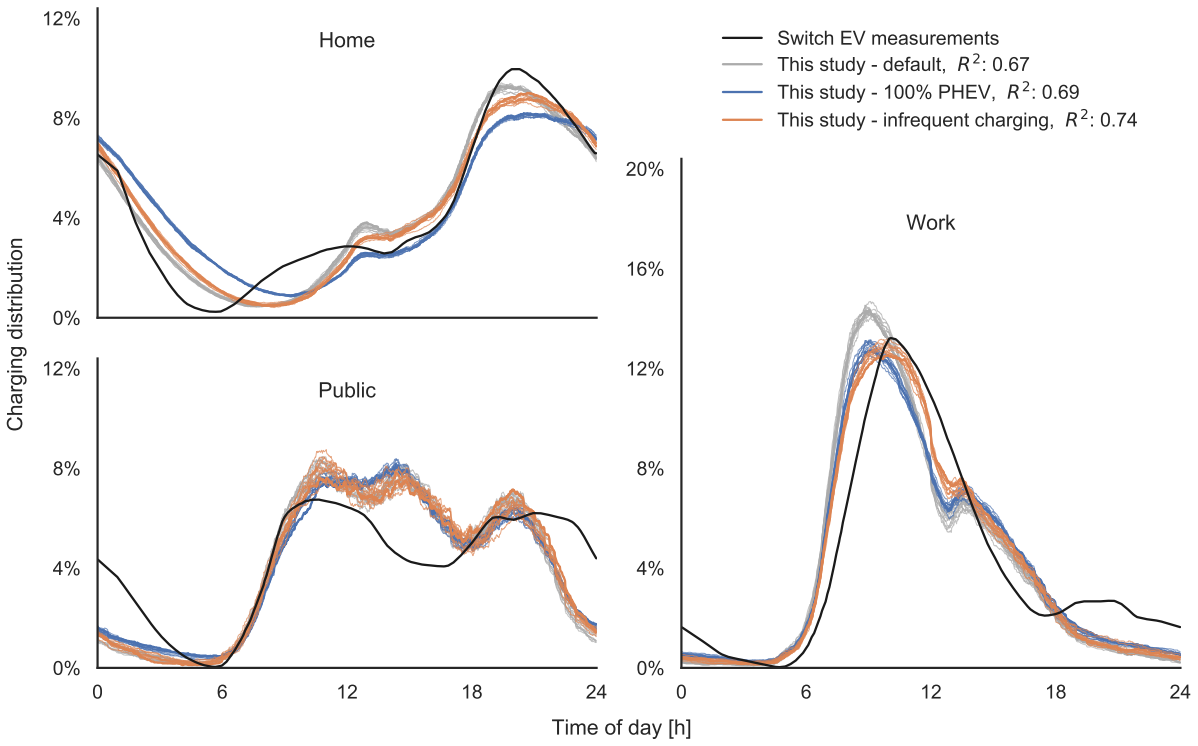

Figure 3.10: Examples of Switch EV CPs obtained with different settings. In blue the case with all cars being PHEVs with the original battery size; in orange the case with alternative behaviour C from Fig. 3.6, i.e. with less frequent charging for high SOC.

for the two previous trials, switching a BEV with a PHEV or expanding the BEVs' battery size both cause an increase in daily electricity consumption. This affects the extension of the CPs more than their peak load and the mismatch with the reference profile is thus retained also after normalisation.

In the Pecan Street trial the CPs obtained with the default settings are among the best performing numerical profiles, supporting the design of the model and its capability to reproduce the on-field trial conditions accurately. The simulated CP from [24] achieves a higher R^2 score, thanks mostly to its capability to capture the morning peak at 8 a.m..

The Switch EV trial exhibits a diversity in R^2 results comparable to Fig. 3.7, meaning that normalisation of CPs to the area does not level out the profiles as much as the peak load normalisation. The highest sensitivity is shown for changes in charging rate, charging losses and BEV battery size, which reflects most of the observations made for Fig. 3.7. Two additional comments are however necessary.

Firstly, the simulated public CPs of Switch EV are often the worst per-

forming in terms of R^2 as is observable in Fig. 3.4. The relative flatness of the reference public CP makes it an easy target for an horizontal fit. Since the coefficient of determination R^2 compares the goodness of the simulated profile to a hypothetical horizontal fit, it becomes a stricter parameter when the latter fits better the reference profile, such as in the case of public CP. This means that a lot of the variance observed in the sensitivity analysis is ascribable to changes in the R^2 score of the simulated public CPs.

Secondly, the mismatches characterising home and work CPs in Fig. 3.4 are small but with opposite sign. This means that even important parameter changes may affect the R^2 results of the two profiles in opposite directions, neutralising the overall impact on the metric. This is the case for the variations in powertrain scenarios, which usually imply longer average charges. When normalising to the area, these longer CPs also manifest a lower peak; consequently, a better reproduction of Work CPs is offset by a worse performance of Home CPs. An example of this effect is presented in blue in Fig. 3.10 for the case with only PHEVs.

The exploratory scenarios of the Switch EV demonstrator occasionally perform better than the default case. The main outlier is the scenario with no public or work charging stations, but the main reason is the exclusion of the poorly performing public CPs from the computation of the overall R^2. In other words, the R^2 score plotted for this test indicates the approximate R^2 generally achieved by the numerical home CPs. A second scenario that performs better than the default case is where the minimum parking time for charging is increased to 4 hours. This change mostly affects stops at public spaces as these locations are more likely to host short parking times. The variation of this parameter does not play an important role in the other 3 trials because of the lower relevance of public CPs in those demonstrators[3]. However, in Switch EV, the R^2 performance of public CPs is a dominant factor of the overall score. Increasing the minimum parking time for charging eliminates several short charges smoothening the synthetic public CPs and reducing the gap with the reference profile. This improvement strongly boosts the overall R^2 result for the scenario.

The last Switch EV scenario that performs better than the default case is when charging behaviour is shifted to point C of Fig. 3.6: this point lies on

[3]Note that public EVSEs in The EV Project account for recharges at both workplaces and public spaces.

the alternative behaviour line and entails less likely charges for high SOCs compared to default. This adjustment mostly impacts stops during the day as EVs are always more likely to charge at home (regardless of behaviour) and end up driving with more depleted batteries in the afternoons than in the mornings. This means that public and work CPs are mostly affected by the behavioural shift to point C, with morning charges becoming less frequent. The orange profiles in Fig. 3.10 illustrate these changes, with morning peaks of all three locations being reduced. The CP improvements at work and public places are particularly responsible for the higher R^2 achieved by this scenario.
All the other scenarios of Switch EV perform similarly to or worse than the default case, hence further validating the architecture of the EV model.

Summary

The above examples demonstrate that the model responds logically to changes in the input parameters although *a priori* the outcome is not always intuitive. The sensitivity analysis shows also that, in few cases, a careful adjustment of some parameters would allow to close the gap with the empirical CPs. However, a more important conclusion is that the uncalibrated model always ranks among the best test cases, managing to capture all important patterns at any location on any day. This work does not intend to promote the use of fine tuning to perfectly match experimental data; rather, it provides evidence that the construction of a thought-out model that adequately describes car usage behaviour and EV charging likelihood is sufficient to robustly replicate the CPs from different contexts.

3.2 Annual mobility

This section assesses the performance of the multi-day mobility model. To test the procedure annual mobility profiles are constructed starting from the both weekly profiles available in NTS and daily profiles in MZMV. The annual target has been chosen since other sources for annual mileage exist and can be used as benchmark. However, the construction of yearly profiles from weeks is more uncertain and a variety of clustering-sampling combinations is possible.

3.2.1 Metrics and nomenclature

The construction of yearly profiles from days or weeks is subject to the following degrees of freedom:

- the variables chosen for clustering weekly data into quasi-homogenous groups;
- the number of clusters, n_{clusters};
- the number of distinctive weeks to be sampled, n_{weeks}.

Weeks are used as fundamental sampling units due to the weekly characterisation of mobility established in Section 2.2.4. Even when starting from single days in MZMV, at least a full week is drawn to describe annual mobility. However, a full yearly profiles may be obtained by sampling $n_{\text{weeks}} < 52$ weeks and repeating multiple times the few sampled ones.
Fig. 3.11 displays the annual mileage distributions that result from different n_{clusters} (columns) and n_{weeks} (rows). In all cases the clusters are formed via the car annual mileage reported by NTS respondents, which will be shown to be the most convenient clustering variable despite its large rounding errors.
Two benchmarks are used for NTS: the car mileages measured in the MOT project introduced in Section 2.2.4 (black curves) and the self-reported annual mileages from NTS, smoothed with Gaussian kernels (red curves). Both references stay constant in all subplots.
The evaluation of the modelled distributions considers two features. First, the PDF of annual mileages should resemble the benchmark distributions, especially the one measured from MOT. This assessment can be carried out qualitatively by visually comparing the distributions and quantitatively with the Kolmogorov–Smirnov (K–S) test. The test returns the maximum distance D between the observed (results of the model) and the reference (MOT) cumulative distribution functions (CDF). Since the null hypothesis of the test is that the observed samples are drawn from the reference distributions, the smaller the p-value the less likely are the samples from that distribution. A good fit between the modelled annual mileages and the MOT distribution would thus entail low D and higher p-value, ideally > 0.05.
The p-value has a more universal interpretability but is a stricter criterion. It decreases namely with the number of samples since it grows the

confidence on the observed data. All distributions from Fig. 3.11 have been produced with 1000 samples for aesthetic reasons, but this impacts the p-value (as it should, since the samples are indeed not from the MOT distribution). The p-value rarely exceeds 0.001 and is not much helpful for assessments.
The K–S statistic D is test-specific but does not depend on the sample size. No general interpretation for it exists, but based on the few cases with an appreciable p-value it can be assumed that the fit is acceptable for $D < 0.080$.
The second feature to consider would be a logical week-to-week variability within each constructed annual profile. No single criterion can fully capture this aspect, which includes plausible destinations and regular working schedules. Given the focus on mobility performance, the standard deviation σ of weekly distances within each annual profile is used as proxy. Fig. 3.11 reports for each distribution the average σ of all annual profiles. Very high σ entails too diverse weekly distances in the same annual profiles, while a low σ denotes mobility patterns with many repeated weeks.
Estimating the best range for σ is also sensitive. The most reliable approach is computing σ within homogeneous groups of the full NTS population. The more homogeneous the groups the more accurate the estimate would be. Grouping NTS in 20 clusters by self-reported annual mileage (as last column of Fig. 3.11) returns $\sigma = 188$ [km][5]. Grouping NTS in 20 clusters by socio-technical variables (as last column of Fig. 3.12) gives $\sigma = 217$. This approach is likely to overestimate the real σ of drivers and 188 should thus be taken as upper bound. Any distribution with $\sigma \leq 188$ can be considered adequate, but too low σ should be regarded with caution as these distributions could miss the heavy tails that make BEV range particularly critical.

3.2.2 Results

NTS, from weeks to year

The first row of Fig. 3.11 is the stochastic version of the *annualised* weekly profiles from Fig. 2.5. Only a week is sampled and is repeated 52.14 times. The internal σ is thus incomputable and the resulting PDF largely misses the empirical ones.

[5] σ is here measured in km, but for sake of conciseness the unit is omitted.

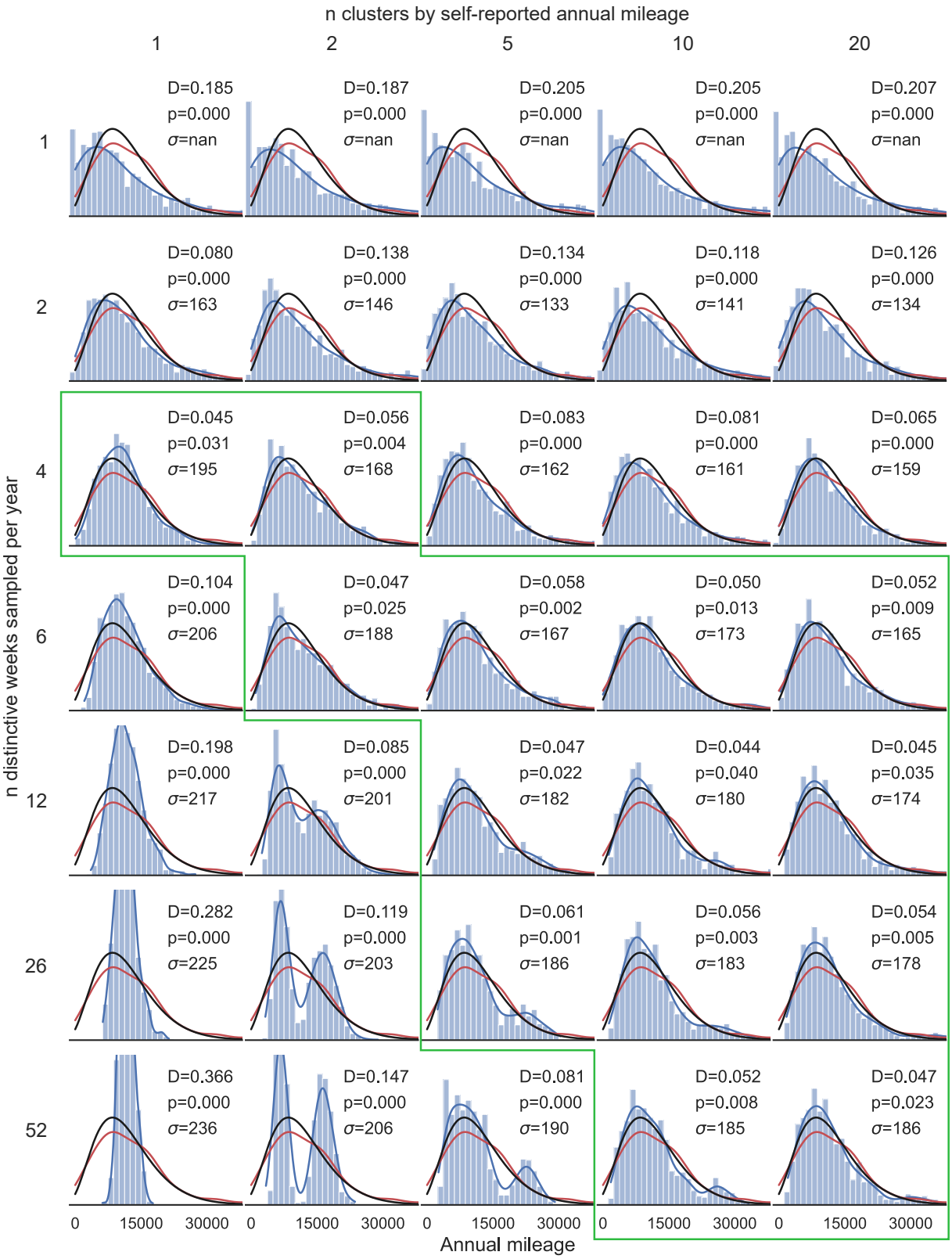

Figure 3.11: Comparison between annual mileages constructed from NTS weeks (blue histograms, weeks clustered by various socio-technical variables), measured in the MOT project (black lines), and reported by NTS respondents (red lines, smoothed). D and p are K–S statistic and p-value of the Kolmogorov–Smirnov test respectively. Low D or high p indicate good fit between sampled mileages and MOT measurements. σ is the average standard deviation of weekly distances within each annual performance. Enclosed in green are the best performing sampling cases.

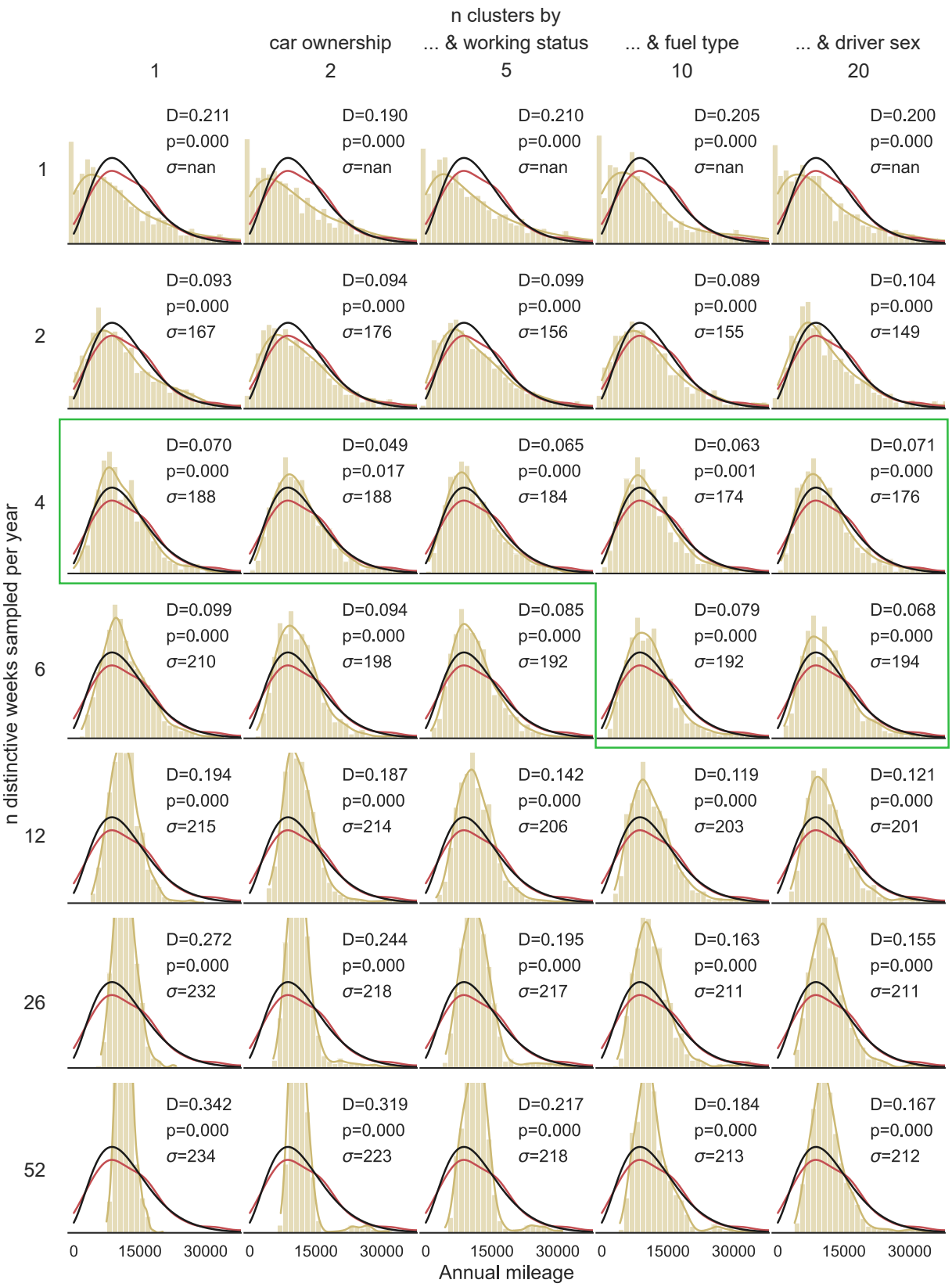

Figure 3.12: Comparison between annual mileages constructed from NTS weeks (yellow histograms, weeks clustered by various socio-technical variables), measured in the MOT project (black lines), and reported by NTS respondents (red lines, smoothed). D and p are K–S statistic and p-value of the Kolmogorov–Smirnov test respectively. Low D or high p indicate good fit between sampled mileages and MOT measurements. σ is the average standard deviation of weekly distances within each annual performance. Enclosed in green are the best performing sampling cases.

The results improve when sampling more weeks. The 0-mileage bin quickly fades and the distribution's mode shifts toward higher mileage. Particularly interesting is the first column case with $n_{\text{clusters}} = 1$ (that is no grouping). In this case the annual distribution is the sum of *independent and identically distributed* variables (the weekly distances) and according to the central limit theorem (CLT) the resulting PDF tends toward a normal distribution. This is visible for $n_{\text{clusters}} = 1$ and $n_{\text{weeks}} \geq 6$, but also for $n_{\text{clusters}} = 2$ and $n_{\text{weeks}} \geq 26$.
From a qualitative point of view the model seems to perform well for a wide range of n_{clusters} and n_{weeks}, especially for medium-large values. These are in fact the cases where also D reaches its lowest values. σ instead grows with n_{weeks}, due to the higher likelihood of encountering outliers, and decreases with n_{clusters}, thanks to the more homogeneous sampling pools. The cases that perform best from a combined point of view are encircled in green.
Interestingly, it is already possible to produce plausible annual PDFs by sampling only 4 weeks from the unclustered data. The p-value exhibits one of its highest values and D almost its minimum. However, σ is rather high, which is expected from sampling 4 random weeks from the entire pool of NTS profiles. But the most robust region is located at $n_{\text{clusters}} \geq 5$ and $n_{\text{weeks}} \geq 6$: the visual and D performances of these cases are still adequate and σ is more contained. No single optimal case stands out but a general guidance can be provided. For lean formulations interested in rapidly matching the target PDF, sampling few weeks from little or no clustered data can suffice. If more accuracy on outliers and high energy days is desired, sampling more weeks from more clusters is recommended.
Fig. 3.11 shows the analogous results with different clustering variables. n_{clusters} increases between columns by progressively adding the following clustering variables:

- car ownership (private/company),
- driver's working status (4 options, but only active professionals may have access to a company-owned car),
- fuel type (petrol/diesel),
- driver's sex (female/male).

These are among the best performing NTS fields in Table 2.3[6] and are supposed to be well correlated with the annual performance. Nevertheless, Fig. 3.11 shows that these variables do not manage to adequately disperse the profiles, resulting in mostly central distributions. Since these variables do not separate NTS entries in significantly distinctive groups, the resulting clusters are not very homogeneous therein but are quite comparable between one another. And the normal distributions predicted by the CLT appear for every column, regardless of n_{clusters}.
Acceptable fits are achieved for $4 \leq n_{\text{weeks}} \leq 6$, i.e. where n_{weeks} is large enough to shift away from the raw weekly PDF and small enough to avoid the CLT. Comparable D levels to Fig. 3.11 are achievable but only in a narrower region. The poor homogeneity within pre-sampling clusters leads to generally higher σ, indicating excessive week-to-week variability in the constructed annual profiles.

MZMV, from days to year

Fig. 3.13 presents the same analysis when constructing annual profiles from the single mobility days available in MZMV. Clusters are formed by self-reported car annual mileage. Rows indicate, as before, the number of sampled weeks but here each day of the week is individually drawn. That is, to sample 4 weeks 28 days are drawn, with 4 Mondays, 4 Tuesdays and so on. The benchmark is the annual mileage PDF derived in [96] by analysing the mileages reported in car-maintenance logs and adjusting for the car age distribution of the Swiss fleet.
The higher number of independent draws compared to NTS means that the CLT establishes for a lower number of weeks (both clustering by self-reported mileage). With $n_{\text{weeks}} > 12$ ($n_{\text{days}} > 84$) the individual normal distributions associated with each cluster become visible except for very high n_{clusters}. The lower correlation between individual days of the week means that more clusters are required to obtain sparse distributions. A minimum of 5 mileage groups seems to be necessary to produce adequate annual mileage PDFs.
D reaches ranges analogous to NTS while the p-value manages to improve in few instances; however, comparisons between the two cases should be treated with caution due to the differences in datasets and benchmarks.

[6] Driver's sex rather than age has been chosen since the latter is heavily correlated with working status and would not bring a significant contribution.

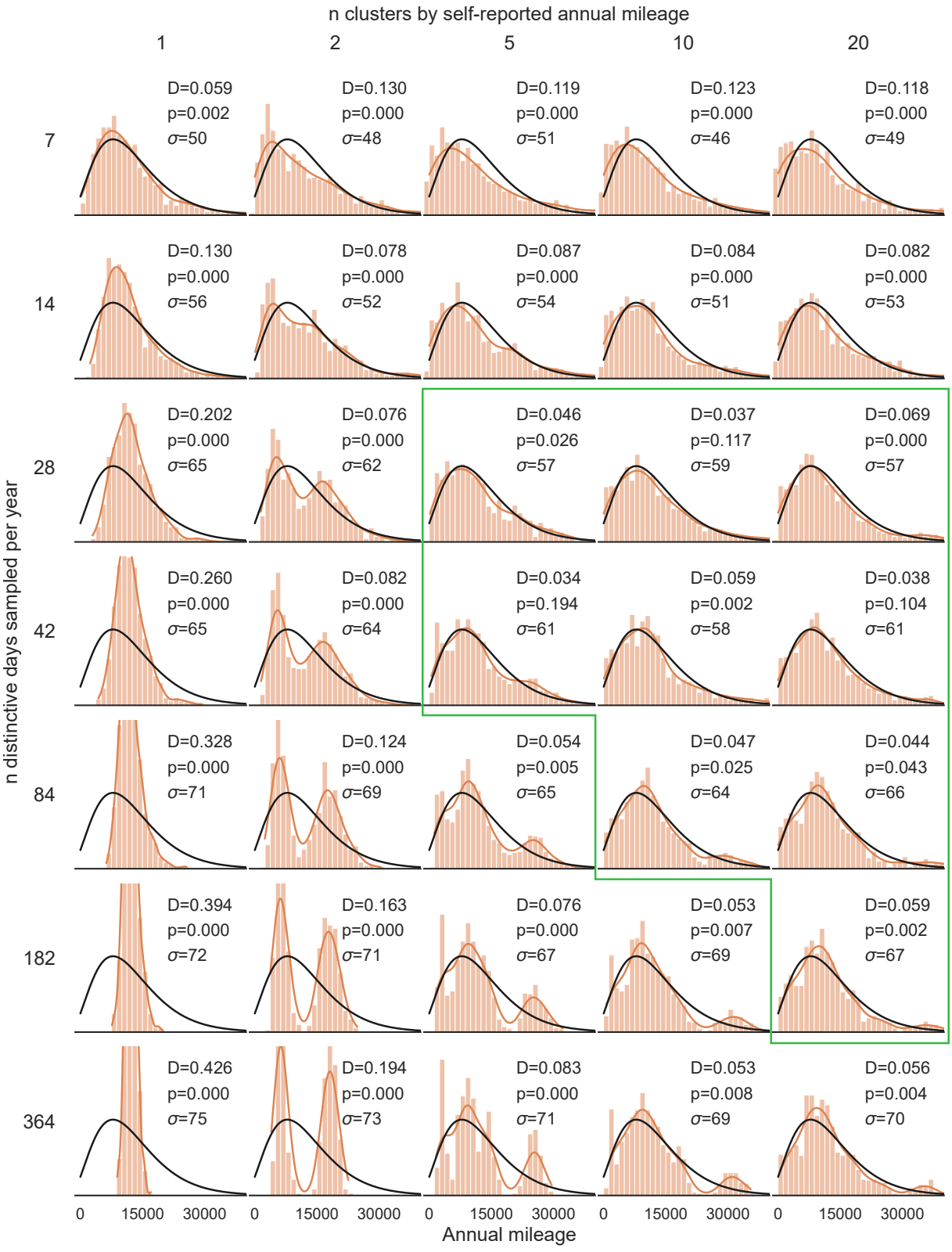

Figure 3.13: Comparison between annual mileages constructed from single days of MZMV (red histograms, days clustered by self-reported mileages) and derived in [96] from car maintenance logs (black lines). D and p are the K–S statistic and p-value of the Kolmogorov–Smirnov test respectively. Low D or high p indicate good fit between sampled mileages and empirical measurements. σ is the average standard deviation of daily distances within each annual performance. Enclosed in green are the best performing sampling cases.

σ in Fig. 3.13 describes the average standard deviation of sampled daily distances within each yearly profile. It exhibits the same general trends of Fig. 3.11 but its incorporation of both within-week and between-weeks variations makes the trends less definite.
Contrary to NTS, sampling from MZMV achieves positive scores even for visually mediocre distributions (e.g. for $n_{\text{days}} = 364,\ n_{\text{clusters}} = 10$). This highlights the need for caution in interpreting a single goodness of fit statistic: the K–S test only measures the maximum difference D between the observed and reference CDFs and can return a good score when the observed PDF smoothly oscillates around the reference PDF.

3.2.3 Summary

The proposed clustering-sampling procedure to construct annual profiles from days or weeks yields accurate results in terms of mileage PDF. The self-reported car annual mileage particularly proves to be an adequate clustering variable to split raw HTS entries in distinctive groups with high inner homogeneity. Realistic annual PDFs are already attainable by sampling 4 independent weeks from unclustered data or 28 individual days from about 5 mileage groups. Increasing the number of sampled days or weeks allows to capture more varied car usages and possible outliers, but it requires a split of the dataset in more groups in order not to fall into the CLT and generate a mixture of normal distributions.

Chapter 4

Applications of EV model

4.1 Electrification potential of BEVs

This section uses the *forward* EV simulation setup and the annual mobility model to assess the fleet electrification potential of BEVs.
The single-day car usage profiles derived form MZMV are used as source. According to Fig. 3.13 adequate annual profiles can be derived with $n_{\text{clusters}} = 10$ and $n_{\text{days}} = 84$ (12 weeks). Since charging opportunities encountered during daily routine play a role in the electrification potential, further consistency in the day-to-day mobility is desired. Specifically charging at workplace is supposed to play an important role, but only professional individuals may take advantage of it. Rather than creating 10 cluster solely by self-reported annual mileage, it is thus preferred to create 10 groups based on 5 mileage categories and 2 working status (active/inactive). This results in an annual mileage PDF slightly tighter than with $n_{\text{clusters}} = 10$, but still more diffuse than $n_{\text{clusters}} = 5$ and with a more consistent day-to-day mobility. The average annual mileage lies around 12260 km/year and the mean driving frequency f_{used} is 64.4%, i.e. about 235 driving days/year.
Three charging scenarios are tested:

- only home charging at 3.7 kW,
- home charging at 3.7 kW and workplace (hereafter "work") charging at 22 kW,
- home charging at 3.7 kW and ubiquitous charging at any other stop at 22 kW.

Since this is an investigation on technical feasibility charging behaviour is not modelled as stochastic but as deterministic: the BEV driver would charge at every possible opportunity if needed.
At the beginning of the simulation each driver is assigned a BEV with a given battery capacity and the corresponding range r. The feasibility assessment checks whether the BEV can fulfil the whole yearly mobility with the available range and charging scenario. A certain tolerance level x_{undone} is granted and is defined as the uppermost share of unfulfillable days for which the annual trip can still be considered electrifiable. How BEV drivers handle those few unfulfillable days is beyond the scope of this investigation: they could resort to *en-route* fast charging, an auxiliary car, or a different mode of transport. Four levels of x_{undone} are tested: 0% (that is, no tolerance), 2%, 5% and 10%.

4.1.1 Single profile example

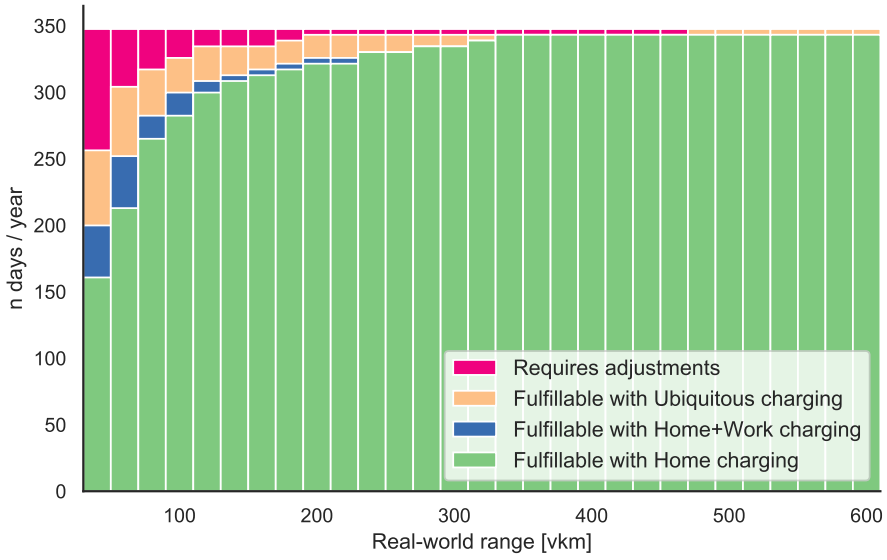

Figure 4.1: Number of mobility days fulfilled with a given BEV range (x-axis) and charging scenario (colour of bars) for a sampled annual profile.

Fig. 4.1 displays how a single annual trip is evaluated. The example refers to a particularly active professional who drives 348 days a year. The bars show, for every possible electric range, how many driving days are fulfillable with the difference charging scenarios.

Home charging is often sufficient to perform the majority of mobility days, but is never capable of singularly satisfying the full annual mobility regardless of the range. Work charging comes in handy at very low r but its importance quickly fades with longer r. The next results show that this observation is rather recurrent. Ubiquitous charging provides a stronger support, but is still incapable of completing the whole year unless for very long r. For any $r < 480$ km this driver would require some kind of "adjustments" for at least few days a year. While they can be bearable for a couple of days (representing less than 2% of annual mobility), these adjustments become discouraging when necessary on a multitude of occasions.

4.1.2 Cars electrification potential

Fig. 4.2 presents the electrification potential for an entire fleet constructed with the afore-described annual mobility model. All results are presented as a function of the "real-world range" r of BEVs and have universal validity regardless of the market segment. The proposed "net battery capacity" instead applies only to the specific mid-size vehicle used as reference.
Blue lines describe the no-tolerance situation, where BEV drivers must solely rely on the available charging opportunities. All charging scenarios perform poorly for low r but greatly benefit from an increase in electric range. A state-of-the-art BEV with a real-world range of 350 km could successfully replace about 60% of existing cars with only home charging[1]. Notably, the addition of work charging plays an inconsequential role especially for longer r. The reason is that commuting distances are commonly within half of the range of these BEVs. With a commuting distance of 60 km work charging starts becoming relevant for $r < 120$ km (see Fig. 4.1). But even then, in a tolerance-zero scenario if the driver once wishes to travel for 150 km to a weekend stay the whole yearly profile is considered non-electrifiable. That is, work charging helps if commuting distance is the limiting factor in determining the electrifiability of the car; or in other words, if the car *never* drives further than twice the commuting distance. This is highly unlikely and the dash-dotted blue line shows this aspect.
However, more flexible tolerance cases may be more reasonable. In these cases the tolerance is mostly absorbed by the longer leisure journeys and

[1]Most sold BEVs in Europe in 2020 were Renault Zoe, Tesla Model 3 and VW ID.3, with real-world ranges rated at 315 (ZE50), 335 (standard range plus) and 350 km (Pro) respectively [97, 98, 99].

commuting distance is more likely to become the determining factor. This is why the gap between home and home+work charging scenarios widens for larger tolerances.

Ubiquitous charging strongly expands the electrification potential of the fleet. The state-of-the-art 350-km BEV can now satisfy almost 80% of car usage profiles in the zero-tolerance scenario. Nevertheless, 20% of drivers travel further than 350 km at least once a year.

Relaxing the tolerance to $x_{\text{undone}} = 2\%$ (about 5 days a year) allows for a greater electrification under any charging scenario. A 350-km BEV can now fulfil more usage profiles with *only home* charging that it could with *ubiquitous* charging for $x_{\text{undone}} = 0\%$. This is quite remarkable, considering that ubiquitous charging entails installing a charging station at every possible stop, while a tolerance of 2% can be facilitated with the installation of few fast *en-route* stations in strategic highway corridors.

For $x_{\text{undone}} = 2\%$ and $r = 350$ km, home and ubiquitous charging electrify 82% and 92% of the fleet. Further increases in range are beneficial but at a lower degree than for shorter r. It seems particularly hard to electrify the last 5% of the fleet, which can be captured at a discouraging rate of about 50-km-range / 1% of the fleet. At the same time, the benefits of ubiquitous charging weaken for longer range. More and more daily routines or weekend trips become electrifiable with the sole home charging and the chances of ubiquitous charging coming handy for the few extremely long journeys become remote. As BEV range is expected to keep growing especially in small and medium market segments, the role of ubiquitous charging might soon become secondary.

A full electrification of the fleet is finally in reach when the tolerance is raised to 5% (about 12 days a year). The 350-km BEV can fulfil 98% and 99.5% of usage profiles with home and ubiquitous charging scenarios respectively. The value of installing a charging station at every possible stop is minimal; the effort should rather go in designing measures to support the remaining 2%, either via different powertrains or by facilitating the adjustments required with BEVs.

Extending the range beyond 350 km brings virtually no benefits. Also further increasing the tolerance level beyond 5% seems unnecessary unless with very small BEVs.

Overall, since to reach high electrification levels an appreciable tolerance degree is required regardless of range and charging scenario, development

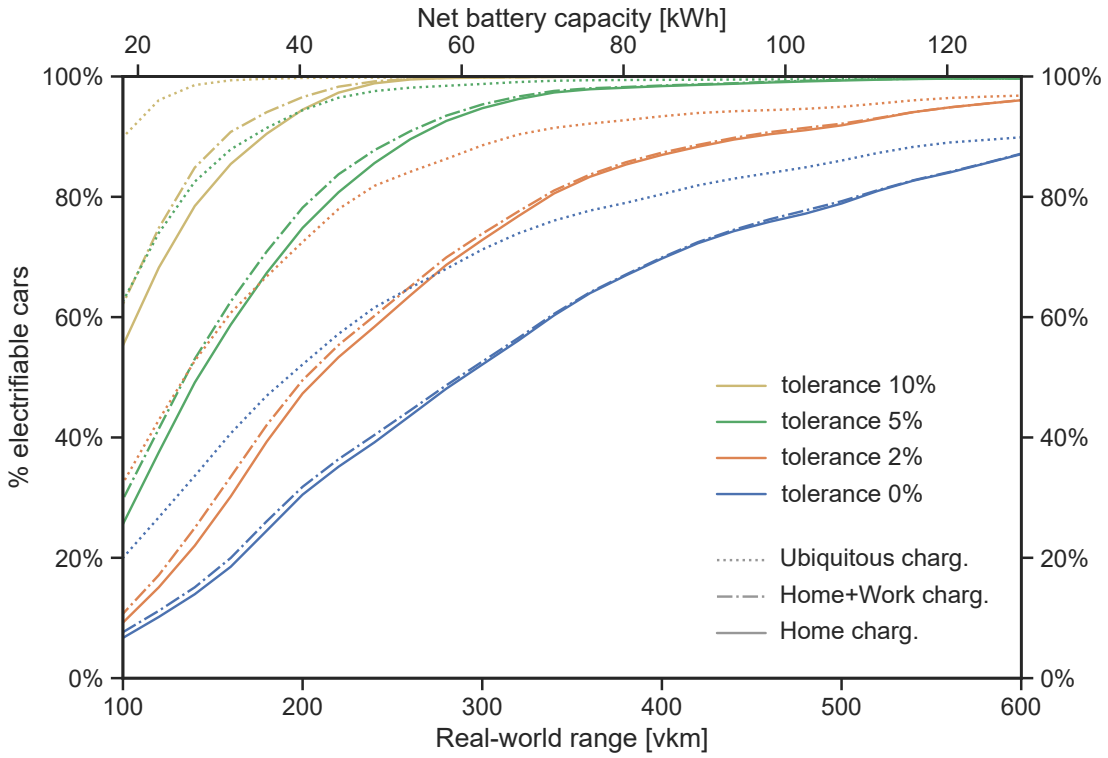

Figure 4.2: Share of cars in the fleet (y-axis) that can be successfully replaced by a BEV with a specific range (x-axis) under a certain charging scenario (line styles). The allowed fractions of unfulfillable days x_{undone} are portrayed with different colours.

plans should focus on facilitating higher tolerance levels. This entails extending the fast charging network, promoting the development and sales of fast-charging-enabled BEVs, supporting the access for BEV owners to other modes of transport. Despite not being directly comparable, improvements in range and "slow" charging network seem to bring relatively lower benefits. While the initial short ranges of BEVs dramatically curbed the electrification potential of the fleet, the currently available 350-km BEVs have already harvested most of the gains possible from range extension. Any further range growth would entail smaller marginal benefits and should be considered only for selected premium BEV models. At the same time, current and future BEV ranges relegate "slow" EV charging to a secondary role: it might be helpful to ease the adoption of BEVs in the short-term but this should not be regarded as a strategic pillar to foster fleet electrification.

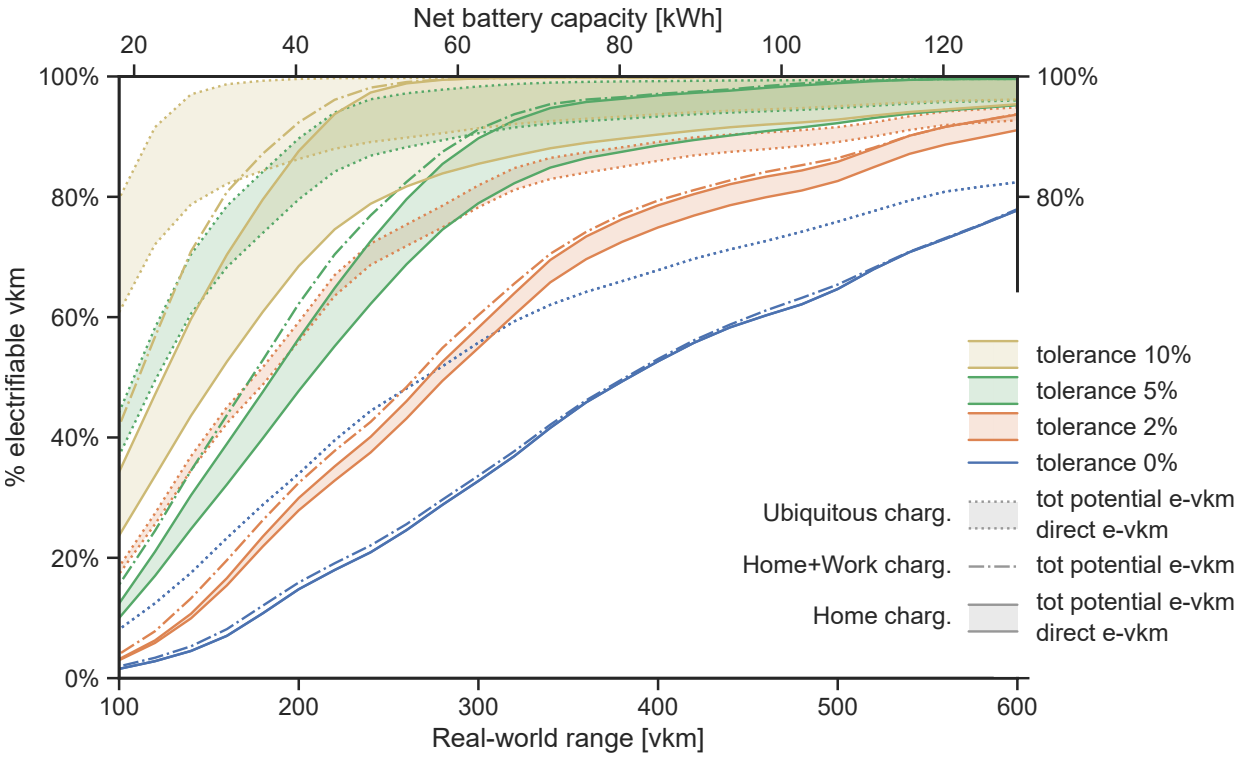

Figure 4.3: Share of vkm performance (y-axis) that can be directly or indirectly electrified by the introduction of BEVs with a specific range (x-axis) under a certain charging scenario (line styles). The allowed fractions of unfulfillable days x_{undone} are portrayed with different colours. For home+work charging scenario only the total electrification potential is displayed for aesthetic reasons.

4.1.3 Vkm electrification potential

Fig. 4.3 shows the actual share of vkm performance that is electrified with the different measures just discussed. The allowance for a tolerance level introduces a distinction between directly electrified vkm (e-vkm) and potential e-vkm. At a given $x_{\text{undone}} > 0\%$, direct e-vkm refer to the performance that all electrifiable cars can undertake without the need for adjustments. Potential e-vkm include also daily trips requiring adjustments. The choice between the two depends on how drivers deal with the non-directly fulfillable days: if they resort to a clean mode of transport (such as train or the same BEV with *en-route* fast charging) then all potential e-vkm are unlocked; if drivers opt for a non-electric alternative (e.g. a rented or owned ICEV, or a flight) then only direct e-vkm are achieved. In case of no-tolerance there is no distinction between the two definitions (blue lines). In order not to clutter the plot and due to its lower importance, for home+work charging scenario only the total potential is displayed.

From a qualitative point of view, Fig. 4.3 displays the same general trends of Fig. 4.2, with work charging playing a marginal role and ubiquitous charging valuable for shorter BEV ranges.
However, the results of Fig. 4.3 confirm what is generally acknowledged and reaffirmed by Tables 2.2 and 2.3: the hardest profiles to electrify (longest journeys) are also the most performing ones (highest annual mileage). The share of electrified vkm (either direct or total) in Fig. 4.3 is thus always smaller than the share of electrified cars from Fig. 4.2.
The 60% of cars replaceable by a 350-km BEV with sole home charging and $x_{\text{undone}} = 0\%$ cover only 45% of the total distance. To reach 60% of performance either ubiquitous charging is installed or a 450-km range is provided.
Also, the 98% fleet electrification achieved by the 350-km model with home charging and $x_{\text{undone}} = 5\%$ is less remarkable from a performance point of view. In the optimistic case with a clean adjustment of unfulfillable days the potential e-vkm reach 95% of the total driven distance. But if other alternatives are employed, the actual share of electrified performance drops to 85%.
The gap between direct and potential e-vkm further widens for larger tolerances. As a last example, with home charging and $x_{\text{undone}} = 10\%$, a 250-km BEV can electrify 99.5% of cars which cover 98% of the total distance, but only 80% of performance is directly electrifiable.
The fact that full fleet electrification requires a substantial tolerance level implies that a direct electrification of all performances is virtually impossible. Measures supporting larger tolerance levels should also make sure that the inevitable adjustments do not jeopardise the gains made by electrifying the fleet.

4.1.4 Home charging availability

An important assumption under all these scenarios is that home charging is always available. This requires that car owners have a reserved parking place at home, ideally in a garage. Section A.4 portrays the home parking situation in Switzerland as of 2015.
On average, in Switzerland there are 0.88 reserved residential parking spots, either rented or owned, per passenger car. The situation improves in rural municipalities but declines in large cities, where the parking availability

can drop to 0.6. This means that the full availability of a home charger is, today, a generous assumption, especially for cities. Nevertheless, the current parking availability is sufficient to accommodate a large share of early adopters and early majority, supporting the idea that these categories do have access to a reserved parking place.
The large electrification scenarios assessed in Fig. 4.3 and 4.2 take necessarily place in a medium-term future, when more residential buildings will be equipped with parking places and infrastructure suitable to the installation of EV charging stations [100].

4.2 Impact of GHG content of electricity

This section presents the results of some exemplary studies where CPs have been used to simulate national electricity systems. In general, power dispatch models are employed to evaluate how future energy systems can punctually supply the demanded electricity (or energy) while optimising between costs, sustainability and security of supply. The goals of these studies vary greatly, but can be summarised to:

- quantify the need for flexible and storage technologies to balance renewable generation [101, 102],
- determine the cheapest evolution of the power plant fleet under CO_2-constraining scenarios [103, 104],
- quantify the frequency and gravity of supply shortages [104],
- compute the average CO_2 or GHG content of the electricity produced or consumed [104, 105].

In all cases, CPs of future EV fleets are an essential component of the projected hourly demand for electricity and the methodology described in Chapter 2 has been used to provide CPs tailored to the application. Among the aforementioned goals, the following discussion focuses on the estimation of the GHG content of electricity, since it has been introduced as one of the key factors determining the sustainability of BEVs [6].
Fig. 4.4 shows the current and future GHG content of the Swiss electricity according to various scenarios and calculation methods. For reference,

the figure includes tipping points where the GHG content of the electricity makes the environmental impact of BEVs worse than the best fossil powertrains. The tipping points are presented as "zones" since two fossil powertrains are used as benchmarks: HEV running on petrol, which delimits the tipping zones to the right, and HEV fuelled with CNG, that sets the left limits since environmentally better than HEV-petrol. Additionally, two environmental assessments are used for the comparison with BEVs. The red tipping zone considers only Well-to-Wheel (WTW) emissions, which account for electricity generation, transmission and charging losses for BEV, and for fuel extraction, distribution and combustion for HEV [6]; this zone lies in the same range as the transition zone between BEV and HEV-CNG showed in Fig. 1.2, which indeed covers only the WTW scope. The yellow tipping zone considers instead the full life-cycle assessment (LCA) of BEV and HEV, hence including manufacturing and scrapping of vehicles [12].

The LCA tipping zone lies on the left of the WTW zone since BEVs entail higher grey emissions linked to vehicles manufacturing (especially the battery) compared to HEVs. This implies that a cleaner electricity mix is required for BEVs to match the LCA footprint of HEVs compared to the WTW assessment. For 2017, the LCA tipping zone lies between 330–480 gCO_2eq/kWh [12], while the WTW one around 520–690 gCO_2eq/kWh [6]. Importantly, the tipping zones might change in the future depending on the relative technological improvements of BEV and HEV. While in the WTW scope no particular innovation is forecasted to shift the balance between the two technologies, the LCA perspective will see different improvements in vehicle manufacturing. The HEV powertrain is rather established and only marginal gains in the manufacturing process are expected; however, the production of batteries for BEVs will experience a remarkable decrease in environmental footprint thanks to the introduction of improved chemistries and the reduction in energy and material inputs (see Section A.2). Future BEVs can thus afford slightly dirtier electricity mixes and the LCA tipping zone shifts to 360–510 gCO_2eq/kWh for 2050 [12][2].

The current production and consumption electricity mixes for Switzerland are 30 and 149 gCO_2eq/kWh respectively [106]. The production mix is

[2]The LCA improvements between 2017 and 2040 presented in [12] have been linearly extrapolated to obtain the trends between 2015 and 2050.

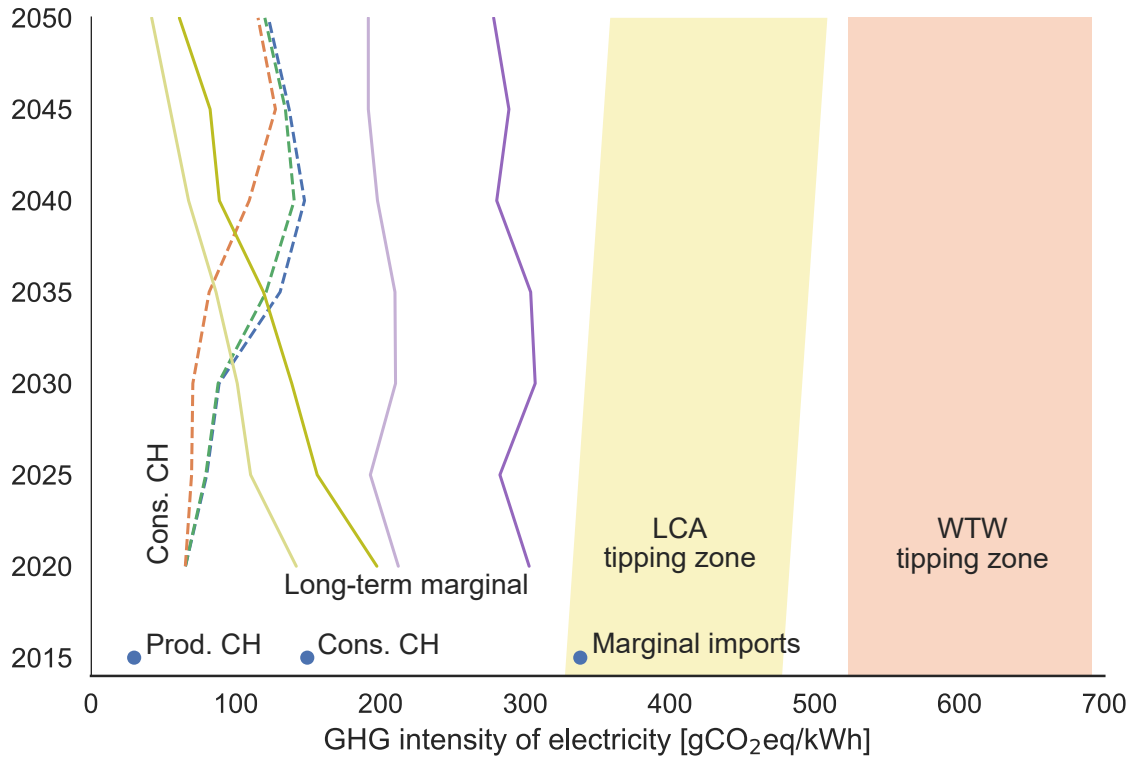

Figure 4.4: Current and future GHG intensity of the Swiss electricity based on different scenarios and calculation methods. Blue dots represent today's situation, dashed lines the consumption mix according to three different scenarios based on [104], solid lines the long-term marginal mix according to four scenarios based on [105]. The yellow LCA tipping zone indicates the GHG intensity of the grid for whom BEV and HEV have comparable life-cycle assessments [12]. The red WTW tipping zone indicates the GHG intensity of the grid for whom BEV and HEV have similar emissions along the electricity/fuel supply and usage chains [6].

very low since the Swiss electricity generation is dominated by nuclear and hydropower. The consumption mix is higher since it accounts for the electricity imported from countries with more fossil generation (primarily Germany). Nevertheless, both values are much smaller than the lowest threshold (LCA comparison against HEV-CNG), promoting BEVs as a much cleaner alternative to conventional powertrains. However, it may be argued that a single additional charging BEV would not consume the average electricity supplied to the country, but it would prompt the increase in production from a specific "marginal" asset. Using this approach can lead to higher CO_2 intensities of the grid, potentially up to 338 gCO_2eq/kWh [107]. This value would fall within the LCA tipping zone, suggesting that a thorough analysis of the origin of electricity is vital to accurately assess the environmental performance of BEV compared to alternative technologies.

Finally, Fig. 4.4 presents some future scenarios on the future evolution of the Swiss electricity mix. The dashed lines represent the average Swiss consumption mix resulting from a power market model of central Europe [104]. The three different lines vary depending on the scenario assumed for the evolution of the Swiss power sector: in blue is the reference scenario, in green stronger support to renewables increases the photovoltaics (PV) installed capacity, in orange the lifetime of nuclear power plants is extended. By supporting renewables or extending nuclear lifetime the reliance on imports decreases and the consumption mix shifts to lower CO_2 intensities. In any case, all scenarios are far from the LCA tipping zone.
The solid lines represent the GHG intensity of the long-term marginal electricity supplied to BEVs resulting from a dispatch model of the entire Europe [105]. This measure is defined long-term marginal since it is the ratio between the additional GHG emissions caused by BEVs and their cumulative electricity demand. It is thus marginal since it only reflects the specific GHG intensity of the electricity supplied to BEVs, and long-term because the power sector can gradually adapt to the expected demand by installing additional capacity. The different lines also vary depending on the assumed scenario:

- the purple lines assume that all electricity imported to Switzerland is generated by combined cycle gas turbine (CCGT), regardless whether it is fed to BEVs or not,
- the green lines assume that electricity is imported from the hourly generation mix of a "low-carbon" Europe, with expanded renewables and wide installation of carbon capture and storage (CCS),
- the darker lines assume a mild penetration of PV in Switzerland, with an annual generation of 13 TWh in 2050,
- the lighter lines assume a large expansion of PV in Switzerland, with an annual generation of 32 TWh in 2050.

In all cases here presented, the excess renewable generation is simply curtailed [105].
As expected, the more renewables are installed in the system (either in Switzerland or in Europe), the lower the marginal GHG intensity. Most importantly, even the worst case scenario with little PV penetration in

Switzerland and CCGT-based imports (dark purple line) remains always below the LCA threshold. This result highlights the strong benefit of the efficient BEV powertrain: even with a comparable primary source (natural gas), the "power plant + transmission + charging + BEV" conversion chain is more efficient than its direct employment in a HEV[3].

[3]In the dark purple scenario not all electricity comes from CCGTs: the marginal GHG intensity is about 300 gCO_2eq/kWh, while CCGT intensity is between 360–423 gCO_2eq/kWh [105], which lies within the LCA tipping zone. However, it is reasonable to expect that at least a small share of electricity fed to BEV will come from cleaner sources, as visible from all 7 scenarios of Fig. 4.4.

Chapter 5

Case study: benefits of BEV sharing

This chapter presents an in-depth analysis of the mutual benefits of shared BEVs and car-sharing systems. Section 4.1 has shown that privately owned BEVs can fulfil the mobility needs of most drivers either when equipped with extremely large batteries or when an adequate level of tolerance is granted. A central operator of shared BEVs (hereafter SEVs) can take advantage of the variance of daily mobility needs to provide the most suitable range to every user on each day, thus minimizing the total battery requirements. This gain comes on top of the typical lower number of cars needed in car-sharing systems, giving an additional edge to SEVs compared to shared ICEVs. Overall, the transition from private BEVs to SEVs entails both environmental benefits concerning the supply of vehicle parts and batteries and economic advantages for SEV users, who gain a cheap access to sustainable private mobility.

5.1 Literature specific to shared BEVs

The employment of BEVs in car-sharing schemes has long been investigated and several companies have adopted BEVs as part of their shared fleets [108, 109, 110]. However, BEVs introduce an additional difficulty in sharing schemes: the regular charging of the batteries [17, 111]. From this point of view, station-based car-sharing — where the vehicle is picked up and dropped at designated parking locations — presents fewer difficulties, as each station can simply be provided with charging connectors used by SEV drivers at the end of their trips. On the other hand, free-floating schemes — where the car can be picked up and dropped anywhere within a designated region — have to rely on individual drivers' responsibility not

to leave the BEV too depleted after their journeys or to sometimes plug it in to a charging station. Alternatively, incentives could be given to SEV users to leave the car plugged in to a charging station, or personnel could be hired to bring the BEVs to a charging point when a certain depletion level is reached. In any case, the SEV free-floating scheme becomes more complex and expensive to run [17, 112].

Regardless of the employment of BEVs, one-way car-sharing — where the vehicle may be dropped at locations other than the start, either in at a station or free-floating — suffers from an additional issue: the unintentional drift towards a spatial imbalance of the fleet [112]. The cost and efficiency of the technique employed to solve this problem is a key factor towards the success of one-way schemes [17, 113, 114]. Multiple strategies have been proposed in literature [112, 115, 116], but the most relied upon enablers are considered autonomous vehicles (AV) [111, 115, 117]. AVs will introduce both important benefits [16, 111] and noteworthy concerns: from the net increase in vkm [16, 111, 117] to the possible positive feedback on the demand for passenger-km (pkm) [118, 119, 120]. The technology enabling full-autonomous cars is progressing quickly [120, 121, 122], but few studies highlight the many barriers still to overcome [17, 123]. Finally, autonomous SEV will require, in order to charge, either a form of wireless charging or an attendant to manually plug in the connector [111].

For these reasons, the following investigation focuses on the leanest car-sharing scheme that exploits all benefits of BEVs while not necessitating further technological advancements: two-way station-based BEV-sharing. Contrary to the cases listed above, this car-sharing scheme is implementable with currently available technology and does not require many attendants nor complex coordination algorithms.

The benefits rising from station-based SEVs have not been thoroughly explored in literature. Authors of [124] consider the driving range of two BEV models to constrain the minimum average range that their optimal station-based shared fleet should offer. However, they also include other powertrain technologies and do not attempt the design of a full-BEV fleet capable to offer the service.

Since the shared fleet operator exploits the variety of mobility patterns, the efficiency of the scheme strongly depends on the size of the shared fleet. This dimension has not received the deserved attention in the community, which usually relies on a constant fleet size [111, 116, 124]. [125] quantifies

the advantages of larger fleets for the case of shared AVs. The following analysis shows that also spatially-constrained station-based SEVs benefit from large fleets thanks to a better integration of the varied demand.

5.2 Methodological adaptations

For this analysis annual usage profiles built from NTS are used as basis. According to Fig. 3.11, sampling 52 whole weeks from 10 mileage groups returns adequately distributed annual profiles. Since the distribution of daily distances matters more than a consistency in day-to-day routines, no further socio-economical clustering is done. The resulting fleet exhibits an average driving frequency $f_{used} = 65.8\%$ (i.e. about 240 days a year).
The next sections detail the sizing of private and shared BEV fleets required to satisfy a given annual mobility demand, both in terms of number of BEVs and individual battery sizes. A certain degree of tolerance x_{undone} is also considered.

Sizing private BEV fleet

The sizing of the private BEV fleet employs the established simulation framework in a *backward* fashion: the electric ranges r of all BEVs in the fleet are determined in order to meet a given (here full) electrification target with a certain tolerance level x_{undone}. Contrary to the simplified cases tested in Section 4.1, this backward simulation returns an assorted distribution of tailored ranges. Eq. 2.13 is then employed to compute the battery capacity to be equipped on every BEV.

Sizing shared BEV fleet

An economic narrative is adopted where the fleet manager tries to minimise the investment in SEVs required to satisfy the target mobility demand of the community. In this two-way whole-day car-sharing system the manager can take advantage of two dynamics:

- users may do not need a car every day, hence reducing the need for a fleet as large as the number of drivers;
- users seldom need to perform long journeys and when they do they can be given the same long-range SEVs on separate days.

The characterisation of the SEV fleet is thus an interdependent problem where all SEVs are simultaneously sized while considering the whole mobility demand of the community. The decision process can abstractly be summarised with the following optimisation problem:

minimise: cost of purchased SEV fleet

such that:

- every SEV is driven by maximum 1 user per day;
- every user drives maximum 1 SEV per day;
- every SEV has a battery capacity to satisfy all assigned daily trips;
- the share of satisfied daily trips in the whole community is larger than $(1 - x_{\text{undone}})$.

To solve this problem an heuristic approach is employed. Although the heuristics may come short of the global optimum achieved by more robust programming environments, it still allows to comparatively assess the benefits of different SEV systems against a fleet of private BEVs. The more conservative estimates produced by the heuristics might also better reflect the projections of potential investors who lack the perfect foresight of simulations.
The heuristic mechanism is schematically summarised in Fig. 5.1. Considering a community with N private cars the goal of the heuristics is to determine the optimal number $n_{\text{cars}}^{\text{opt}}$ of SEVs that, while accounting for the required battery capacity, minimise the fleet purchase costs C_{fleet}. The purchase costs and embedded emissions used in this analysis are listed in Table 5.1.

	per BEV w/o battery	per kWh of battery
purchase costs $(C_{\text{car}}, C_{\text{kWh}})$ [€]	23500	315
embedded emissions [kg CO_2e]	11700	108

Table 5.1: Purchase costs and embedded emissions assumed in this study.

All figures refer to a mid-size BEV manufactured in 2017 [12]. However, the battery manufacturing process is improving quickly and both specific costs and emissions are projected to be cut by more than half by 2040 [12, 126].

The relative importance of the battery pack on the overall environmental or economic assessment of BEVs will thus lessen in the future.
The range of values n can assume is limited. On the upper side, the maximum number $n_{\max}$ of SEVs required to satisfy the whole mobility demand is equal to the maximum number of private cars used on the same day. On the lower end, the lowest acceptable number $n_{\min}$ is such that, by compacting as many daily trips as possible on $n_{\min}$ SEVs the share of unserved trips does not exceed x_{undone}. Section A.5.1 details the precise steps for estimating $n_{\min}$ and $n_{\max}$.
The optimal number $n^{\text{opt}}_{\text{cars}}$ of SEVs must lie between $n_{\min}$ and $n_{\max}$. Algorithm 6 in the Appendix presents the detailed estimation procedure. Conceptually, the heuristics evaluates every feasible n in terms of fleet purchase costs C_{fleet} and finally selects the cheapest option $n^{\text{opt}}_{\text{cars}}$. For every n, the heuristics selects the most convenient trips to be disregarded within the tolerance x_{undone} in order to either reduce the number of required SEVs or to limit the longest trip to be served.

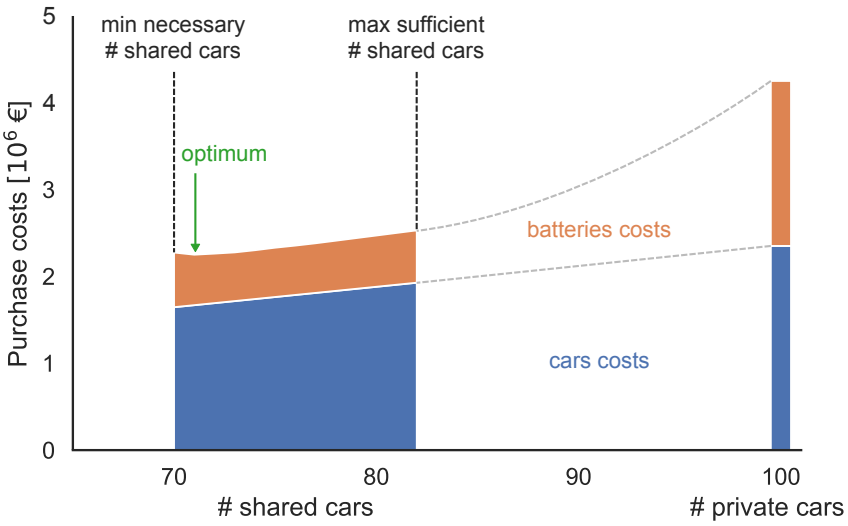

Figure 5.1: Total purchase costs for a fleet of 100 private BEVs (on the right) and a shared fleet that fulfils the same mobility demand (on the left). Various SEV fleet sizes are feasible and the goal of the heuristic algorithm is to select the cheapest option after exploring all possibilities. The cars contribution to the purchase costs (in blue) is proportional to the fleet size, while the investment in batteries (in orange) is substantially higher for private BEVs than SEVs.

The output of the heuristics for a community of $N = 100$ private cars is shown in Fig. 5.1. With $x_{\text{undone}} = 2\%$, $n_{\min}$ and $n_{\max}$ resulted in 70 and 84 SEVs respectively. However, by always removing 2% of the trips

no more than 82 SEVs ever resulted to be necessary. In addition to the costs output of the heuristic optimiser, the costs for the private case with 100 individually sized BEVs are depicted on the right. The breakdown of the purchase costs shows that the contribution of the cars is simply proportional to the fleet size. The costs of batteries is where SEVs perform particularly better than private BEVs. This is evident from Fig. 5.2, which shows the distribution of batteries selected by the model for the two fleets (with $n_{\text{cars}} = 71$ for the shared case). The need to satisfy every individual range requirement forces private BEVs to often accommodate large batteries. Contrarily, the flexibility of the shared scheme allows the fleet manager to dedicate only few SEVs to the fulfilment of long journeys, leaving the majority of the fleet to operate short daily trips. More than 80% of SEVs are equipped with the minimum battery size of 20 kWh. The maximum battery capacity assigned also reduces from 123 to 98 kWh thanks to the possibility of the shared fleet operator to neglect the overall longest trips from the whole community mobility demand.

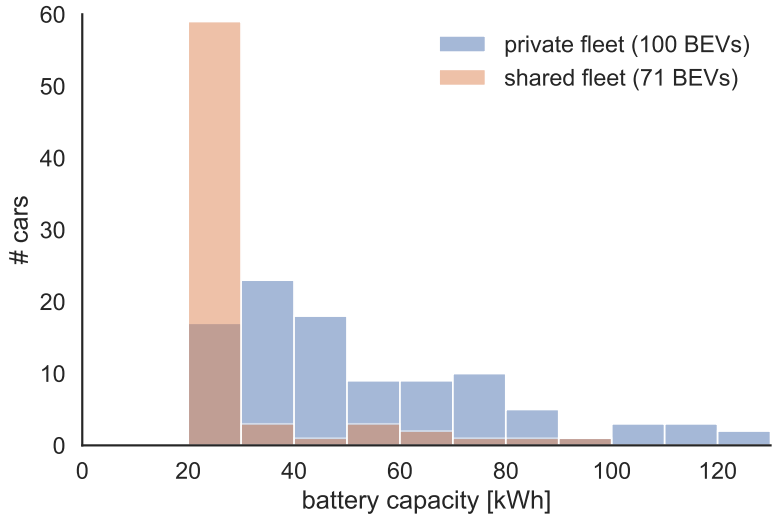

Figure 5.2: Distributions of battery requirements for a private and shared fleets that satisfy the same share of mobility demand. A minimum battery size of 20 kWh is set for both cases.

The cost of batteries for different sizes of the shared fleet in Fig. 5.1 seems fairly constant and inconsequential except near n_{min}. The general constant trend is due to the dominance of 20-kWh-SEVs for most n. However, for low n the tolerance x_{undone} is almost entirely used by trips occurring on days with more demand than n, leaving few degrees of freedom for the removal of longest journeys. The fewer SEVs may thus be assigned larger

batteries which raise the costs. This characteristic moves the optimum closer to $n_{\min}$ but usually not at exactly $n_{\min}$.

5.3 Results

In order to show the benefits of changing the ownership model of BEVs, most results present the relative cost savings of a SEV fleet with respect to the private BEV fleet that satisfies the same share of mobility demand. Costs and emissions have not been modelled at the refinement level required to make robust conclusions on the absolute values. However, the consistent and conservative assumptions applied to private and shared BEVs make the following relative results particularly useful and reliable. Fig. 5.1 can be used to visualise the actual cost numbers behind the relative trends.
The results investigate various aspects of the problem, but the largest focus is on the community size N. This is because the dimension of the problem can enable the scale effects that only the shared fleet operator can exploit to size the fleet.

5.3.1 Private BEV ownership

As mentioned in the methodology, sizing the fleet of private BEVs only requires the computation of individual battery requirements. Each BEV battery capacity depends solely on the driver's traveling pattern and is thus independent from the mobility demand of the community or its size N.
Fig. 5.3 shows the battery requirements for 1000 private BEVs for different shares of unserved individual mobility demand x_{undone}. The average battery capacity expectedly drops with increasing x_{undone}, but the steepest reduction occurs when the longest 2% of daily trips is excluded from battery sizing. Further omissions of long trips lead to lower marginal benefits. The box plots and the mean line show that the battery distribution is not symmetric and is markedly skewed towards higher values. This is consistent with the intuition that the distribution of "longest trips of the year" is in some way related to the distribution of total annual mileages shown in Fig. 3.11.
Beyond the raw share x_{undone}, the x-axis of Fig. 5.3 displays the average number of unserved trips per year. While each bin depicts the battery

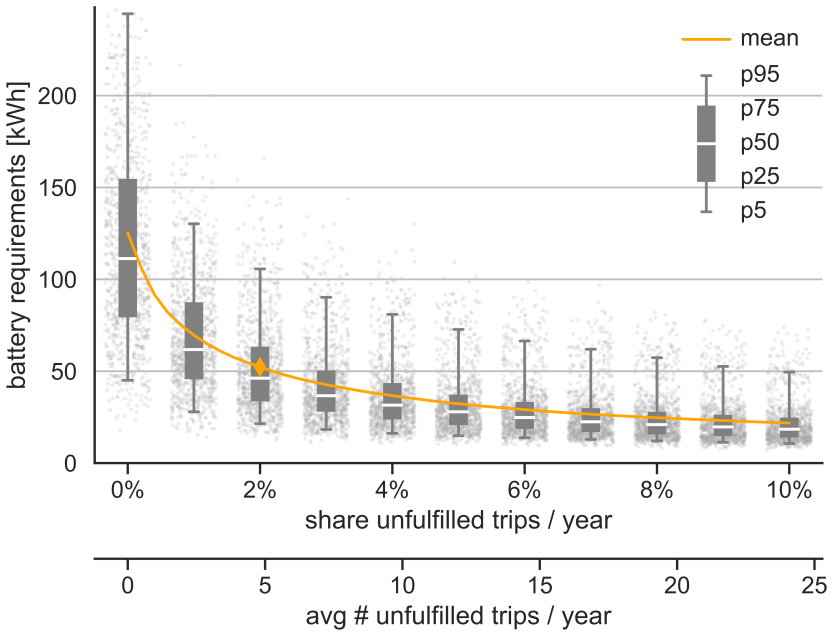

Figure 5.3: Distribution of battery requirements for private BEV owners for various shares of unfulfilled mobility x_{undone}. Each boxplot refers to a specific x_{undone}, which entails on average $240 \cdot x_{\text{undone}}$ unserved trips a year.

requirements of 1000 cars at the same x_{undone}, the actual number of unfulfilled trips depends on the individual mobility behaviour. The second x-axis is based on the average sampled driving frequency of 240 days a year.

The plot shows that at $x_{\text{undone}} = 2\%$ most users are satisfied with battery sizes currently available in the market, with the mean (orange diamond in Fig. 5.3) around the typical 50 kWh of top-selling state-of-the-art BEVs [98]. At the same time, $x_{\text{undone}} = 2\%$ implies that BEV drivers need to resort to fast *en-route* charging or different transport modes for about 5 trips a year, which seems a reasonable discomfort to bear [127, 128]. For these reasons the subsequent analysis sets

$$x_{\text{undone}} = 2\%$$

as default unfulfilment rate for both private and shared fleets.

5.3.2 Shared vs Private BEV fleets

Fig. 5.4 presents the economic and environmental benefits of reorganizing private BEV fleets of various size into shared BEV fleets. The grey lines

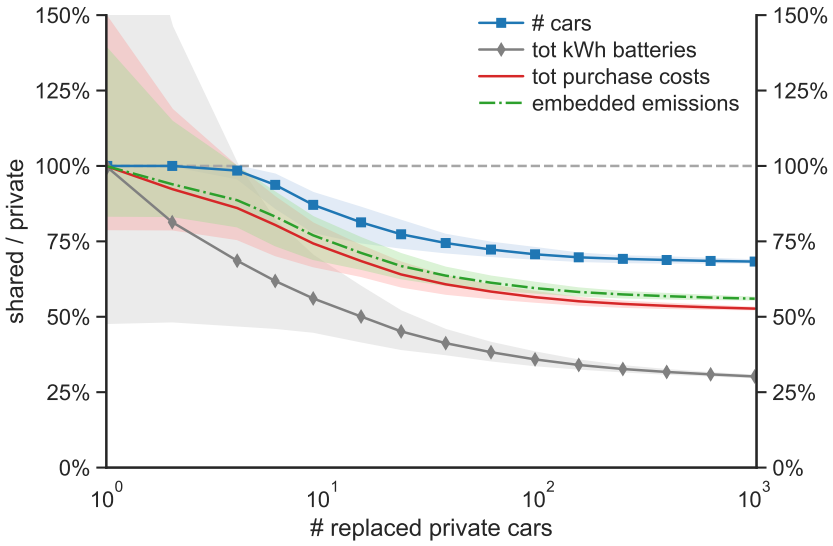

Figure 5.4: Net reduction in various indicators when substituting a fleet of private BEVs with a fleet of SEVs that satisfy an equivalent mobility demand. The reductions depend on the number of replaced private cars (x-axis, logarithmic scale). Purchase costs and embedded emissions are a function of the number of cars and the kWh of batteries installed.

with squares and diamonds represent the reductions in number of cars and total installed battery capacities respectively. When only a single driver joins the shared scheme there is no technical difference between private and shared ownership and neither the number of cars nor the battery capacity is affected by the change.

As observed in Fig. 5.1, when multiple drivers quit private ownership the decrease in battery capacities is more pronounced than the drop in BEVs employed. Specifically, the shared fleet operator can already take advantage of very few users to distribute short and long journey between the owned SEVs, hence optimizing the installed battery capacities. However, the operator needs to reach a threshold of about 6 users before the opportunity to entirely remove cars arises. That is, when the community counts 6 or more private cars, on any day of the year there will be at least one car that is not driven.

The benefits in number of cars and batteries installed keep widening for larger communities until a few hundreds users are reached, after which a saturation effect is observed. If 1000 people were to give up their private cars and join a shared scheme, they would need 30% fewer cars and 70% less kWh of total battery capacity.

The solid red line and the green dash-dotted line represent the reductions

in total purchase costs and embedded emissions respectively. These indicators use the inputs of Table 5.1 to weigh the relative benefits induced by the fewer cars and the smaller batteries. The two measures display a similar pattern that starts decreasing for very few users thanks to the batteries optimisation, and further plunges when also the number of cars gets reducible. Similarly to the two underlying quantities, also purchase costs and emissions stabilise when the community reaches a few hundreds members, landing at about 50–55% of the original value.
Notably, purchase costs and embedded emissions exhibit very similar relative improvements due to the comparable ratios between car-specific and kWh-specific values presented in Table 5.1 (75 and 108 for costs and emissions respectively). The improvement in battery manufacturing process will lead to an increase of both ratios, but in a comparable manner. Therefore, the reduction in purchase costs can be regarded as an acceptable proxy for the environmental benefits in embedded emissions. In order not to crowd the following plots, the environmental gains are not explicitly presented but can be considered "captured" by the economic benefits. In addition, the closeness between economic and environmental improvements signifies that similar results are attained when optimizing the system for minimal embedded CO_2 emissions rather than for minimal purchase costs.
The shaded areas in Fig. 5.4 describe the uncertainty faced by the shared fleet operator. Specifically, for every private fleet size N, 100 different scenarios are simulated where:

- N annual trips are sampled;
- the N private BEVs are assigned an adequate battery size;
- the shared fleet manager determines the optimal fleet of SEVs.

The shaded areas represent the possible fleets that the SEVs operator should provide depending on the community to be addressed. In order to make the shared fleets comparable, they are all normalised to the same average private fleet. The shaded areas span from the 5^{th} to the 95^{th} percentile that the shared fleets achieve in every indicator.
The variability visibly drops when shifting towards larger communities. This intuitively follows from the law of large numbers. On the left side, sizing a shared fleet for a single user is equivalent to sizing the battery for a private owner. The uncertainty in battery capacity for one user is thus

analogous to the variance depicted in Fig. 5.3 (with $x_{\text{undone}} = 2\%$). To the contrary, the variability in number of cars for very small communities ($N < 6$) is null, due to the certain need to provide as many SEVs as the replaced private BEVs. Similarly to the mean lines, also the variance of purchase costs and embedded emissions results from the weighted average between the variances of the two underlying assets.
Considering a risk-averse entrepreneur, the 95^{th} line of total purchase costs may offer an indication of the number of drivers to reach to confidently approach lower investment costs. With $N < 6$ the high mobility uncertainty makes the sizing of a suitable shared fleet particularly difficult and the result might be more expensive (and unsustainable) than the original set of private BEVs. If a profit margin of at least 20% is desirable, the community size threshold moves to about $N = 10$.
Finally, Fig. 5.4 highlights the significant role that BEVs play in supporting the transition towards shared ownership. If both private and shared cars were ICEVs, the net environmental and economic benefits of the proposed car-sharing scheme would approximately follow the "number of cars" line[1]. The operator of SEVs can instead exploit the additional optimisation of batteries allocation to further increase the benefits of car-sharing: by 13% for small communities and by about 16% for larger ones.

Role of community taxonomy

In Fig. 5.4 the community is composed of drivers whose mobility patterns are extracted from any socio-demographic background. The following discussion refines this approach by building annual trips from more specific and homogeneous categories of the society. This is more consistent with the scenario of a station-based car-sharing system that manages to address only the community in its surroundings.
Income. Fig. 5.5 presents reductions in number of BEVs, battery capacity and purchase costs for two segments of society: lower income (blue solid lines) and higher income population (dashed orange lines).[2] Income is a well-known factor influencing mobility behaviour [20, 129, 130, 131]. Specifically, higher income people tend to be more mobile (see Table 2.3),

[1] A minor change would occur as the minimiser of Fig. 5.1 would select the fleet with least cars rather than with least costs.

[2] Income segments are defined by quintiles of the population, with the lower being the 1^{st} and 2^{nd} and the upper the 4^{th} and 5^{th}.

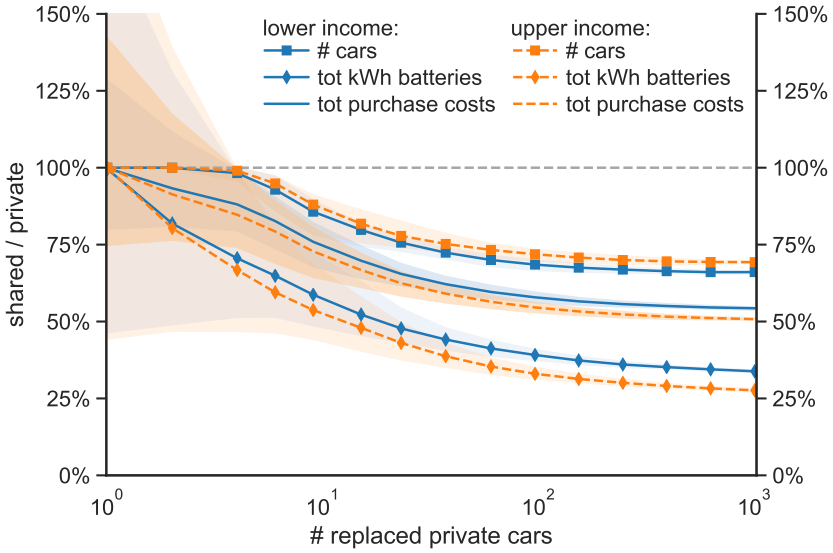

Figure 5.5: Net reductions in number of cars, battery storage and purchase costs when switching from private BEVs to SEVs for two segments of society: lower income (blue solid lines) and higher income (dashed orange lines) communities.

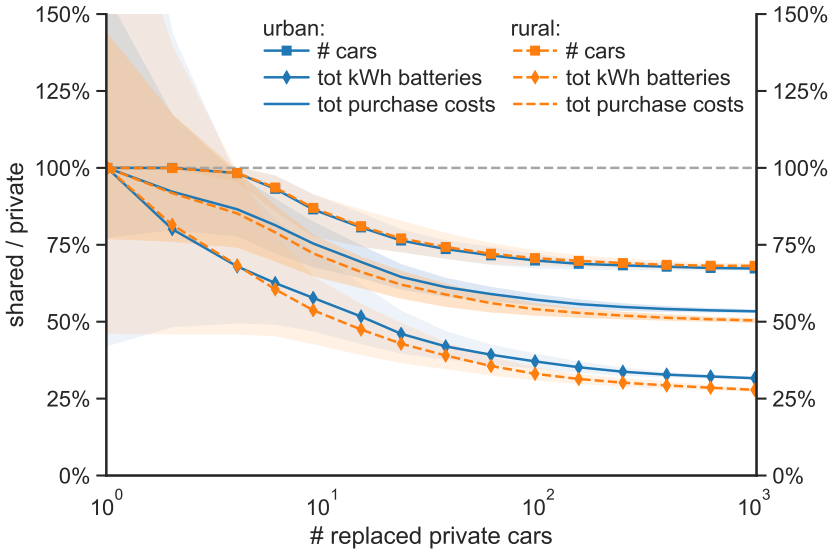

Figure 5.6: Net reductions in number of cars, battery storage and purchase costs when switching from private BEVs to SEVs for types of settlement area: urban (blue solid lines) and rural (dashed orange lines).

drive longer distances and rely more often on private means of transport such as the car. This is the reason why their potential car reduction when switching to SEVs (lines with squares) is less than for lower income communities: their frequent usage of cars increases the number of SEVs needed on any given day ($n_{\max}$) and limits the cars-saving benefit of shared own-

ership.

At the same time, the average longer distances driven by higher income individuals increase their need for long-range BEVs in the private scenario. The above discussions showed that the shared scheme is particularly efficient in optimizing the set of batteries to install on the SEVs. This explains why higher income communities benefit more than lower incomes ones in terms of battery capacity optimisation.

Ultimately, the reduction in total battery capacity outweigh the drop in number of BEVs and the higher income group nets higher cuts in purchase costs than the lower income one. If a large higher income community were to adopt the proposed station-based car-sharing scheme, it could benefit from a 50% reduction in purchase costs.

Settlement. Fig. 5.6 presents the same analysis when segmenting society by type of settlement area, that is urban in contrast to rural[3]. In this classification the rural segment is the one characterised by higher mobility needs, especially by car, both in terms of frequency and distances [130, 132]. This is why the SEV benefits exhibited by this classification neatly follow the same patterns of the income analysis, with rural areas playing the role of higher income communities.

The major difference between Figures 5.5 and 5.6 is the smaller gap between the different settlement curves compared to the ones differentiated by income. That is, income plays a larger role than settlement type in shaping the mobility characteristics that determine the benefits potential of SEVs. This finding aligns well with the correlation coefficients observed in Table 2.3.

Nevertheless, the preference for rural counties seems to contradict the general acknowledgement that urban areas are more suited for car-sharing than rural counties [17, 111, 125, 133]. However, Fig. 5.6 only considers the different mobility behaviours, disregarding another important feature of urban areas: high population density. Section 5.3.3 expands the analysis by addressing the role of population density.

Overall, higher income and rural areas exhibit a higher potential reduction in purchase costs with respect to lower income and urban communities. Similar conclusions can be drawn for embedded emissions. However, since emissions weigh the number of BEVs more heavily than purchase costs,

[3]Area types defined by the settlement size: urban with population $>$ 250000 residents, rural with population $<$ 10000 inhabitants.

the net environmental gains of higher income and rural communities is narrower than on the basis of purchase costs.

Impact of varying satisfaction rates

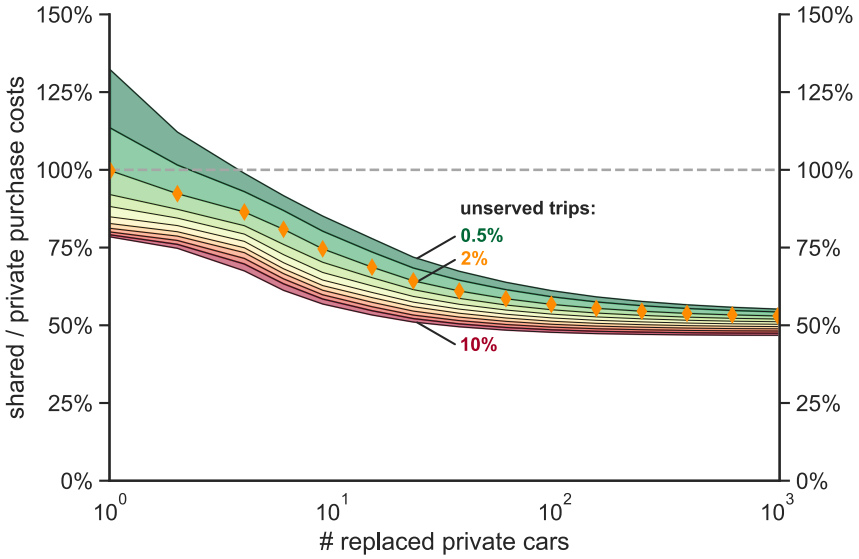

Figure 5.7: Mean purchase costs reduction for varying SEV tolerance level $x_{\text{undone}}^{\text{shared}}$ and constant private tolerance level $x_{\text{undone}}^{\text{private}} = 2\%$.

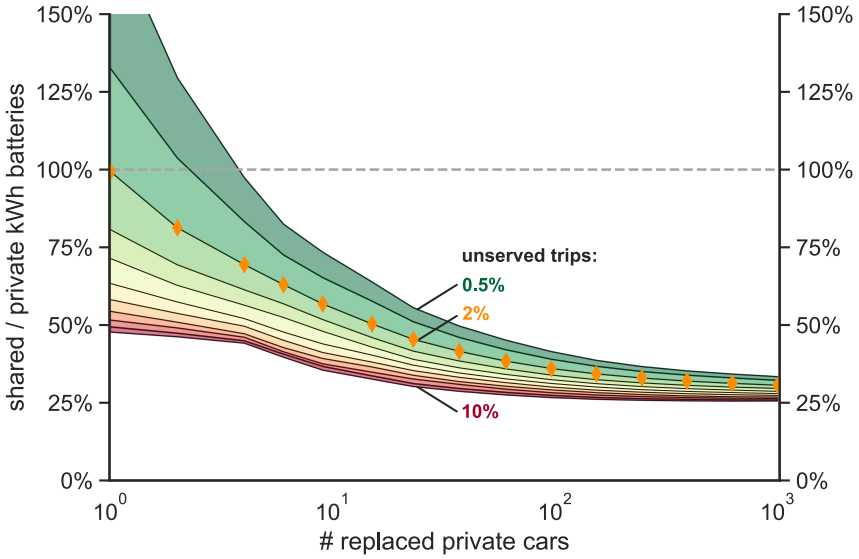

Figure 5.8: Mean total battery capacity reduction for varying SEV tolerance level $x_{\text{undone}}^{\text{shared}}$ and constant private tolerance level $x_{\text{undone}}^{\text{private}} = 2\%$.

This section explores the consequences of the car-sharing operator sizing the fleet for an unfulfilment rate $x_{\text{undone}}^{\text{shared}}$ other than the one applied by

private owners $x_{\text{undone}}^{\text{private}}$. This is not a sensitivity analysis on the $x_{\text{undone}}^{\text{private}}$ assumed for private buyers when making their purchase decision. It is rather an assessment of the business choice faced by the shared fleet operator when deciding upon the quality of the service provided. Therefore, in the following plots $x_{\text{undone}}^{\text{shared}}$ is varied from 0.5% to 10%, while $x_{\text{undone}}^{\text{private}}$ is kept constant at 2%.

Fig. 5.7 shows the purchase costs reduction achieved by the shared fleet operator for varying $x_{\text{undone}}^{\text{shared}}$ with respect to a private fleet sized for $x_{\text{undone}}^{\text{private}} = 2\%$. Although many realisations are run like for Fig. 5.4, only the mean line is shown. Predictably, the lower the tolerance rate, the higher the total purchase costs. However, for any community larger than 4 drivers the shared model is able to reduce costs even while improving the overall satisfaction rate. For higher $x_{\text{undone}}^{\text{shared}}$ the shared fleet is able to achieve even lower costs, but with diminishing marginal savings. A large community joining a shared scheme with $x_{\text{undone}}^{\text{shared}} = 10\%$ can save up to 53% of the original private costs. At the same time, the same community may enjoy a better service with only $x_{\text{undone}}^{\text{shared}} = 0.5\%$ and save 45% of the original costs nonetheless.

Fig. 5.7 can be used by the shared fleet manager as design table to link the three main features of the provided service: size of the community addressed N, purchase costs of the shared fleet C_{fleet} and related savings, and quality of the service offered $x_{\text{undone}}^{\text{shared}}$. If the community size is fixed (due for instance to the population density, as explored in Sec. 5.3.3), the fleet manager may opt to worsen the quality of the service in order to offer a cheaper alternative to private mobility.

Fig. 5.4 showed that battery sizing is the main driver of the variability in fleet costs. This is analogously the case when adjusting the satisfaction rate $x_{\text{undone}}^{\text{shared}}$ of the shared fleet. Fig. 5.8 shows the total battery capacity required by SEVs for varying $x_{\text{undone}}^{\text{shared}}$ with respect to a private fleet sized for $x_{\text{undone}}^{\text{private}} = 2\%$. The impact of $x_{\text{undone}}^{\text{shared}}$ is particularly large for small communities. Specifically, sizing the battery for a single user is the same as for a private owner: the variability of E_{batt} for $N = 1$ in Fig. 5.8 is thus the same as the mean line shown in Fig. 5.3, with the battery capacity for $x_{\text{undone}} = 1\%$ (10%) being 33% larger (52% smaller) than for $x_{\text{undone}} = 2\%$.

Also the battery capacity variability decreases for larger communities, with the amount of kWh converging towards 30% of the original capacity.

5.3.3 The role of population density

The above results presented the potential reduction in total purchase costs — and, as a proxy, in embedded emissions — achievable with varying:

- size of the addressed community N;
- mobility patterns, by income or by settlement size;
- quality of the service provided by the shared fleet $x^{\text{shared}}_{\text{undone}}$.

Of these 3 dimensions, the size of the problem plays the largest role, with the potential to alone reduce costs by up to 50% *ceteris paribus*. The possibility to reach and trigger the substitution of a large number of private cars is not trivial for station-based car-sharing systems. These are necessarily conditioned by the context where they are located and suffer from the need for users to reach the station to pick up the vehicles. If the integration of car-sharing services in a multimodal system is ignored, the potential reach of a station-based scheme is thus proportional to the population density ρ that surrounds the station. This is particularly the case for the two-way service here addressed, where users drive the SEVs on home-to-home round trips.
The following paragraphs aim at framing the discussion on costs reduction potential in terms of population density ρ rather than in number of replaced private cars N.

Linking population density and community size

Since N is an absolute quantity while ρ is defined per unit of surface area, the first step is the characterisation of the area A on which N is defined. Without multimodal transitions, A can be interpreted as the circular area of radius R that people feel comfortable to walk to reach the car-sharing station. R is here set to the distance walked in 5 minutes at the speed of 1.4 m/s [134, 135, 136], hence:

$$R = 420 \text{ m} \quad \text{and} \quad A = \pi R^2 = 0.554 \text{ km}^2$$

All the relevant quantities can now be linked with:

$$N = A \cdot \rho \cdot M \tag{5.1}$$

where M is the motorisation rate, i.e. the number of private cars per resident of any age. However, car ownership can vary greatly between city and countryside and thus correlates with the population density ρ [137, 138]. Section A.5.2 quantifies this correlation and Eq. 5.1 becomes:

$$N = A \cdot \rho \cdot \left(\frac{4506}{\rho - 7601} + 0.021 \right) \tag{5.2}$$

which directly relates the population density ρ to the number of private cars N expected in a given area A.

Car-sharing potential at varying population density

Eq. 5.2 estimates the number of *all* private cars N^{all} in reach of a station-based car-sharing service. However, the actual number of replaced private cars N can also be smaller than N^{all}. A new degree of freedom thus arises: the density ρ sets the market potential N^{all} of the car-sharing service, but the shared fleet operator may choose to address only a subset N of the available market. More precisely, the car-sharing business may offer a fleet of n SEVs that does not aim to saturate the available market.
Fig. 5.9(a) unfolds the main results of Fig. 5.4 against the two introduced degrees of freedom: population density ρ on the x-axis and number of provided SEVs n on the y-axis. Specifically, every point of the contour plot indicates the purchase cost reduction achievable when offering a shared fleet of n SEVs at a location with local density ρ. The same $x_{\text{undone}} = 2\%$ is assumed for sizing all private and shared fleets and the influence of income or settlement typology on mobility is neglected due to its very low impact (see Fig. 5.5, 5.6).
The diagonal grey dashed line of Fig. 5.9(a) is the output of Eq. 5.2 and represents the maximum number of private cars N^{all} for varying ρ. The squared grey line indicates the number n^{all} of SEVs that cost-optimally replace all N^{all} private cars[4]. These two grey lines are the projections onto the new space of the analogous-style lines of Fig. 5.4, namely the reference and the "number of cars" lines.
The contour lines crossed by the squared grey line indicate the relative shared fleet costs when replacing all N^{all} private cars; these are the same

[4] n^{all} should not be confused with $n_{\max}$: the former is the usual $n < n_{\max}$ obtained with the heuristics for $N = N^{\text{all}}$.

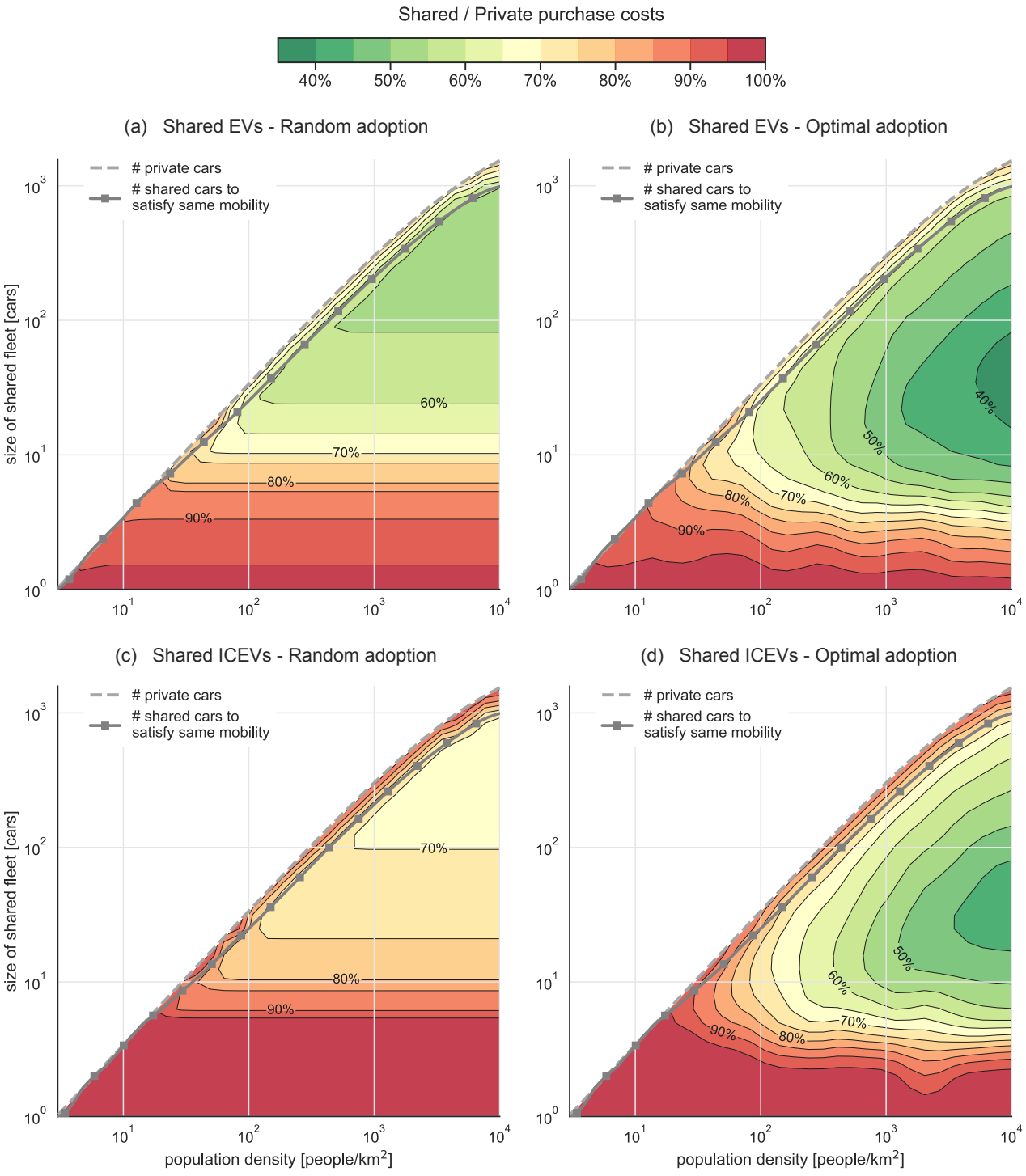

Figure 5.9: Contour plots of the purchase costs of the shared fleet relative to the private fleet being replaced; results for different local densities ρ (x-axis) and shared fleet sizes n (y-axis). The squared grey line indicates the size n required to replaced all private cars in reach (dashed grey line). When n cannot replace all private cars, cases (a) and (c) assume a random selection of the drivers joining the car-sharing scheme, while (b) and (d) assume that the least driving residents join the scheme until the mobility capacity of n is saturated. Cases (a) and (b) apply to private and shared fleets composed of BEVs, while (c) and (d) to fleets of ICEVs.

purchase costs reductions captured by the red line in Fig. 5.4. Any point between the two grey lines represents a situation where the shared fleet n is over-dimensioned and the additional SEVs are unused. The purchase costs thus sharply rise in this region. All points above the diagonal dashed line are not investigated as they would entail the illogical business choice of offering $n > N^{\text{all}}$.

For all points below the squared grey line the introduced n SEVs cannot saturate the market and may only replace a subset N of the private cars in reach. The actual number N and the related cost savings depend, beyond on n, on which private drivers choose to join the car-sharing scheme. A new adoption uncertainty emerges that links the car-sharing efficiency to the particular driving patterns of its members.

Random adoption. Fig. 5.9(a) presents the case where the people adopting SEVs are randomly sampled from the community in reach of the station. Since for any ρ mobility patterns are assumed to be the same, N private cars at high ρ drive *on average* similarly to N private cars at low ρ. This is why the purchase cost reduction in Fig. 5.9(a) do not depend on ρ but solely on n. Specifically, n SEVs manage to replace the same amount N of private cars for any ρ with at least N private cars (that is, for any ρ with $N^{\text{all}} \geq N$). With the same mobility patterns, also the gains in battery capacity are unaffected and the overall purchase cost savings remain constant.

Nonetheless, only large ρ contain enough private cars to make large n sensible and profitable. For example, only for $\rho > 700$ people/km^2 the shared fleet manager can offer $n > 90$ SEVs that, if allocated, ensure a cost reduction of more than 45%. This is where the urban context gains an edge over the rural one: only high densities entail the large fleet sizes that unlock, following Fig. 5.4, the profitable scale effects of car-sharing systems.

Optimal adoption. Fig. 5.9(b) displays the relative purchase costs when only the most suitable drivers within the pertinent zone decide to join the shared scheme. For n SEVs made available to the public, a varying N of private cars may get replaced depending on the compatibility of their mobility patterns. In this work, the propensity to join the car-sharing system is set proportional to the number of days the private car is not driven. When $n < n^{\text{all}}$ SEVs are offered at a location, only the $N < N^{\text{all}}$ cars with the least driving days are dropped in favour of SEVs. N is

determined so that the usage capacity of the n SEVs is saturated.

If the $(N+1)^{th}$ driver has a better mobility compatibility with the shared fleet than the N^{th} driver, the latter is still chosen to join the shared scheme due to its lower number of driving days. The selection is thus greedy and made from the point of view of the private car owner, who decides whether to join the car-sharing scheme independently from other mobility patterns. Nonetheless, the car-sharing scheme greatly profits from this selection process, as infrequent drivers occupy SEVs for fewer days leaving room for more members to join.

When shifting towards higher ρ, the pool of drivers that can join the car-sharing system widens. It thus gets more likely to encounter particularly non-driving candidates. This explains the sharper decline in fleet costs of Fig. 5.9(b) compared to Fig. 5.9(a).

This freedom of choice vanishes when n approaches the n^{all} squared line. In these cases the n^{all} SEVs are aiming to replace all N^{all} cars available in the area, leaving no room for selective adoption. Therefore, the relative shared fleet costs in the region between n^{all} and N^{all} are the same as in Fig. 5.9(a).

For medium-to-high ρ the cheapest adoptions are achieved for compromising fleet sizes: when n grows the aforementioned selective adoption weakens; with smaller n the beneficial scaling effects of car-sharing remain locked. This results in an "optimal" middle pathway, that provides the ideal shared fleet size n^{opt} at any given ρ. A smooth approximation of this optimal pathway is shown in Fig. 5.10 with the square-dotted orange line. These optimal fleets manage to accomplish much lower costs than their random counterpart in Fig. 5.9(a), approaching 38% of the original private costs at high ρ.

Sharing of ICEVs. Figures 5.9(c) and (d) show the same results with both the private and shared fleets composed of ICEVs. When replacing the private fleet with the shared one, the minimisation of purchase costs of Fig. 5.1 simplifies to the direct selection of $n_{\min}$.

The trends exhibited by the two ICEV plots are the same shown by the BEVs graphs. In the random adoption case (c) the cheapest fleet conversions are still achieved for high ρ and n, but the resulting costs reductions are significantly smaller than in the BEV case (a). In the optimal adoption approach (d), the gap from the BEV performance (b) decreases, with the ICEV shared fleet achieving important cost reductions for high ρ and

middle n. The reason for the narrower gap in the optimal case is that the selection of the N "optimal" drivers is based on the number of driving days and ignores the distances driven. This approach affects BEVs and ICEVs in the same way and does not enhance the SEVs capability to absorb long-range requirements in fewer cars. Nonetheless, the optimal adoption of SEVs unlocks larger costs reductions than optimally shared ICEVs since the efficient allocation of battery capacities still rewards the costs ratios of BEVs.

Summary. The expanded analysis of Fig. 5.9 confirms the observation made for Fig. 5.4 that BEVs multiply the economic and environmental convenience of shared ownership. This holds true regardless of the adoption behaviour assumed. Nevertheless, optimal adoption can lead to significant cost reductions, especially for high ρ, making the urban context even more vital for the success of car-sharing.

Beyond enabling further economic savings, optimal adoption shifts the best strategy of the shared fleet manager to more practical fleet sizes, with $20 < n < 90$. If the fleet manager can convince the most suitable drivers of high density areas to join the shared scheme, the best fruits of car-sharing can be harvested without reaching hundreds of vehicles in the fleet. Additionally, the car-sharing subscribers may feel more comfortable when sharing their vehicles with fewer users. However, the fleet manager has no certainty that the optimal adoption scenarios (b) or (d) will occur rather than the random (a) or (c). Realistically, any case in between may materialise depending on people's awareness of their travel behaviour and the economic rationality of their decisions. The next section explores how this adoption uncertainty affects the cost-benefit analysis of the shared fleet operator.

Attainability of optimal SEVs adoption.

This last section investigates the car-sharing profitability under two fleet sizing strategies: one that aims at replacing all private cars in reach of the station and another that hopes to persuade only the most convenient subset of drivers in the area. Both approaches are described by the respective pathways in Fig. 5.10: the grey lines depict the replace-all plan, while the orange ones focus on the optimal subset; in both cases, the squared lines indicate the number of SEVs and the dash(-dotted) lines the number of replaced private cars.

The optimal pathway is defined by setting the number of replaced private

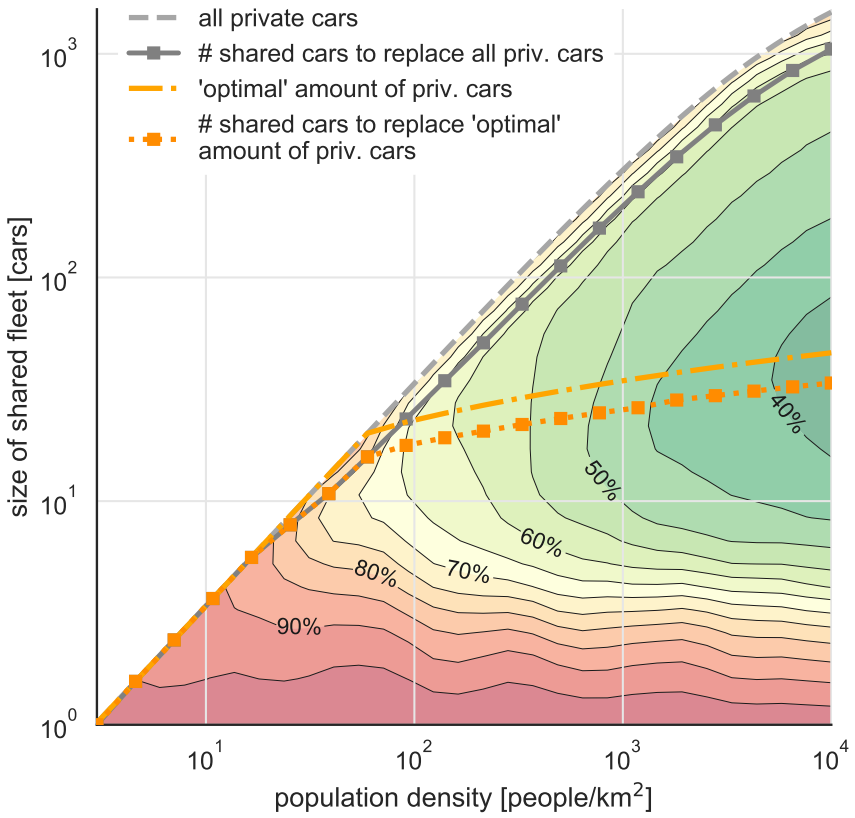

Figure 5.10: Two pathways used to design the shared fleet: by addressing all private cars in reach (grey lines) or only a subset of them (orange lines). The relative shared fleet costs indicated by the contour lines are achieved if the subset is optimally selected with the least driving residents in the area.

cars N^{opt} equal to:

$$\begin{cases} N^{\text{opt}} = \text{Eq. 5.2 } (\rho) & \text{for } \rho \leq 60 \\ N^{\text{opt}} = 5 \log \rho & \text{for } \rho > 60 \end{cases} \tag{5.3}$$

The optimal size of the shared fleet n^{opt} is generated by the simulation and depends on the individual realisations. The average size depicted by the orange squared line in Fig. 5.10 can be approximated by:

$$\begin{cases} n^{\text{opt}} = 0.34\rho - 0.0013\rho^2 & \text{for } \rho \leq 60 \\ n^{\text{opt}} = 3.8 \log \rho & \text{for } \rho > 60 \end{cases} \tag{5.4}$$

Beyond comparing the profitability of the two pathways, this sections aims to investigate the uncertainties involved. To this end, the iterative Alg. 4 is employed.

Algorithm 4 Iterative process to derive uncertainties of Fig. 5.11. For every private or shared fleet the respective purchase costs are computed.

1: **for** each ρ **do**
2: $N^{\text{all}} = \text{Eq. 5.2 } (\rho)$
3: $N^{\text{opt}} = \text{Eq. 5.3 } (\rho)$
4: **for** *scenario* j **in** $[1:30]$ **do**
5: generate N_j^{all} individual annual trips
6: compute n_j^{all}
7: **for** *realisation* k **in** $[1:30]$ **do**
8: sample $N_{j,k}^{\text{opt}}$ random trips from N_j^{all}
9: compute corresponding $n_{j,k}^{\text{rand}}$
10: **end for**
11: $n_j^{\text{opt}} = \sum_k n_{j,k}^{\text{rand}}/30$
12: assuming optimal adoption, determine the most profitable N_j^{opt} and the resulting n_j^{best}
13: assuming worst adoption, determine the least profitable N_j^{opt} and the resulting n_j^{worst}
14: **end for**
15: **end for**

This iterative approach addresses the two uncertainties faced by the shared fleet designer:

- the location uncertainty, i.e. the variability in mobility patterns encountered in the area where the station is located: it is explored via different *scenarios* for the same ρ (lines 4–6);
- the adoption uncertainty, i.e. the variability of which users living in the area would actually join the car-sharing scheme: it is explored by testing various random *realisations* within the same *scenario* (lines 7–11); additionally, the best (optimal) and worst possible adoption cases are simulated for each *scenario* (lines 12–13).

The results of this procedure are shown in Fig. 5.11. The graph is analogous to Fig. 5.4, although only the number of cars (squared lines) and the total purchase costs (unmarked lines) are shown for both strategies. Each x-coordinate refers to a unique ρ and the corresponding private fleet sizes N^{all} and N^{opt} as determined by the pathways.

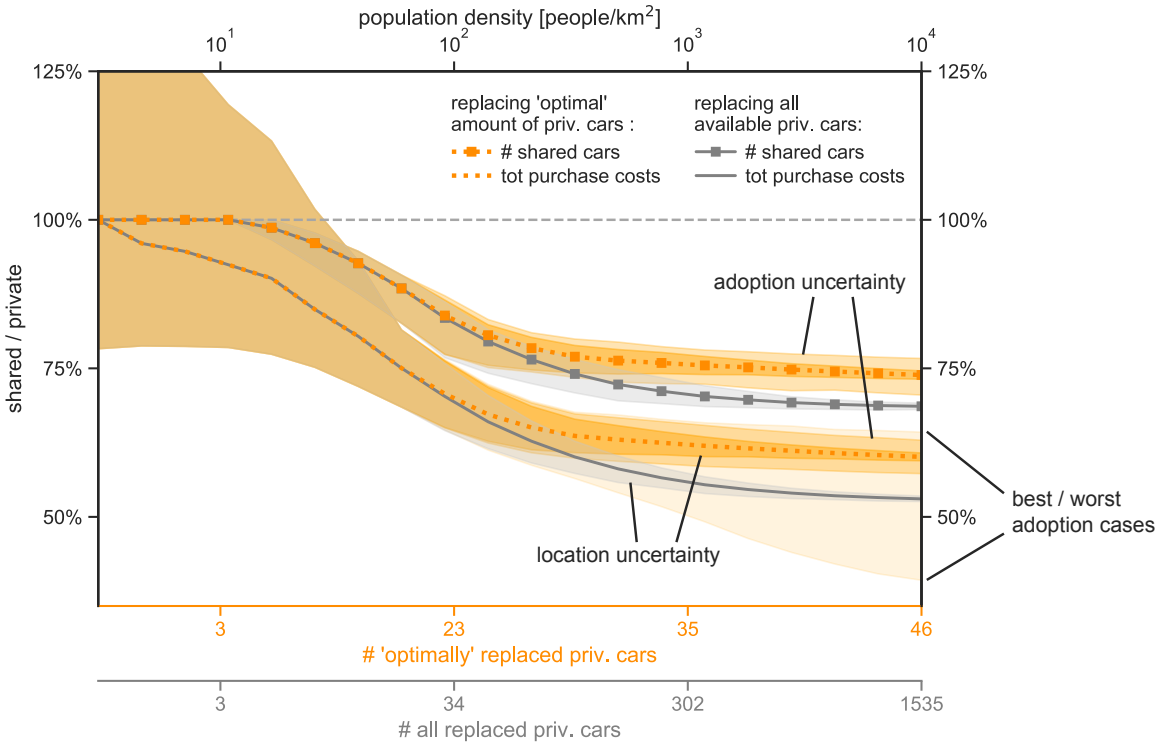

Figure 5.11: Purchase costs (unmarked lines) and number of cars (squared lines) of the shared fleet relative to the private fleet being replaced; results for two design strategies: by replacing all cars in reach (grey x-axis and lines) or only a subset of them (orange x-axis and lines). Shaded areas depict the variances involved: $5^{th} - 95^{th}$ percentiles for location and adoption uncertainties, and the best/worst adoption outcomes of the subset approach. Best/worst cases are not shown for the number of cars in order not to crowd the figure.

The grey solid lines and shaded areas represent the replace-all strategy with its uncertainties (displayed as $5^{th} - 95^{th}$ percentiles range). The patterns follow the same results exhibited in Fig. 5.4, as this also assumed a replacement of all private cars in reach. As in that case, the costs variance is solely due to the location uncertainty and is inversely related to the population density: the lower ρ the least predictable the mobility needs of the few drivers in the area. Higher ρ entails larger fleets that, with the law of large numbers, help reducing the variability in mobility patterns and shared fleet costs.

The orange dotted lines and shaded areas describe the economic potential of replacing only a subset of the private cars in the addressed area. The mean number of cars and purchase costs are always higher than the respective trends of the replace-all strategy. This is because the smaller private fleet size does not lead to profitable scale effects if the subscribers

are randomly selected. This is the same phenomenon displayed in Fig. 5.9(a), where N randomly selected drivers achieve the same profitability regardless of the density they are extracted from.
The subset approach is however subject to multiple uncertainties, which are displayed in Fig. 5.11 with different shades of orange. The darkest inner shade represents the location uncertainty, which, being a function of ρ, affects this strategy in the same way as the replace-all one. The second middle shade describes the adoption uncertainty, depicted by the $5^{th} - 95^{th}$ percentiles resulting from all random *realisations*. The random selection of N^{opt} drivers does not achieve significant costs reductions compared to the average case: the most convenient 5^{th} percentile is more expensive than the replace-all approach for any $\rho > 400$ people/km^2.
To reach significant savings, the adoption behaviour has to be optimally managed as done in Fig. 5.9(b). This enables the costs reductions depicted by the faintest orange shade of Fig. 5.11, which achieves 38% of the original private fleet costs for $N^{\text{opt}} = 46$. These relative fleet costs cannot be achieved by the replace-all approach for any fleet size, but require an ideal adoption behaviour which might not occur. When choosing the strategy to adopt at high ρ, the shared fleet manager is weighing the profitable scale effects of larger fleets against the possibility to exploit the easier integration of the least frequent drivers in the area. The latter solution may grant lower capital expenditures but is subject to more uncertainty.

5.4 Potential applicability

Fig. 5.12 shows for every British MSOA[5] the purchase costs of the shared BEV fleet relative to the dismissed private BEV fleet, assuming the replace-all approach. Apart from the least inhabited regions, every MSOA can lower fleet costs by more than 20%, with urban areas approaching 50% reduction.
These robust results represent a technical potential, which assumes that private owners in the area give up their cars to join the car-sharing system until there is capacity; i.e. the shared fleet is never overdimensioned or left unused. Equivalently, each driver is modelled as a *homo economicus*

[5]In this work, MSOAs refer to the British census output areas, i.e. the smallest geographical units used to cluster census data. These areas namely are the Middle layer Super Output Areas of England and Wales and the intermediate zones of Scotland.

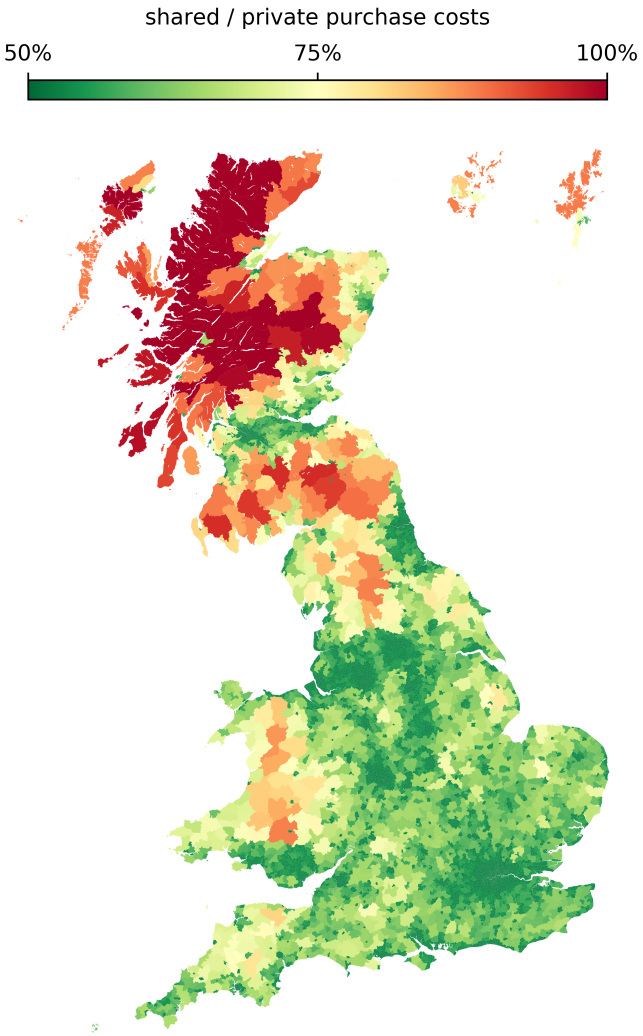

Figure 5.12: Relative fleet costs when shifting from private to shared BEVs. Every MSOA[5] of Great Britain has different potential depending on the local population density.

who would join the car-sharing scheme whenever possible in order to benefit from the lower costs. While this is an acceptable first-order approximation, non-monetary considerations such as comfort or model choice should also be considered.

Importantly, all environmental and economical operational aspects have been neglected. Purchase costs have principally been employed as proxy variable to account for both the number of BEVs and the total battery storage installed. To assess the effective economic soundness and sustainability potential of SEVs, more dedicated and comprehensive analyses should be carried out. Finally, the quick improvements of battery manufacturing processes entail that the number of vehicles will weigh more toward the proxy purchase cost variable. Results such as Fig. 5.4 might thus see a

slight increase in purchase cost and embedded emissions relative to the equivalent private BEV fleet.

Chapter 6

Conclusions and Outlook

This thesis deepens the comprehension of private passenger transportation in order to adequately address the most pressing needs surrounding electric vehicles (EV). EVs are one of the essential strategies to decarbonise passenger transportation but their introduction entails a series of problems whose resolution requires, among other aspects, an extremely refined picture of car usage cases. This level of detail is available, in raw form, in traditional household travel surveys (HTS), which are also characterised by statistically significant samples and advantageous spatio-temporal distributions. This thesis expands the descriptive power of HTSs and presents a validation of their employment in EV simulations to legitimate this kind of use case. The subsequent applications of HTS-based EV models provide helpful insights into the technical potentials and limitations of EVs.

This thesis in a nutshell

This work starts by characterising HTSs and proposing solutions to some of their possible shortcomings. Firstly, a procedure is provided to derive the actual driving frequency of cars from HTSs which do not have a full picture of car mobility. Secondly, a methodology to synthesise long-term car usage profiles (e.g. annual) from the daily and weekly records typically available in HTSs is proposed. The usage profiles so obtained are suitable for any analysis which simultaneously requires an accurate picture of both intra-day and multi-day mobility.
To specifically address EVs, their energy flows have then been modelled. Among charging strategies the focus has been given to plain plug-and-charge schemes due to their easier reproducibility and hence suitability for the subsequent validation. This straightforward charging behaviour

has nevertheless been refined in order to emulate the realistic plugging-in propensity of EV drivers. The favourable comparison between the charging loads obtained from the resulting model and the empirical loads measured in four different EV trials supports the soundness of the entire simulation chain.
The annual mobility model has then been used to explore the electrification potential of private BEVs when accounting for both the variety of car use cases and the variability of day-to-day mobility needs throughout the year. The marginal benefits offered by longer BEV range, opportunity charging and consent to alternative means have been investigated.
As an exemplary application of the charging profiles developed in this thesis, a brief discussion on the output of power dispatch models is presented. Particular focus is given to the simulated greenhouse gas (GHG) content of the electricity fed into BEVs since it has a strong impact on the overall environmental performance of BEVs.
Finally, the annual mobility model is applied to investigate the potential of EV-sharing setups to reduce the overall demand for vehicles and battery capacity.

Key insights

The validation of the HTS-based EV model presented in Chapter 3 gives legitimacy to all studies that employ analogous approaches. The aforementioned advantages of HTSs justified their extensive employment in many EV investigations, but a comprehensive validation of such utilization was missing. Future EV research can keep fairly relying on traditional HTSs even when stemming from rather unelectrified fleets.
The annual mobility model proposed in Section 2.2 is helpful for all those analyses that require an adequate picture of the variance in mobility performance beyond its mean value. Applications such as the eligibility to join a car-sharing service, the design of an optimal fleet portfolio or the estimation of the fleet-average utility factor of plug-in hybrid EVs (PHEV) can return widely different results depending on the degree of inclusion of mobility variance.
Section 2.3 shows that the charging behaviour observed in various EV trails can be elegantly reduced to a single stochastic function where the decision to plug in the battery electric vehicles (BEV) solely depends on the battery state of charge. This decision function can be easily integrated into future

EV studies to model the charging propensity in plug-and-charge scenarios. The analysis on the electrification potential of BEVs presented in Section 4.1 reveals that, when considering the entire annual mobility, extending BEV range is not enough to successfully replace a large share of conventional cars. The possibility to charge at work is also superfluous if home charging is accessible since commuting distances are rarely the critical factor. However, ubiquitous charging is quite helpful, especially with short-to-medium BEV ranges, because it unlocks many leisure trips that would otherwise be inaccessible. But the largest potential is unlocked by providing drivers with alternatives for the few very long trips of the year: these alternatives can be simple *en-route* fast chargers, rentable HEVs or public modes of transport. For instance, a 300-km BEV with only home charging can satisfy the same demand of a 600-km BEV with ubiquitous charging with only 7 additional days requiring adaptation.
Section 4.2 aggregates a typical outcome of power dispatch models that make use of EV charging profiles: the GHG intensity of the electricity supplied to EVs. The results from two different dispatch models show that in any investigated scenario the GHG intensity of the Swiss grid will remain rather low, making BEV the most sustainable powertrain even when compared to a gas-fuelled hybrid vehicle over the full life-cycle. In general, the very high efficiency of the powertrain makes BEV the most sustainable car technology whenever the GHG content of the electricity is lower than the output of a combined cycle gas turbine.
Finally, the EV-sharing investigation of Chapter 5 shows that tangible benefits are possible for a wide range of service sizes, but that the largest gains are achievable in dense areas. These contexts link the possibility to reach many users and benefit from scaling effects with the higher likelihood of encountering particularly inactive drivers who are the most suitable profiles to join car-sharing systems.

Proposals for improvements and expansions

Data sources. The presented mobility model heavily relies on HTSs, especially for the description of intra-day mobility. This approach is successful also thanks to the high quality of the two specific HTSs here employed (MZMV from Switzerland and NTS from the United Kingdom). Both HTSs track every single movement of the respondents and take note of which household car is driven in any leg. However, there are HTSs that

solely ask for the longest or more relevant trip of the day [139]. Nevertheless, access to high-quality mobility data should not be at risk in the future: on one side national statistical offices are comprehending the importance of reliable travelling information about their citizens, on the other smarter mobility tracking systems are becoming available [139, 140].

Additionally, HTSs manage to properly track, as the name suggests, *household* mobility. HTSs may miss vehicles and movements purely related to professional duties. The share of national mobility missed by HTSs depends on the specific boundaries of the survey. The British HTS, for instance, includes cars available to the household but owned by a firm; it however asks not to report legs related to carrying people or goods for professional reasons. For investigations on the electrification of captive or business fleets, the relevant mobility sources should be employed.

Methodology. While the construction of long-term car profiles presented in Section 2.2 is flexible, the best results in terms of mileage distribution are obtained when clustering HTS records by the self-reported car annual mileage. Unfortunately, this information is severely rounded and approximated by respondents. An impartially measured annual mileage would be a considerably more reliable source for this methodology. However, datasets that simultaneously contain intra-day mobility details and reliable annual information would be expensive to build and are currently extremely rare. Nevertheless, the validation in Section 3.2 shows that the annual mobility profiles constructed from the self-reported car mileages can already capture much of the existing variance.

The stochastic charging behaviour proposed in Section 2.3.2 has been derived from EV trials with BEVs with rather small battery capacities. It is not guaranteed that drivers of larger BEVs would exhibit the same charging decision process. Once access to the relevant data is provided, an estimation of the charging behaviour of larger BEVs can be carried out with the same methodology here applied to smaller BEVs.

An estimation of the charging behaviour of PHEV drivers would be extremely useful since it could inform about the actual sustainability of this powertrain. The methodology here applied to BEVs could, with few extensions, be employed to perform this assessment. However, the importance of this evaluation urges for dedicated and extensive on-field measurement campaigns [141].

The proposed BEV charging likelihood function could be used as a first-

order approximation of the plugging-in decision process in smart charging contexts. Specifically, it could be argued that BEV drivers would welcome actively managed charging only when assured about the low intrusiveness of the system: BEV drivers might then keep behaving as with plug-and-charge schemes [48]. Nevertheless, this may not fully hold true, especially in case the local operator offers incentives to keep the BEV plugged in as much as possible. However, assuming that BEV drivers would indeed always plug in the car at every opportunity as currently done in most smart charging studies can also represent a dangerous over-simplification [142, 143]. It is thus recommended to investigate the specific plugging-in propensity of BEV drivers under different smart charging designs and incentive schemes.

Charging costs have been neglected. The proposed function in terms of state of charge seems to successfully describe the behaviour of EV drivers, but it has been tested in contexts with few charging options. When competing charging alternatives are available it is possible that the different costs of charging influence the plugging-in preferences of drivers. Future works should take this into account by modelling EV drivers' elasticities and their monetisation of range anxiety.

Validation. These limitations of HTSs and charging behaviour curb the applicability of the charging load validation proposed in Section 3.1. EV simulations and trials involving larger BEVs would be required to give a stronger legitimacy to HTS-based EV models. However, the current validation already fills an important gap of the research field and the current success of HTS-based models suggests that further efforts towards an enhancement of the validation may be unnecessary. Furthermore, EV introduction in fleets is proceeding at a high rate and it will soon be possible to directly rely on the EV subset of HTSs from particularly electrified countries (such as Norway or California). Such data will combine the high statistical power of HTSs with the specific driving routines of EVs.

EV-sharing systems. Chapter 5 analyses the case for shared EVs in the form of two-way station-based schemes since these are the prototypical form of car-sharing. It is of course important to also investigate the employment of EVs in less traditional sharing schemes such as with free-floating cars.

The proposed two-way car-sharing system could be analysed in a zero-dimensional fashion, ignoring the spatial distribution of mobility patterns. The assessment of more asymmetric systems would necessitate an accurate

modelling of this spatial component with the consequential higher demand for mobility data and computational power.
Shared EVs have been here analysed only in terms of initial investment and footprint, that is their operation has been neglected. Complete and discounted techno-economical analyses should be carried out to assess the actual sustainability and profitability of these mobility systems.

Outlook to the future

Beyond enhancing the understanding of car usage, supporting EVs diffusion requires further investigations in complementary fields.
EV charging. While plug-and-charge schemes can be fully addressed by the proposed model, smart charging necessitates a deeper understanding of drivers' propensity to share their batteries and of the monetary value assigned to this choice. Additionally, the legal framework in terms of privacy guarantees and accountability has to be developed; the general IT architecture to efficiently and securely manage these systems should also be established [142, 144].
These argumentations apply to both mono- and bi-directional smart charging. However, the latter may entail serious advantages for the whole system, which could then rely on a large and distributed electricity storage to handle intra-day production fluctuations [145, 146]. This would be particularly important for countries that cannot rely on other short-term storage systems such as pumped-hydro power [101].
Carbon intensity of charged electricity. While the specific CO_2 intensity of the grid impacts the environmental performance of EVs, more precise estimations of the exact mix used to charge the EV may be unnecessary. The urgent (and faster) decarbonisation of the power sector is shifting electricity mixes towards ranges where EVs would unlikely fall behind other powertrains under any conditions. Exact specifications of the charged mix would thus not bring substantial value in determining the most sustainable technological option.
Nevertheless, after the successful uptake of EVs, legislators may wish to adopt a more technology-neutral approach and could thus resort to WTW or LCA approaches accounting for the CO_2 content of the electricity. In this scenario, the average electricity mix could be used as a good first approximation. If more differentiation is desired, certificates of origin (i.e. electricity labels) could then be employed: these would be simple for tax

offices to check and would not require complex tracing systems of the physical electrical flow.

BEV range. As already acknowledged in literature and here reaffirmed, the limited range of BEVs is often a rhetorical argument with no substantial foundation, apart from some specific use cases [51]. Long trips are extremely rare and usually occur on specific arterial roads. It is thus more convenient to strategically place fast-charging stations in those segments. Nevertheless, drivers may be discouraged by the longer "refuelling" times of these *en-route* stops. Efforts should thus go on one side towards the enhancement and standardisation of fast charging technology and on the other towards a strategic placement and expansion of charging stations in arterial roads [147]. Analogously, battery swapping technology seems unnecessary given the few times a year the swap would occur. While some users may benefit from this fast recharging option, existing alternatives such as fuel-cell or plug-in hybrid cars could also serve the purpose.

Future of mobility. All these arguments apply to today's mobility paradigm. However, important technological and cultural disruptions are on the horizon, especially autonomous vehicles and mobility as a service [122]. While their profitability will largely determine when and how they may succeed, regulators must make sure that these innovations, including EVs, stay on a sustainable track. This includes environmental concerns such as the rise in vehicle-km, hence energy demand, likely caused by driverless cars [120, 119]. However, sustainable development also involves social considerations like the working conditions of extraction points of raw materials for batteries and electronics [148, 149] or the reallocation of jobs lost in the traditional automotive industry due to the reduced demand for vehicles and parts [150]. The discussion should not neglect the role of public transport since, despite its problematic profitability, it is a necessary pillar for efficient passenger transportation systems [123].

Appendix

A.1 Car locations on different days of the week

This sections presents a more detailed breakdown of the locations of Swiss active cars on specific days of the week. Fig. A.1 provides the same information of Fig. 2.4, but for average weekdays (Monday–Friday), Saturdays and Sundays. As usual, all the plots refer solely to cars which have been driven on those days.

The graphs show that the car patterns drastically change between different days, hence affecting the charging opportunities the EVs may encounter. Weekdays expectedly show the highest percentage of vehicles parked at Work, whose share reaches 40% in the morning. Weekdays also present the largest rush hour, with 13% of the cars being mobile between 5 p.m. and 6 p.m.

Saturdays and Sundays present a considerably higher share of cars at Home. Since all plotted vehicles are being driven, this observation reveals that weekends' car movements are combined with rather short stops away from Home. The only significant exceptions are stays at Other people's Houses, such as friends or family members. Two last noteworthy patterns are stops at Services on Saturdays and visits to Food & Drink businesses on Sundays. All these observations endorse the plausibility of the underlying data, but also introduce uncertainty regarding viability and influence of charging at points of interest.

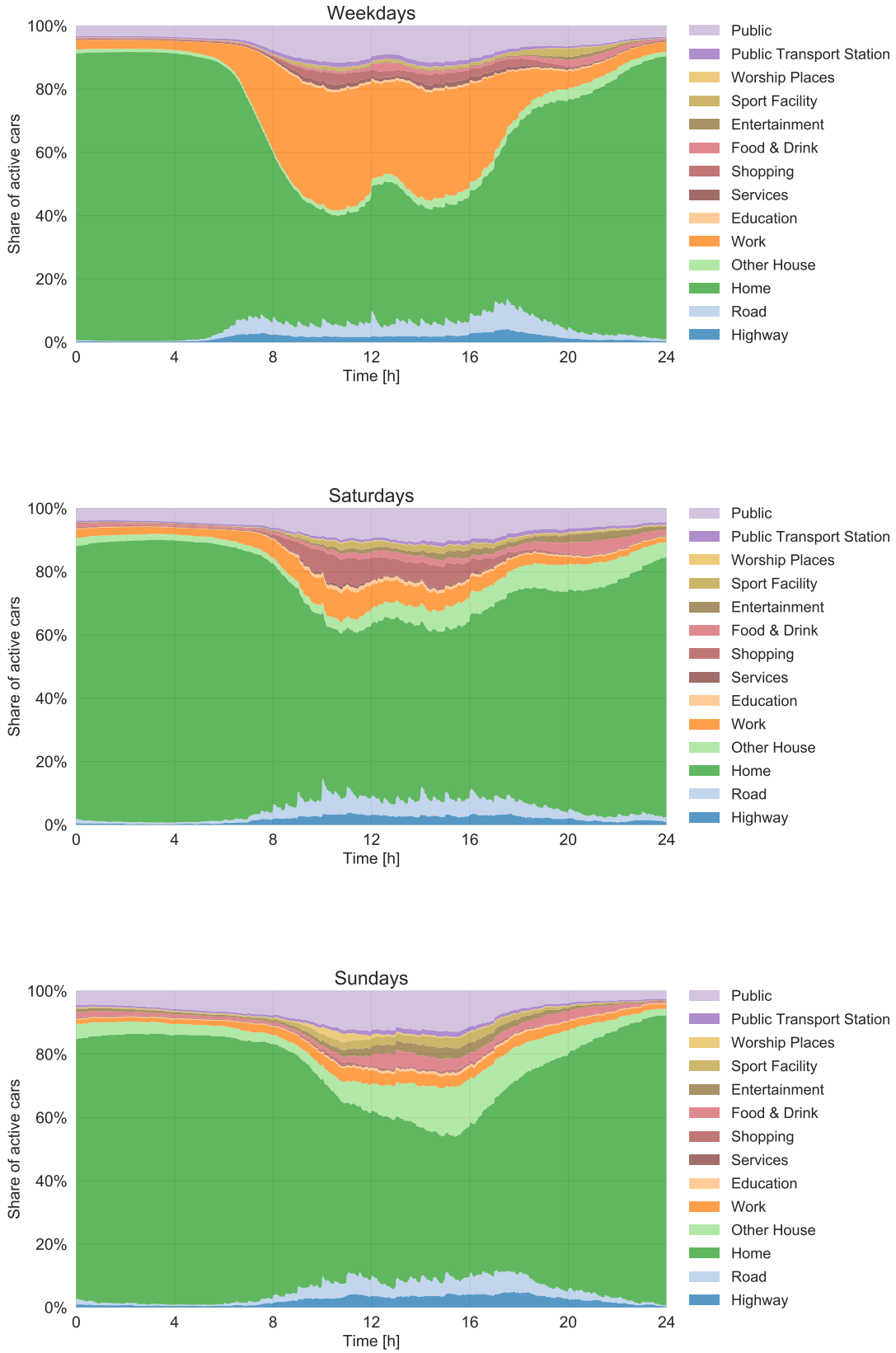

Figure A.1: Car locations and activities on specific days of the week. Only cars which are used at least once during the day are included.

A.2 EV battery properties

Battery technology is evolving very rapidly, with both improvements in the manufacturing of established technologies and the development of more advanced chemistries (cite EU2020). This progress will improve various EV performance indicators (range, environmental footprint, price) and will shift the favour of typical powertrain assessments closer to EVs. This thesis employs the specifications of state-of-the-art Li-ion batteries and the results thus reflect today's technological status. This implies that most results can be regarded as conservative estimates of future trends.
To contextualise the assumptions made in this thesis, the foreseen improvements in battery technology are here presented. Fig. A.2 shows the current and future estimates of battery energy densities from various sources [6, 12, 151, 152, 153, 154, 155]. All values refer to the energy content per kg of battery pack, thus including sealing and casing.

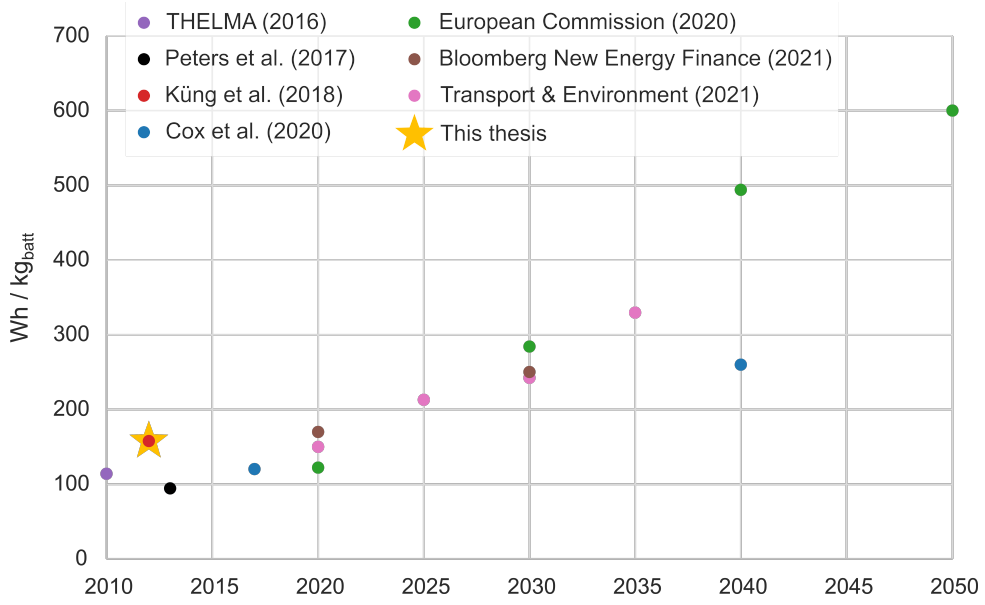

Figure A.2: Present and future estimates for the energy density of EV batteries with respect to the weight of the entire battery pack.

Current state-of-art batteries energy densities lie around 150 Wh/kg, but quick improvements to up to 600 Wh/kg are foreseen for the mid of century. Some studies ignore the introduction of new battery chemistries (e.g. Transport & Environment [155]) and thus display lower gains compared to analyses that model the introduction of solid-state or Na-ion batteries (e.g. the European Commission report [153]). This thesis uses the value of

157.5 Wh/kg as proposed by L. Küng [6] following the 2012 specification of cell energy density by Panasonic of 225 Wh/kg. This measure is higher than other estimates from the same time period, but can reflect the status of battery technology at the time of writing (2021) and in the near future. However, there is general agreement that battery energy densities higher than 200 Wh/kg should be assumed after 2025.

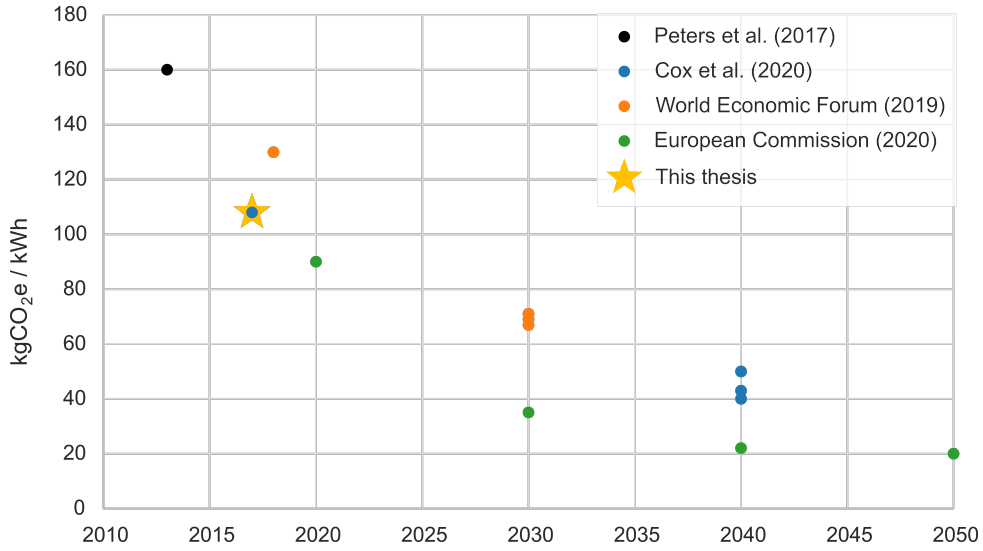

Figure A.3: Present and future estimates for the life-cycle emissions of EV batteries considering the production of the entire battery pack.

Figure A.3 displays the current and future estimates of greenhouse gas (GHG) emissions from life-cycle assessments (LCA) of EV batteries [12, 126, 152, 153]. As in the former plot, emissions related to entire battery system are considered. Current LCAs place the footprint of batteries at around 120 $kgCO_2e/kWh$ but this estimate is subject to large uncertainties due to the difficulty in modelling all energy and material flows linked to battery manufacturing. Nevertheless, all studies foresee a dramatic reduction in life-cycle emissions thanks both to the decarbonization of energy inputs and to the lower material needs per energy content shown in the previous plot. This thesis uses the estimate for 2017 provided by Cox *et al.* [12] of 108 $kgCO_2e/kWh$, considered representative for state-of-the-art batteries at the time of writing. However, the quick foreseen improvements may make such value quickly obsolete and LCA footprints lower than 80 $kgCO_2e/kWh$ should be assumed after 2030.

A.3 Charging behaviours

This section reports in detail all charging behaviours of the analysed trials and of the tested scenarios. Charging behaviours are here presented with the S curves introduced in Fig. 2.9 and 2.10, curves that indicate the likelihood of plugging in an EV for a given SOC of its battery. In other words, these S curves are the survival function (i.e. inverse of the cumulative distribution function) of the normally distributed SOC threshold below which the EV would be plugged in.

A.3.1 EV trials

Figure A.4 and Table A.1 report the charging behaviours extracted from the EV trails with the Algorithms 2 and 3 in Section 2.3.2. This procedure is applied only to charging data of BEVs and the SOC threshold is thus modelled by normal distributions truncated on the lower tail. This is the reason why all curves start from a probability of 1 with a depleted battery.

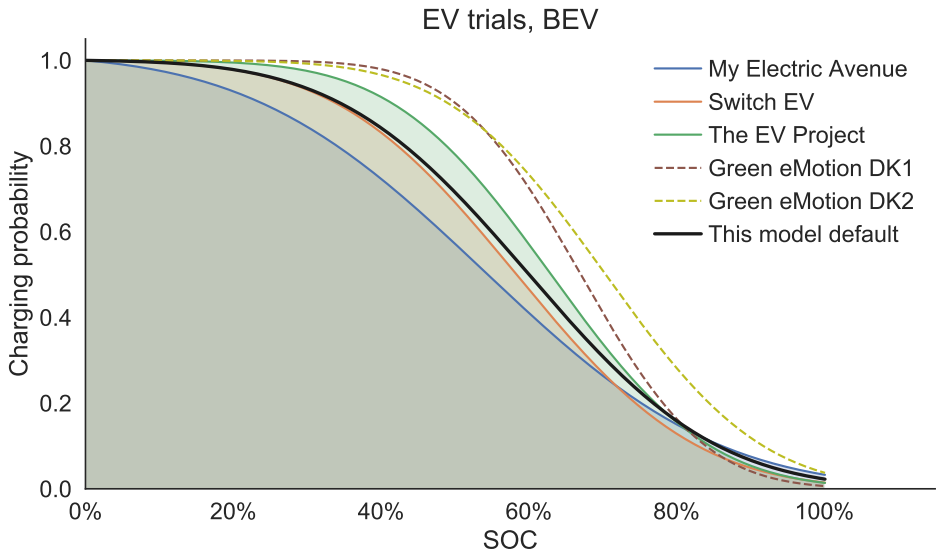

Figure A.4: Charging behaviours derived from the empirical data reported by the EV trials. The curves are derived only for BEVs.

With the data reported by the Green eMotion trial [84] Algorithm 2 can be directly applied to two of its demo regions — DK1 and DK2. The resulting charging behaviours are shown with dash lines. With the incomplete information from the other three trials — My Electric Avenue [70], Switch EV [81], The EV Project [82] — the iterative Algorithm 3 must

	μ	σ	weight
Green eMotion DK1	0.67	0.13	1
Green eMotion DK2	0.70	0.17	1
My Electric Avenue	0.54	0.25	4
Switch EV	0.58	0.19	4
The EV Project	0.63	0.17	4
This study default	0.6	0.2	

Table A.1: Parameters of truncated normal distributions extracted from the EV trials. The default settings for this study are obtained as weighted average of the single trails' parameters.

be applied. This procedure returns multiple charging behaviours for each field test (see Fig. 2.11). The solid lines in Figure A.4 and the values in Table A.1 illustrate the charging behaviours that each trial converges to. This thesis adopts the weighted average of the single trials' parameters as default charging behaviour. The weights approximately measure the quality of the data provided by the demonstrators. Specifically, the use case of the BEVs employed in the Green eMotion trials is either unknown (DK2) or unsuitable (a captive fleet is tracked in DK1).[1] The resulting charging behaviour has parameters:

$$\mu = 0.6 \quad \sigma = 0.2$$

and is illustrated by the black in Fig. A.4. As discussed in Section 2.3.2, due to the lack of sufficient data the same default charging behaviour is assumed for both BEVs and PHEVs.

A.3.2 Sensitivity analysis

Table A.2 summarises all charging settings explored in the sensitivity analysis in Section 3.1.4. These parameters are always simultaneously changed in the charging mechanisms of both BEVs and PHEVs. The only difference is that the former samples the threshold SOC from a truncated distribution.

[1] There is no specific reason for setting the weights to 4 rather than, for example, 2. However, the change would be marginal: setting the higher weights to 2 shifts the weighted average to: $\mu = 0.61$ $\sigma = 0.19$.

		μ	σ	
Raw sensitivities	$\mu + 10\%$	0.64[†]	0.2	Fig. A.5
	$\mu - 10\%$	0.56[†]	0.2	
	$\sigma + 10\%$	0.6	0.22	
	$\sigma - 10\%$	0.6	0.18	
Exploratory scenarios	always charge	1	0	Fig. A.6
	empirical behav. 1	0.9	0	
	empirical behav. 2	0.7	0.12	
	empirical behav. 3	0.5	0.28	
	empirical behav. 4	0.3	0.44	
	alternative behav. A	0.9	0.44	Fig. A.7
	alternative behav. B	0.7	0.28	
	alternative behav. C	0.5	0.12	
	alternative behav. D	0.3	0	

Table A.2: Parameters of the charging behaviours tested in the sensitivity analysis.

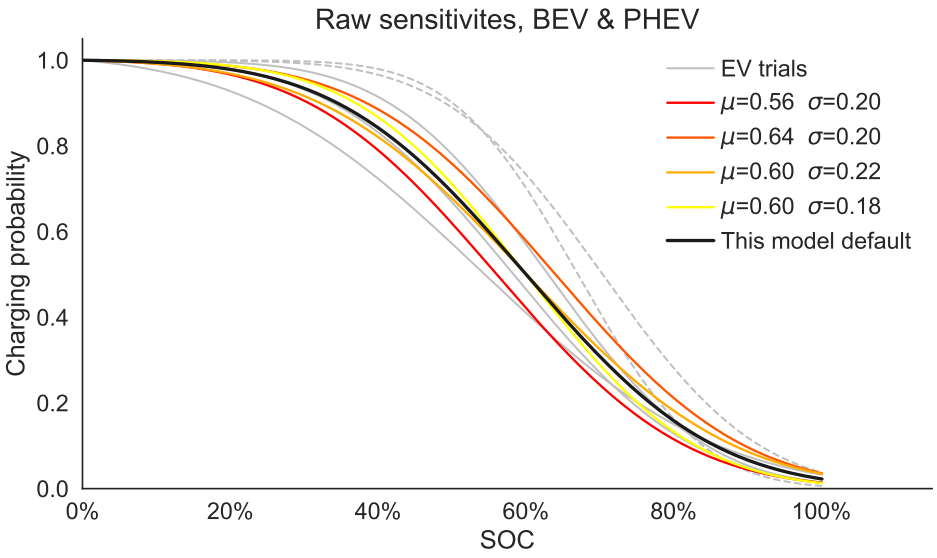

Figure A.5: Charging behaviours tested in the raw sensitivities. The curves for BEVs and PHEVs are essentially identical and no difference can be appreciated.

The charging probabilities resulting from the raw sensitivities are illustrated in Fig. A.5. The curves' deviation from the default behaviour is marginal, and this explains the minor impact on the coefficient of determination R^2 observed in Section 3.1.4. In addition, all curves, including the default behaviour, exhibit no difference between BEVs and PHEVs. This

[†]The $\pm 10\%$ shift of μ is applied in terms of battery depletion (i.e. on a basis of 0.4), rather than in terms of absolute SOC.

is due to the steepness of the curves, which quickly approach the probability of 1 even when not truncated (PHEV case). The truncation on the lower tail (BEV case) thus plays almost no role, as it tries to enforce a charging probability of 1 when this is already in place.

Figure A.6 shows the charging probabilities tested in the exploratory scenarios that follow an *empirical* behaviour. The name for this set of scenarios comes from an examination of Figure A.4, which presents the charging behaviours observed in the EV trials, i.e. *empirical*. They are united by similar charging probabilities at high SOC and by more disperse attitudes for depleted batteries. This gives rise to the linear trend between μ and σ observed in Fig. 2.11.

The empirical set of exploratory scenarios positions itself in the same trend, anchoring to stable charging behaviours at high SOC and exploring more attitudes at low SOC. This is evident from Fig. A.6, where particularly behaviours 2–4 wrap the charging probabilities drawn by the EV trials. Empirical behaviour 1 theoretically falls in the same pattern, but its null standard deviation makes it look like a sharp step function. The plot also includes the "always charge" scenario, which represents the most conservative approach with a charging probability always equal to 1.

Contrary to the previous examples, empirical behaviours 3 and 4 manifest a difference between BEVs and PHEVs. The higher σ of these scenarios allows PHEVs to have a lower-than-1 probability to charge even with a fully depleted battery. This behaviour is technically viable, as PHEVs can rely on a second on-board energy carrier. However, first studies seem to show that PHEVs drivers may tend to charge their car very often in order to minimize the consumption of the liquid fuel [156]. Further research should be carried out to better understand the charging practices of PHEV drivers.

Finally, Figure A.7 presents the charging probabilities investigated in the exploratory scenarios that do not follow the empirical pattern from above. This set of scenarios is named *alternative* and is designed in a symmetrical manner compared to the empirical behaviour (see Table A.2 or Fig. 3.6). Therefore, these alternative scenarios share similar charging probabilities to the default case at low SOC, but explore more diverse behaviours for charged batteries.

Figure A.7 shows that these alternative scenarios cut through the empirical behaviours observed in the EV trials. Also this set includes a scenario with null σ, behaviour D, that resembles a step function. However, in this

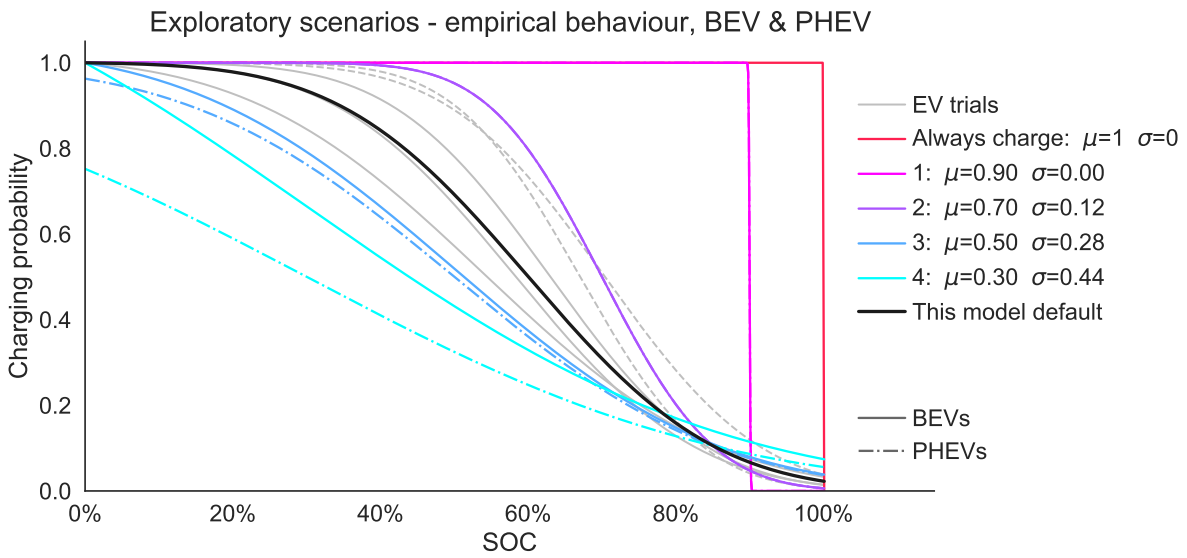

Figure A.6: Charging probabilities tested in the exploratory scenarios that follow the empirically observed behaviour. For the same behavioural parameters (colours), BEV (solid lines) and PHEVs (dash-dotted lines) may exhibit different charging probabilities.

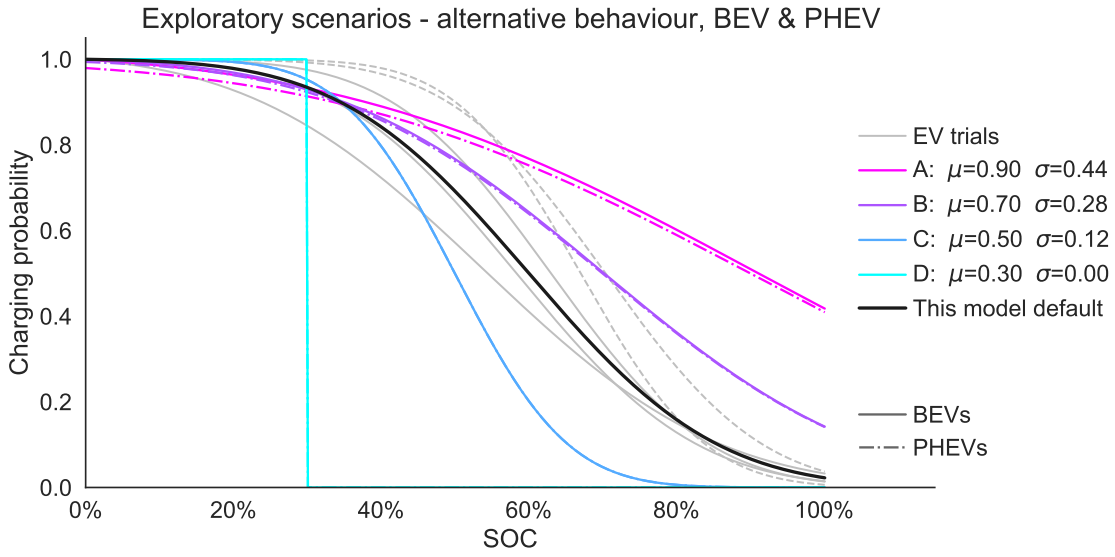

Figure A.7: Charging probabilities tested in the exploratory scenarios that follow a behaviour antithetical to the one empirically observed. For the same behavioural parameters (colours), BEV (solid lines) and PHEVs (dash-dotted lines) exhibit slightly different charging probabilities.

situation it represents a very risky approach, as the EV would never be plugged in for SOCs higher than 30%.

BEVs and PHEVs perform similarly also in this set of scenarios. The reason is that the charging probabilities are so designed to resemble the

default behaviour at low SOC. And this behaviour does not exhibit difference between BEVs and PHEVs. The diversity added by the alternative scenarios rather occurs at high SOCs, but this has a minor role on the BEV charging threshold, being this truncated only on the lower tail.

A.4 Availability of reserved home parking place

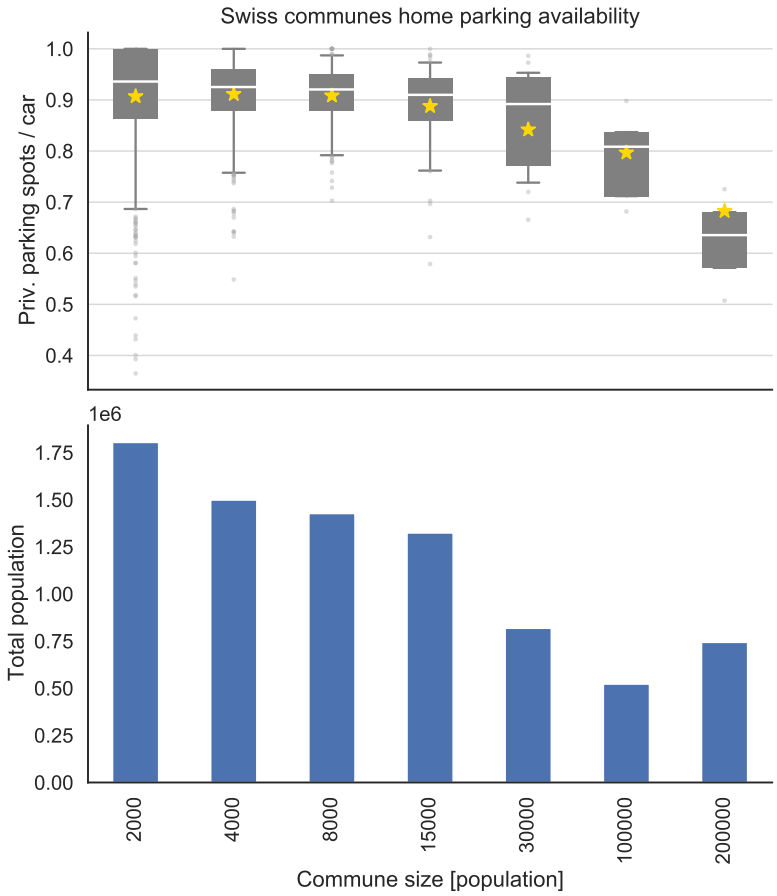

Figure A.8: *Above:* average number of home reserved parking spots per owned car by Swiss commune. Communes are horizontally split by population size. Stars indicate the average private parking availability for the whole commune size category. Whiskers define the 5^{th} and 95^{th} percentiles. *Below:* distribution of the Swiss population among commune size categories.

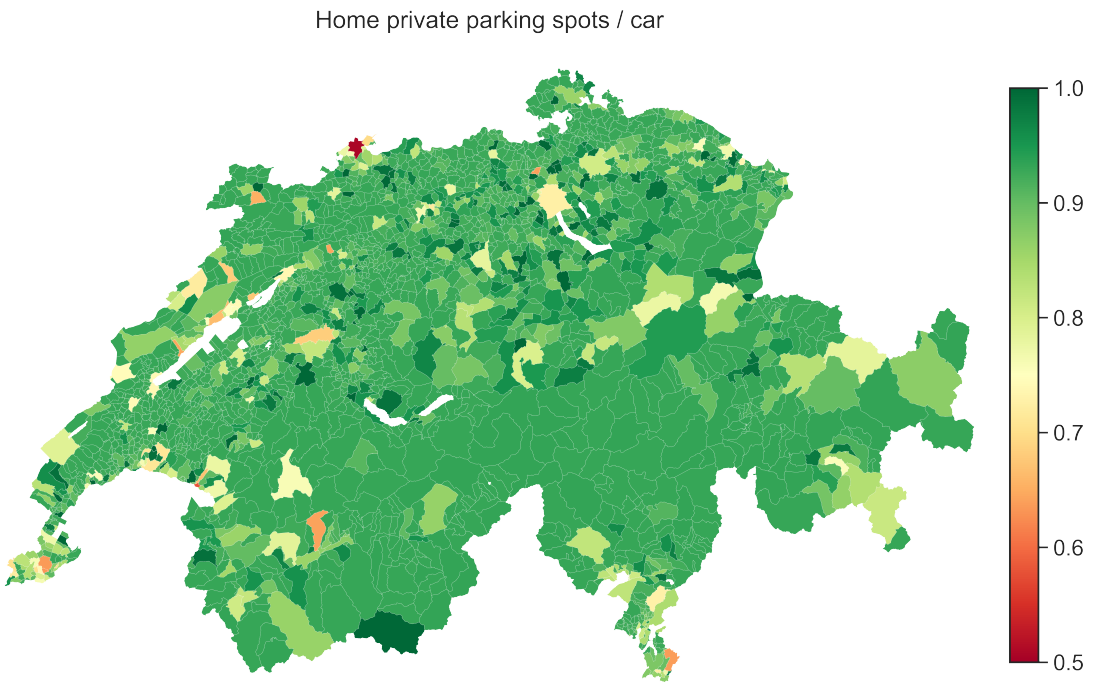

Figure A.9: Average number of home reserved parking spots per owned car by Swiss commune. Communes with fewer than 16 entries in MZMV have been fit according to their population density.

A.5 Benefits of shared BEVs

A.5.1 Sizing of a shared BEV fleet

Let's assume a community with N private cars that perform $T \in \mathbb{R}^{365 \times N}$ trips during the year. T_{ij} represents the total daily distance of j^{th} private car on the i^{th} day of the year. The goal of the heuristic algorithm is to determine the optimal number n of SEVs that, while accounting for the required battery capacity, minimize the fleet purchase costs C_{fleet}.

The maximum number $n_{\max}$ of SEVs sufficient to satisfy the whole mobility demand T equals the maximum number of private cars used on the same day d:

$$n_{\max} = \max\left[\text{count}\left(T_{d*}\right) \textbf{ for } d \textbf{ in } [1:365]\right]$$

where T_{d*} denotes the entire row d and *count* counts the elements greater than zero, i.e. the number of trips.

By reducing n some trips of the community remain unserved. The maxi-

mum number of unfulfillable trips U is exogenously given by:

$$U = \text{round}\left(\text{count}\left(T\right) \cdot x_{\text{undone}}\right)$$

Algorithm 5 details the computation of the minimum number $n_{\min}$ of SEVs such that only U or fewer trips are left unserved.

Algorithm 5 Derivation of the minimum number $n_{\min}$ of SEVs required to leave fewer than U day trips unserved.

```
1:  for d in [1 : 365] do
2:      sort T_{d*} ascendingly
3:  end for
4:  trips_undone = 0
5:  for c in [1 : N] do
6:      trips_undone = trips_undone + count(T_{*c})
7:      if trips_undone > U then
8:          n_min = N − c + 1
9:          break for
10:     end if
11: end for
```

Algorithm 6 is then employed to evaluate every feasible n in terms of fleet purchase costs C_{fleet} and finally select the cheapest option (lines 1, 21–26). The heuristic approach considers the total number of unfulfillable trips U as a budget that can be spent in two ways:

- to reduce the number of required SEVs: this is a function of the n being evaluated and costs k_d trips for every day d with more driving private cars than n (lines 3–6);
- to remove the longest daily trips from the overall mobility demand X: the number of erased trips is given by the budget that remains after the previous step (lines 7–8)[2].

After all U trips have been removed (i.e. set to 0), the algorithm computes the minimum battery requirements b_c for each shared car c. The idea is to maximize the utilisation of any battery b_c by assigning to c the longest

[2] X is just a copy of T that is reinitiated at every loop to preserve the original mobility demand (line 2).

Algorithm 6 Heuristic approach employed to size fleet and batteries of SEVs.

1: **for** n **in** $[n_{\min} : n_{\max}]$ **do**
2: $X = T$
3: **for** d **in** $[1 : 365]$ **do**
4: $k_d = \max\left(\text{count}\left(X_{d*}\right) - n, 0\right)$
5: remove k_d longest trips from X_{d*}
6: **end for**
7: $U = U - \sum_{d=1}^{365} k_d$
8: remove U longest trips from whole X
9: **for** d **in** $[1 : 365]$ **do**
10: sort X_{d*} descendingly
11: **end for**
12: $n_{\text{cars}} = n$
13: **for** c **in** $[1 : n]$ **do**
14: $r_c = \max\left(X_{*c}\right)$
15: **if** $r_c = 0$ **then**
16: $n_{\text{cars}} = c - 1$
17: **break for**
18: **end if**
19: $b_c =$ Eq. 2.13 (r_c)
20: **end for**
21: $C_{\text{fleet}} = n_{\text{cars}} \cdot C_{\text{car}} + \sum_{c=1}^{n_{\text{cars}}} b_c \cdot C_{\text{kWh}}$
22: **if** $C_{\text{fleet}} < C_{\text{fleet}}^{\text{opt}}$ **then**
23: $C_{\text{fleet}}^{\text{opt}} = C_{\text{fleet}}$
24: $n_{\text{cars}}^{\text{opt}} = n_{\text{cars}}$
25: **end if**
26: **end for**

trips it can fulfil, as long as they occur on different days. The journeys on each day are thus ordered by total distance (lines 9–11) and each column of the resulting matrix X is assigned a SEV. The range requirement r_c for each SEV is given by the largest journey assigned (line 14) and the corresponding battery size b_c is computed from Eq. 2.13 (line 19).

After all U trips are removed in the upper part of the routine (lines 3–

8), some of the n SEVs may have no trips assigned: in those cases the actual number of sized SEVs n_{cars} can be lower than n and the superfluous battery capacities are ignored (lines 12, 15–18). Finally, the purchase costs of the resulting fleet are computed and compared against the provisional optimum (lines 21–25).

A.5.2 Correlation between population density and motorisation rate

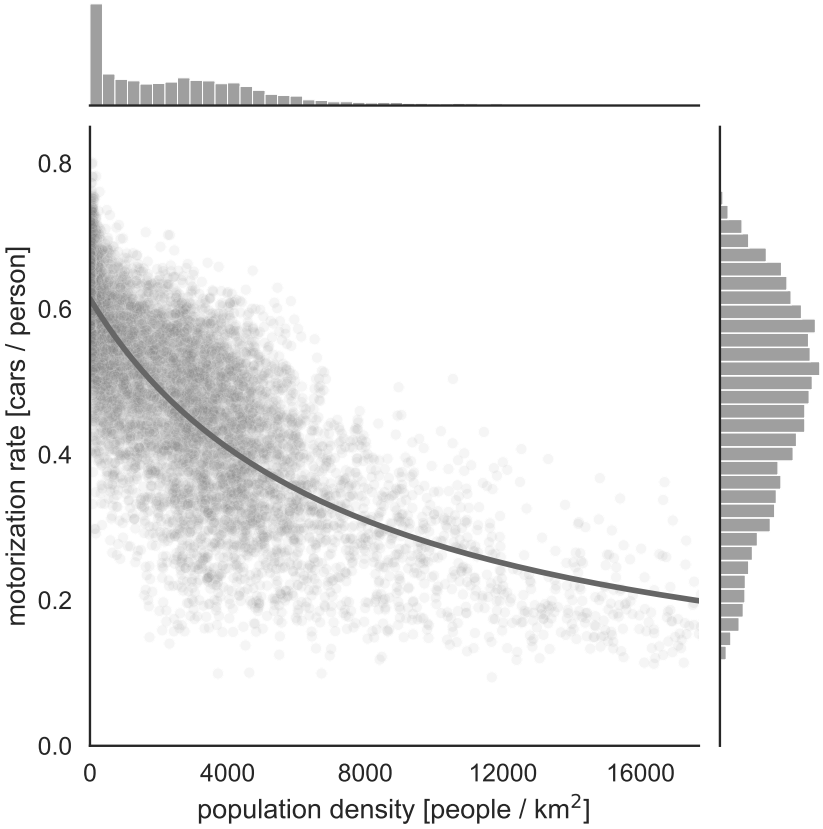

Figure A.10: Correlation between motorisation rate and population density in every MSOA of Great Britain.

Fig. A.10 shows the relation between ρ and M for every census area (MSOA[3]) of Great Britain [157]. Predictably, the higher the population density the lower the car ownership level. Very rural areas reach motorisation rates of about 0.7 cars/person, while inner cities see a drop in ownership rate below 0.3 cars/person.

[3]In this work MSOAs refer to both the Middle layer Super Output Areas of England and Wales as well as the intermediate zones of Scotland.

A least square fit of the data points returns the following rectangular hyperbola:

$$(\rho - 7601) \cdot (M - 0.021) = 4506 \tag{A.1}$$

with ρ expressed in people/km^2.
The hyperbolic formulation has been chosen so that Eq. 5.2 can be potentially reversed with the quadratic formula to obtain the population density ρ as a function of N.

Nomenclature

Acronym	Description
BEV	Battery Electric Vehicle
CCGT	Combined Cycle Gas Turbine
CCS	Carbon Capture and Storage
CDF	Cumulative Distribution Function
CH	Switzerland
CLT	Central Limit Theorem
CNG	Compressed Natural Gas
CP	Charging Profile (electricity demand caused by EV charging)
DoD	Depth of Discharge
EV	Electric Vehicle (either BEV or PHEV)
EVSE	Electric Vehicle Supply Equipment
FCEV	Fuel Cell Electric Vehicle
GB	Great Britain
GHG	GreenHouse Gas
HEV	Hybrid Electric Vehicle
HTS	Household Travel Survey
ICEV	Internal Combustion Engine Vehicle
K–S	Kolmogorov–Smirnov (test or metric)
LCA	Life-Cycle Assessment
MZMV	Mikrozensus Mobilität und Verkehr (CH)
NTS	National Travel Survey (GB)
PDF	Probability Distribution Function
PFCEV	Plug-in Fuel Cell Electric Vehicle
PHEV	Plug-in Hybrid Electric Vehicle
pkm	person-km
PV	Photovoltaic

Acronym	Description
SEV	Shared battery Electric Vehicle
SOC	State Of Charge
UF	Utility Factor
UK	United Kingdom
US	United States
vkm	vehicle-km
WTW	Well-To-Wheel

Symbol	Description
A	surface area in reach of a car-sharing station
b	gross energy capacity of batteries
c	energy consumption per unit distance
C	purchase costs
d_{car}	average daily distance of a car
$d_{\text{car used}}$	average daily distance of a car when driven
D	K–S statistic of the Kolmogorov–Smirnov test
E_{batt}	gross energy capacity of batteries
f_{used}	average driving frequency of a car
M	motorisation rate
N	number of private cars
n	number of shared cars
p	p-value
r	range of BEVs
R	radius of influence area of car-sharing station
x_{undone}	tolerance level, i.e. share of unfulfillable trips
η	association coefficient
μ	mean of a statistical distribution
ρ	population density
σ	standard deviation of a statistical distribution

List of Tables

List of Figures

Bibliography

[1] IEA. CO_2 emissions from fuel combustion, 2019. URL https://webstore.iea.org/co2-emissions-from-fuel-combustion-2019.

[2] IPCC. Global warming of 1.5°C. An IPCC Special Report on the impacts of global warming of 1.5°C above pre-industrial levels and related global greenhouse gas emission pathways, in the context of strengthening the global response to the threat of climate change, sustainable development, and efforts to eradicate poverty, 2018. URL https://www.ipcc.ch/sr15/.

[3] P. Friedlingstein, M. O'Sullivan, M. W. Jones, R. M. Andrew, J. Hauck, A. Olsen, G. P. Peters, W. Peters, J. Pongratz, S. Sitch, C. Le Quéré, J. G. Canadell, P. Ciais, R. B. Jackson, S. Alin, L. E. O. C. Aragão, A. Arneth, V. Arora, N. R. Bates, M. Becker, A. Benoit-Cattin, H. C. Bittig, L. Bopp, S. Bultan, N. Chandra, F. Chevallier, L. P. Chini, W. Evans, L. Florentie, P. M. Forster, T. Gasser, M. Gehlen, D. Gilfillan, T. Gkritzalis, L. Gregor, N. Gruber, I. Harris, K. Hartung, V. Haverd, R. A. Houghton, T. Ilyina, A. K. Jain, E. Joetzjer, K. Kadono, E. Kato, V. Kitidis, J. I. Korsbakken, P. Landschützer, N. Lefèvre, A. Lenton, S. Lienert, Z. Liu, D. Lombardozzi, G. Marland, N. Metzl, D. R. Munro, J. E. M. S. Nabel, S.-I. Nakaoka, Y. Niwa, K. O'Brien, T. Ono, P. I. Palmer, D. Pierrot, B. Poulter, L. Resplandy, E. Robertson, C. Rödenbeck, J. Schwinger, R. Séférian, I. Skjelvan, A. J. P. Smith, A. J. Sutton, T. Tanhua, P. P. Tans, H. Tian, B. Tilbrook, G. van der Werf, N. Vuichard, A. P. Walker, R. Wanninkhof, A. J. Watson, D. Willis, A. J. Wiltshire, W. Yuan, X. Yue, and S. Zaehle. Global carbon budget 2020. *Earth System Science Data*, 12(4):3269–3340, 2020. doi: 10.5194/essd-12-3269-2020. URL https://essd.copernicus.org/articles/12/3269/2020/.

[4] IPCC. Fifth Assessment Report, 2014. URL https://www.ipcc.ch/assessment-report/ar5/.

[5] IEA. ETP clean energy technology guide, 2019. URL https://www.iea.org/articles/etp-clean-energy-technology-guide.

[6] Lukas Küng, Thomas Bütler, Gil Georges, and Konstantinos Boulouchos. Decarbonizing passenger cars using different powertrain technologies: optimal fleet composition under evolving electricity supply. *Transportation Research Part C: Emerging Technologies*, 95:785 – 801, 2018. ISSN 0968-090X. doi: https://doi.org/10.1016/j.trc.2018.09.003. URL http://www.sciencedirect.com/science/article/pii/S0968090X18302043.

[7] IEA. Tracking clean energy progress, 2019. URL https://www.iea.org/reports/tracking-transport-2019.

[8] IEA. Global EV Outlook, 2019. URL https://www.iea.org/reports/global-ev-outlook-2019.

[9] EEA. CO_2-emission intensity from electricity generation, 2020. URL https://www.eea.europa.eu/data-and-maps/daviz/sds/co2-emission-intensity-from-electricity-2/@@view.

[10] Bundesamt für Statistik / Bundesamt für Raumentwicklung (2017). Verkehrsverhalten der Bevölkerung. Ergebnisse des Mikrozensus Mobilität und Verkehr 2015, Neuchâtel und Bern, 2017. URL https://www.bfs.admin.ch/bfs/de/home/statistiken/mobilitaet-verkehr/erhebungen/mzmv.html.

[11] Department for Transport. National travel survey, 2002-2017. [data collection] 13th edition, 2019. URL http://doi.org/10.5255/UKDA-SN-5340-10. UK Data Service. SN: 5340.

[12] Brian Cox, Christian Bauer, Angelica Mendoza Beltran, Detlef P. van Vuuren, and Christopher L. Mutel. Life cycle environmental and cost comparison of current and future passenger cars under different energy scenarios. *Applied Energy*, 269:115021, 2020. ISSN 0306-2619. doi: https://doi.org/10.1016/j.apenergy.2020.115021. URL http://www.sciencedirect.com/science/article/pii/S030626192030533X.

[13] Elsa A Olivetti, Gerbrand Ceder, Gabrielle G Gaustad, and Xinkai Fu. Lithium-ion battery supply chain considerations: analysis of potential bottlenecks in critical metals. *Joule*, 1(2):229–243, 2017.

[14] Qiang Dai, Jarod C Kelly, Linda Gaines, and Michael Wang. Life cycle analysis of lithium-ion batteries for automotive applications. *Batteries*, 5(2):48, 2019.

[15] Makena Coffman, Paul Bernstein, and Sherilyn Wee. Electric vehicles revisited: a review of factors that affect adoption. *Transport Reviews*, 37(1):79–93, 2017.

[16] Erick C. Jones and Benjamin D. Leibowicz. Contributions of shared autonomous vehicles to climate change mitigation. *Transportation Research Part D: Transport and Environment*, 72:279–298, jul 2019. ISSN 13619209. doi: 10.1016/j.trd.2019.05.005.

[17] Richard Mounce and John D. Nelson. On the potential for one-way electric vehicle car-sharing in future mobility systems. *Transportation Research Part A: Policy and Practice*, 120:17–30, feb 2019. ISSN 09658564. doi: 10.1016/j.tra.2018.12.003. URL `https://linkinghub.elsevier.com/retrieve/pii/S0965856417315331`.

[18] Andreas Horni, Kai Nagel, and Kay W Axhausen. *The multi-agent transport simulation MATSim*. Ubiquity Press, 2016.

[19] Claire Weiller. Plug-in hybrid electric vehicle impacts on hourly electricity demand in the United States. *Energy Policy*, 39(6):3766–3778, jun 2011. ISSN 03014215. doi: 10.1016/j.enpol.2011.04.005. URL `https://www.sciencedirect.com/science/article/pii/S0301421511002886`.

[20] Jarod C. Kelly, Jason S. MacDonald, and Gregory A. Keoleian. Time-dependent plug-in hybrid electric vehicle charging based on national driving patterns and demographics. *Applied Energy*, 94:395–405, jun 2012. ISSN 03062619. doi: 10.1016/j.apenergy.2012.02.001. URL `https://www.sciencedirect.com/science/article/pii/S0306261912000931?via{%}3Dihub{#}f0035`.

[21] Florian Salah, Jens P. Ilg, Christoph M. Flath, Hauke Basse, and Clemens van Dinther. Impact of electric vehicles on distribution

substations: A Swiss case study. *Applied Energy*, 137:88–96, jan 2015. ISSN 03062619. doi: 10.1016/j.apenergy.2014.09.091. URL http://dx.doi.org/10.1016/j.apenergy.2014.09.091.

[22] Guzay Pasaoglu, Davide Fiorello, L Zani, A Martino, Alyona Zubaryeva, and Christian Thiel. Projections for electric vehicle load profiles in Europe based on travel survey data, 2013. URL http://europa.eu/.

[23] Sonja Babrowski, Heidi Heinrichs, Patrick Jochem, and Wolf Fichtner. Load shift potential of electric vehicles in Europe. *Journal of Power Sources*, 255:283–293, jun 2014. ISSN 03787753. doi: 10.1016/j.jpowsour.2014.01.019. URL https://www.sciencedirect.com/science/article/pii/S0378775314000342.

[24] Chioke B. Harris and Michael E. Webber. An empirically-validated methodology to simulate electricity demand for electric vehicle charging. *Applied Energy*, 126:172–181, aug 2014. ISSN 03062619. doi: 10.1016/j.apenergy.2014.03.078. URL https://www.sciencedirect.com/science/article/pii/S0306261914003183?via{%}3Dihub.

[25] Jairo Quiros-Tortos, Alejandro Navarro Espinosa, Luis F. Ochoa, and Tim Butler. Statistical Representation of EV Charging: Real Data Analysis and Applications. In *2018 Power Systems Computation Conference (PSCC)*, number June, pages 1–7. IEEE, jun 2018. ISBN 978-1-910963-10-4. doi: 10.23919/PSCC.2018.8442988. URL https://ieeexplore.ieee.org/document/8442988/.

[26] Sulabh Sachan and Nadia Adnan. Stochastic charging of electric vehicles in smart power distribution grids. *Sustainable Cities and Society*, 40:91–100, jul 2018. ISSN 22106707. doi: 10.1016/j.scs.2018.03.031. URL https://www.sciencedirect.com/science/article/pii/S221067071830338X?via{%}3Dihub.

[27] Jun Su, T.T. Lie, and Ramon Zamora. Modelling of large-scale electric vehicles charging demand: A New Zealand case study. *Electric Power Systems Research*, 167:171–182, feb 2019. ISSN 03787796. doi: 10.1016/j.epsr.2018.10.030. URL https://www.sciencedirect.com/science/article/pii/S0378779618303535?dgcid=raven{_}sd{_}recommender{_}email{#}fig0040.

[28] Niancheng Zhou, Xicong Xiong, and Qianggang Wang. Probability Model and Simulation Method of Electric Vehicle Charging Load on Distribution Network. *Electric Power Components and Systems*, 42 (9):879–888, jul 2014. ISSN 1532-5008. doi: 10.1080/15325008.2014.903537. URL `http://www.tandfonline.com/doi/abs/10.1080/15325008.2014.903537`.

[29] Alicja Lojowska, Dorota Kurowicka, Georgios Papaefthymiou, and Lou van der Sluis. Stochastic modeling of power demand due to EVs using copula. *IEEE Transactions on Power Systems*, 27(4): 1960–1968, nov 2012. ISSN 0885-8950. doi: 10.1109/TPWRS.2012.2192139. URL `http://ieeexplore.ieee.org/document/6193193/`.

[30] Nima H. Tehrani and Peng Wang. Probabilistic estimation of plug-in electric vehicles charging load profile. *Electric Power Systems Research*, 124:133–143, jul 2015. ISSN 03787796. doi: 10.1016/j.epsr.2015.03.010. URL `https://www.sciencedirect.com/science/article/pii/S037877961500070X`.

[31] Hamidreza Jahangir, Hanif Tayarani, Ali Ahmadian, Masoud Aliakbar Golkar, Jaume Miret, Mohammad Tayarani, and H. Oliver Gao. Charging demand of Plug-in Electric Vehicles: Forecasting travel behavior based on a novel Rough Artificial Neural Network approach. *Journal of Cleaner Production*, 229:1029–1044, aug 2019. ISSN 09596526. doi: 10.1016/j.jclepro.2019.04.345. URL `https://linkinghub.elsevier.com/retrieve/pii/S0959652619314428`.

[32] Dai Wang, Junyu Gao, Pan Li, Bin Wang, Cong Zhang, and Samveg Saxena. Modeling of plug-in electric vehicle travel patterns and charging load based on trip chain generation. *Journal of Power Sources*, 359:468–479, aug 2017. ISSN 03787753. doi: 10.1016/j.jpowsour.2017.05.036. URL `https://www.sciencedirect.com/science/article/pii/S0378775317306687{#}fig1`.

[33] David Fischer, Alexander Harbrecht, Arne Surmann, and Russell McKenna. Electric vehicles' impacts on residential electric local profiles – A stochastic modelling approach considering socio-economic, behavioural and spatial factors. *Applied Energy*, 233-234:

644–658, jan 2019. ISSN 03062619. doi: 10.1016/j.apenergy.2018.10.010. URL https://www.sciencedirect.com/science/article/pii/S0306261918315666?via{%}3Dihub.

[34] Yue Wang and David Infield. Markov Chain Monte Carlo simulation of electric vehicle use for network integration studies. *International Journal of Electrical Power & Energy Systems*, 99:85–94, jul 2018. ISSN 01420615. doi: 10.1016/j.ijepes.2018.01.008. URL https://www.sciencedirect.com/science/article/pii/S0142061517307226?via{%}3Dihub{#}f0055.

[35] Azhar Ul-Haq, Carlo Cecati, and Ehab El-Saadany. Probabilistic modeling of electric vehicle charging pattern in a residential distribution network. *Electric Power Systems Research*, 157:126–133, apr 2018. ISSN 03787796. doi: 10.1016/j.epsr.2017.12.005. URL https://www.sciencedirect.com/science/article/pii/S0378779617304765?via{%}3Dihub{#}fig0005.

[36] Alicja Lojowska, Dorota Kurowicka, Georgios Papaefthymiou, and Lou van der Sluis. From transportation patterns to power demand: Stochastic modeling of uncontrolled domestic charging of electric vehicles. In *2011 IEEE Power and Energy Society General Meeting*, pages 1–7. IEEE, jul 2011. ISBN 978-1-4577-1000-1. doi: 10.1109/PES.2011.6039187. URL https://ieeexplore.ieee.org/document/6039187/.

[37] Ali Ashtari, Eric Bibeau, Soheil Shahidinejad, and Tom Molinski. PEV Charging Profile Prediction and Analysis Based on Vehicle Usage Data. *IEEE Transactions on Smart Grid*, 3(1):341–350, mar 2012. ISSN 1949-3053. doi: 10.1109/TSG.2011.2162009. URL http://ieeexplore.ieee.org/document/6017151/.

[38] John Brady and Margaret O'Mahony. Modelling charging profiles of electric vehicles based on real-world electric vehicle charging data. *Sustainable Cities and Society*, 26:203–216, oct 2016. ISSN 22106707. doi: 10.1016/j.scs.2016.06.014. URL https://www.sciencedirect.com/science/article/pii/S221067071630124X.

[39] Mariz B. Arias, Myungchin Kim, and Sungwoo Bae. Prediction of electric vehicle charging-power demand in realistic urban

traffic networks. *Applied Energy*, 195:738–753, jun 2017. ISSN 03062619. doi: 10.1016/j.apenergy.2017.02.021. URL https://www.sciencedirect.com/science/article/pii/S0306261917301459.

[40] Eamon Keane and Damian Flynn. Potential for electric vehicles to provide power system reserve. In *2012 IEEE PES Innovative Smart Grid Technologies (ISGT)*, pages 1–7. IEEE, jan 2012. ISBN 978-1-4577-2159-5. doi: 10.1109/ISGT.2012.6175701. URL http://ieeexplore.ieee.org/document/6175701/.

[41] Yue Zhou, Ruoxi Wen, Hewu Wang, and Hua Cai. Optimal battery electric vehicles range: A study considering heterogeneous travel patterns, charging behaviors, and access to charging infrastructure. *Energy*, 197:116945, apr 2020. ISSN 03605442. doi: 10.1016/j.energy.2020.116945. URL https://linkinghub.elsevier.com/retrieve/pii/S0360544220300529.

[42] Thomas Franke and Josef F. Krems. Understanding charging behaviour of electric vehicle users. *Transportation Research Part F: Traffic Psychology and Behaviour*, 21:75–89, nov 2013. ISSN 13698478. doi: 10.1016/j.trf.2013.09.002. URL https://www.sciencedirect.com/science/article/pii/S1369847813000776{#}f0005.

[43] The "My Electric Avenue" project. URL http://myelectricavenue.info/.

[44] Thomas Franke, Isabel Neumann, Franziska Bühler, Peter Cocron, and Josef F. Krems. Experiencing Range in an Electric Vehicle: Understanding Psychological Barriers. *Applied Psychology*, 61(3):368–391, jul 2012. ISSN 0269994X. doi: 10.1111/j.1464-0597.2011.00474.x. URL http://doi.wiley.com/10.1111/j.1464-0597.2011.00474.x.

[45] Ankita Chaudhary. *Impact of range anxiety on driver route choices using a panel-integrated choice latent variable model*. PhD thesis, The University of Texas at Austin, 2014. URL http://hdl.handle.net/2152/28254.

[46] Peyman Ashkrof, Gonçalo Homem de Almeida Correia, and Bart van Arem. Analysis of the effect of charging needs on battery electric vehicle drivers' route choice behaviour: A case study in the Netherlands. *Transportation Research Part D: Transport and Environment*, 78:102206, jan 2020. ISSN 13619209. doi: 10.1016/j.trd.2019.102206. URL https://linkinghub.elsevier.com/retrieve/pii/S1361920919309757.

[47] Yeongmin Kwon, Sanghoon Son, and Kitae Jang. User satisfaction with battery electric vehicles in South Korea. *Transportation Research Part D: Transport and Environment*, 82:102306, may 2020. ISSN 13619209. doi: 10.1016/j.trd.2020.102306. URL https://linkinghub.elsevier.com/retrieve/pii/S1361920919308296.

[48] EA Technology. My Electric Avenue - An assessment of the public acceptance of demand side responses of EV charging using Esprit, Oct 2015. URL http://myelectricavenue.info/sites/default/files/documents/9.6.pdf.

[49] Justin Woodjack, Dahlia Garas, Andy Lentz, Thomas Turrentine, Gil Tal, and Michael Nicholas. Consumer Perceptions and Use of Driving Distance of Electric Vehicles. *Transportation Research Record: Journal of the Transportation Research Board*, 2287(1): 1–8, jan 2012. ISSN 0361-1981. doi: 10.3141/2287-01. URL http://journals.sagepub.com/doi/10.3141/2287-01.

[50] Nadine Rauh, Thomas Franke, and Josef F. Krems. Understanding the Impact of Electric Vehicle Driving Experience on Range Anxiety. *Human Factors: The Journal of the Human Factors and Ergonomics Society*, 57(1):177–187, feb 2015. ISSN 0018-7208. doi: 10.1177/0018720814546372. URL http://journals.sagepub.com/doi/10.1177/0018720814546372.

[51] Lance Noel, Gerardo Zarazua de Rubens, Benjamin K. Sovacool, and Johannes Kester. Fear and loathing of electric vehicles: The reactionary rhetoric of range anxiety. *Energy Research & Social Science*, 48:96–107, feb 2019. ISSN 22146296. doi: 10.1016/j.erss.2018.10.001. URL https://linkinghub.elsevier.com/retrieve/pii/S2214629618304456.

[52] Guzay Pasaoglu, Alyona Zubaryeva, Davide Fiorello, and Christian Thiel. Analysis of European mobility surveys and their potential to support studies on the impact of electric vehicles on energy and infrastructure needs in Europe. *Technological Forecasting and Social Change*, 87:41–50, sep 2014. ISSN 00401625. doi: 10.1016/j.techfore.2013.09.002. URL https://www.sciencedirect.com/science/article/pii/S004016251300228X?via{%}3Dihub.

[53] FSO, Swiss population. URL https://www.bfs.admin.ch/bfs/en/home/statistics/population.html.

[54] *Rapport méthodologique: plan d'échantillonage, taux de réponse et pondération*. Number 4262242. Neuchâtel, Jan 2018. URL https://www.bfs.admin.ch/hub/api/dam/assets/4262242/master.

[55] Department for Transport. NTS0901: Annual mileage of cars by ownership and trip purpose: England, since 2002, 2020. URL https://www.gov.uk/government/statistical-data-sets/nts09-vehicle-mileage-and-occupancy.

[56] Chioke B. Harris and Michael E. Webber. Quantifying the effect of plug-in electric vehicles on future grid operations and ancillary service procurement requirements. volume Volume 11: Emerging Technologies of *ASME International Mechanical Engineering Congress and Exposition*, 04 2014. doi: 10.1115/IMECE2013-63335. URL https://doi.org/10.1115/IMECE2013-63335.

[57] Piet Rietveld. Rounding of arrival and departure times in travel surveys: an interpretation in terms of scheduled activities. *Journal of Transportation and Statistics*, 5:71–82, 2001. ISSN 1094-8848. URL https://trid.trb.org/view.aspx?id=646385.

[58] *Verkehrsverhalten der Bevölkerung*. Number 1840477. Bundesamt für Statistik (BFS), Neuchâtel, May 2017. ISBN 978-3-303-11262-5. URL https://www.bfs.admin.ch/hub/api/dam/assets/1840477/master.

[59] Peter Cornick, Christos Byron, Iain Templeton, and John Hurn. National travel survey 2018 - technical report. URL https://www.gov.uk/government/statistics/national-travel-survey-2019.

[60] Zhaoxi LIU, Qiuwei WU, Linda CHRISTENSEN, Antti RAUTIAINEN, and Yusheng XUE. Driving pattern analysis of Nordic region based on National Travel Surveys for electric vehicle integration. *Journal of Modern Power Systems and Clean Energy*, 3(2):180–189, jun 2015. ISSN 2196-5625. doi: 10.1007/s40565-015-0127-x. URL http://link.springer.com/10.1007/s40565-015-0127-x.

[61] Patrick Plötz, Till Gnann, and Martin Wietschel. Total ownership cost projection for the german electric vehicle market with implications for its future power and electricity demand. In *7th conference on energy economics and technology infrastructure for the energy transformation*, volume 27, page 12, 2012.

[62] Patrick Plötz, Niklas Jakobsson, and Frances Sprei. On the distribution of individual daily driving distances. *Transportation research part B: methodological*, 101:213–227, 2017. ISSN 0191-2615. doi: https://doi.org/10.1016/j.trb.2017.04.008. URL http://www.sciencedirect.com/science/article/pii/S0191261516309067.

[63] A Blum. *Electro-mobility: statistical analysis of human mobility patterns*. PhD thesis, Master Thesis, infernum, Wuppertal, 2014.

[64] FSO. Leistungen des privaten Personenverkehrs auf der Strasse, 2019. URL https://www.bfs.admin.ch/bfs/de/home/statistiken/kataloge-datenbanken/publikationen.assetdetail.9867227.html.

[65] Mot - motoring and vehicle ownership trends in the uk, 2016. URL https://environment.leeds.ac.uk/transport-research/dir-record/research-projects/754/mot-motoring-and-vehicle-ownership-trends-in-the-uk.

[66] SD Ball, P Emmerson, J Anable, S Cairns, RE Wilson, and T Chatterton. Understanding variation in car use: exploration of statistical metrics at differing spatial scales using data from every private car registered in great britain, 2016.

[67] Peter Weldon, Patrick Morrissey, John Brady, and Margaret O'Mahony. An investigation into usage patterns of electric vehicles

in Ireland. *Transportation Research Part D: Transport and Environment*, 43:207–225, mar 2016. ISSN 13619209. doi: 10.1016/j.trd.2015.12.013. URL https://www.sciencedirect.com/science/article/pii/S1361920915002230?via{%}3Dihub{#}f0005.

[68] Marco Giacomo Flammini, Giuseppe Prettico, Andreea Julea, Gianluca Fulli, Andrea Mazza, and Gianfranco Chicco. Statistical characterisation of the real transaction data gathered from electric vehicle charging stations. *Electric Power Systems Research*, 166: 136–150, jan 2019. ISSN 03787796. doi: 10.1016/j.epsr.2018.09.022. URL https://www.sciencedirect.com/science/article/pii/S037877961830316X?vi.

[69] Idaho National Laboratory. EV Project electric vehicle charging infrastructure summary report, 2014. URL https://avt.inl.gov/sites/default/files/pdf/EVProj/EVProjectInfrastructureReportJan13Dec13.pdf.

[70] EA Technology. My Electric Avenue - An assessment of how much headroom an Esprit type technology would yield, Nov 2015. URL http://myelectricavenue.info/sites/default/files/documents/9.8%20-%20vol%201.pdf.

[71] Maximilian Held, Lukas Küng, Emir Çabukoglu, Giacomo Pareschi, Gil Georges, and Konstantinos Boulouchos. Future mobility demand estimation based on sociodemographic information: A data-driven approach using machine learning algorithms. In *18th Swiss Transport Research Conference (STRC 2018)*. STRC, 2018.

[72] Jacob Cohen. *Statistical power analysis for the behavioral sciences*. Academic press, 2013.

[73] Office for National Statistics. The national statistics socio-economic classification (ns-sec), 2020. URL https://www.ons.gov.uk/methodology/classificationsandstandards/standardoccupationalclassificationsoc/soc2020/soc2020volume3thenationalstatisticssocioeconomicclassificationnsse
structure-and-flexibility.

[74] International Labour Organization. The international standard classification of occupations (isco), 2020. URL http://www.ilo.org/public/english/bureau/stat/isco/index.htm.

[75] Lukas Küng. *Exploration of Systemic Strategies to Decarbonize Swiss Passenger Cars with a Focus on Vehicle Real-World Energy Demand*. PhD thesis, ETH Zurich, 2020.

[76] Lukas Küng, Thomas Bütler, Gil Georges, and Konstantinos Boulouchos. How much energy does a car need on the road? *Applied Energy*, 256:113948, 2019. ISSN 0306-2619. doi: https://doi.org/10.1016/j.apenergy.2019.113948. URL http://www.sciencedirect.com/science/article/pii/S0306261919316356.

[77] Improved battery technology: the key to superior ev performance & affordability, 2021. URL https://blog.wallbox.com/9-leading-ev-influencers-discuss-the-innovations-that-will-shape-t#index_1.

[78] A.P. Robinson, Phil T. Blythe, M.C. Bell, Yvonne Hübner, and Graeme A. Hill. Analysis of electric vehicle driver recharging demand profiles and subsequent impacts on the carbon content of electric vehicle trips. *Energy Policy*, 61:337–348, oct 2013. ISSN 03014215. doi: 10.1016/j.enpol.2013.05.074. URL https://doi.org/10.1016/j.enpol.2013.05.074.

[79] Ramteen Sioshansi and Paul Denholm. Emissions impacts and benefits of plug-in hybrid electric vehicles and vehicle-to-grid services. *Environmental Science & Technology*, 43(4):1199–1204, 2009. doi: 10.1021/es802324j. URL https://doi.org/10.1021/es802324j.

[80] Myriam Neaimeh, Graeme Hill, Phil T. Blythe, Robin Wardle, Jialiang Yi, and Phil Taylor. Integrating smart meter and electric vehicle charging data to predict distribution network impacts. In *IEEE PES ISGT Europe 2013*, pages 1–5. IEEE, oct 2013. ISBN 978-1-4799-2984-9. doi: 10.1109/ISGTEurope.2013.6695238. URL http://ieeexplore.ieee.org/document/6695238/.

[81] Myriam Neaimeh, Robin Wardle, Andrew M. Jenkins, Jialiang Yi, Graeme Hill, Padraig F. Lyons, Yvonne Hübner, Phil T. Blythe,

and Phil C. Taylor. A probabilistic approach to combining smart meter and electric vehicle charging data to investigate distribution network impacts. *Applied Energy*, 157:688–698, nov 2015. ISSN 03062619. doi: 10.1016/j.apenergy.2015.01.144. URL https://www.sciencedirect.com/science/article/pii/S0306261915001944.

[82] James Francfort. EVs and PHEVs charging habits, 2016. URL https://inldigitallibrary.inl.gov/sites/sti/sti/Sort_11067.pdf.

[83] The Green eMotion project. URL http://www.greenemotion-project.eu/.

[84] Elisabetta Cherchi, Patrick Morrissey, Margaret O'Mahony, and Peter Weldon. Deliverable 9.1 - Consumers' preferences and attitudes to, demand for, and use of electric vehicles (EV), Mar 2015. URL http://www.greenemotion-project.eu/.

[85] The North East's "Switch EV" electric vehicle trial. URL https://www.ncl.ac.uk/engineering/research/civil/transport/projects/switchev/.

[86] The EV Project. URL https://avt.inl.gov/project-type/ev-project.

[87] Graeme A. Hill, Myriam Neaimeh, Phil T. Blythe, and Yvonne Hübner. Routing systems to extend the driving range of electric vehicles. *IET Intelligent Transport Systems*, 7(3):327–336, sep 2013. ISSN 1751-956X. doi: 10.1049/iet-its.2013.0122. URL https://digital-library.theiet.org/content/journals/10.1049/iet-its.2013.0122.

[88] Idaho National Laboratory. Nissan Leafs and Chevrolet Volts reporting data in The EV Project through December 2013, 2014. URL https://avt.inl.gov/sites/default/files/pdf/EVProj/LeafsVoltsByRegionThroughQ42013.pdf.

[89] Idaho National Laboratory. Characterize the demand and energy characteristics of residential electric vehicle supply equipment, 2015. URL https://avt.inl.gov/sites/default/files/pdf/EVProj/CharacterizeEnergyDemandResidentialEVSE.pdf.

[90] Idaho National Laboratory. Demand and energy characteristics of non-residential alternating current level 2 electric vehicle supply equipment, 2015. URL https://avt.inl.gov/sites/default/files/pdf/EVProj/DemandACL2NonresidentialEVSE.pdf.

[91] Charging stations statistics UK. URL https://www.zap-map.com/statistics/.

[92] Idaho National Laboratory. Characterize clustering of non-residential alternating current level 2 electric vehicle supply equipment, 2015. URL https://avt.inl.gov/sites/default/files/pdf/EVProj/CharacterizeClusteringOfACL2NonResidentialEVSE.pdf.

[93] Adam Evans, Andrew Kelly, and Matthew Slocombe. National Travel Survey: England 2018, 2019. URL https://www.gov.uk/government/statistics/national-travel-survey-2018.

[94] Part-time employment rate OECD. URL https://data.oecd.org/emp/part-time-employment-rate.htm.

[95] American National Household Travel Survey 2017. URL https://nhts.ornl.gov/.

[96] Michele Bolla, Maximilian Held, Lukas Küng, Gil Georges, and Konstantinos Boulouchos. Vehicle motion patterns for energy research: Comparison of annual mileage using vehicleand person-based data. In *18th Swiss Transport Research Conference (STRC 2018)*. STRC, 2018.

[97] European alternative fuels observatory, 2020. URL https://www.eafo.eu/.

[98] Lower-range bevs are seeing strong sales in europe, 2020. URL https://cleantechnica.com/2020/08/02/lower-range-bevs-are-seeing-strong-sales-in-europe/.

[99] Electric vehicle database, 2021. URL https://ev-database.org/.

[100] Directive (eu) 2018/844 of the european parliament and of the council of 30 may 2018 amending directive 2010/31/eu on the energy performance of buildings and directive 2012/27/eu on energy efficiency, 2018. URL http://data.europa.eu/eli/dir/2018/844/oj.

[101] Mattia Maeder, Olga Weiss, and Konstantinos Boulouchos. Assessing the need for flexibility technologies in decarbonized power systems: A new model applied to central europe. *Applied Energy*, 282:116050, 2021.

[102] Loris Di Natale, Luca Funk, Martin Rüdisüli, Bratislav Svetozarevic, Giacomo Pareschi, Philipp Heer, and Giovanni Sansavini. The potential of vehicle-to-grid to support the energy transition: A case study on switzerland. *Energies*, 14(16):4812, 2021.

[103] Evangelos Panos, Tom Kober, Ramachandran Kannan, and Stefan Hirschberg. Long term energy transformation pathways: Integrated scenario analysis with the swiss times energy systems model, 2021. URL `https://sccer-jasm.ch/JASMpapers/JASM_results_stem.pdf`.

[104] Olga Weiss, Giacomo Pareschi, Gil Georges, and Konstantinos Boulouchos. The swiss energy transition: Policies to address the energy trilemma. *Energy Policy*, 148:111926, 2021.

[105] Martin Rüdisüli, Christian Bach, Christian Bauer, Didier Beloin-Saint-Pierre, Urs Elber, Gil Georges, Robert Limpach, Giacomo Pareschi, Ramachandran Kannan, and Sinan L Teske. Prospective life-cycle assessment of greenhouse gas emissions of electricity-based mobility options. *Applied Energy*, 306:118065, 2022.

[106] Annika Messmer and Rolf Frischknecht. Umweltbilanz Strommix Schweiz 2014, 2016. URL `https://treeze.ch/fileadmin/user_upload/downloads/589-Umweltbilanz-Strommix-Schweiz-2014-v3.0.pdf`.

[107] Giacomo Pareschi, Gil Georges, and Konstantinos Boulouchos. Assessment of the marginal emission factor associated with electric vehicle charging. In *1st E-Mobility Power System Integration Symposium. E-Proceedings*. Energynautics GmbH, 2017.

[108] Susan A. Shaheen and Adam P. Cohen. Carsharing and Personal Vehicle Services: Worldwide Market Developments and Emerging Trends. *International Journal of Sustainable Transportation*, 7(1): 5–34, jan 2013. ISSN 1556-8318. doi: 10.1080/15568318.2012.

660103. URL https://www.tandfonline.com/doi/full/10.1080/15568318.2012.660103.

[109] Share now: facts and figures. URL https://brandhub.share-now.com/web/6570a0eb69e15b2f/factsheets/.

[110] Zipcar: electric car sharing. URL https://www.zipcar.com/en-gb/flex/electric.

[111] T. Donna Chen, Kara M. Kockelman, and Josiah P. Hanna. Operations of a shared, autonomous, electric vehicle fleet: Implications of vehicle & charging infrastructure decisions. *Transportation Research Part A: Policy and Practice*, 94:243–254, dec 2016. ISSN 09658564. doi: 10.1016/j.tra.2016.08.020. URL https://linkinghub.elsevier.com/retrieve/pii/S096585641630756X.

[112] Maurizio Bruglieri, Alberto Colorni, and Alessandro Luè. The relocation problem for the one-way electric vehicle sharing. *Networks*, 64(4):292–305, dec 2014. ISSN 00283045. doi: 10.1002/net.21585. URL http://doi.wiley.com/10.1002/net.21585.

[113] Marion Lagadic, Alia Verloes, and Nicolas Louvet. Can carsharing services be profitable? A critical review of established and developing business models. *Transport Policy*, 77:68–78, may 2019. ISSN 0967070X. doi: 10.1016/j.tranpol.2019.02.006. URL https://linkinghub.elsevier.com/retrieve/pii/S0967070X18307480.

[114] Diana Jorge, Cynthia Barnhart, and Gonçalo Homem de Almeida Correia. Assessing the viability of enabling a round-trip carsharing system to accept one-way trips: Application to logan airport in boston. *Transportation Research Part C: Emerging Technologies*, 56:359–372, 7 2015. ISSN 0968090X. doi: 10.1016/j.trc.2015.04.020. URL https://linkinghub.elsevier.com/retrieve/pii/S0968090X15001618.

[115] Chiara Boldrini and Raffaele Bruno. Stackable vs autonomous cars for shared mobility systems: A preliminary performance evaluation. In *2017 IEEE 20th International Conference on Intelligent Transportation Systems (ITSC)*, volume 2018-March, pages 232–237. IEEE, oct 2017. ISBN 978-1-5386-1526-3. doi: 10.

1109/ITSC.2017.8317960. URL http://ieeexplore.ieee.org/document/8317960/.

[116] Diana Jorge, Goran Molnar, and Gonçalo Homem de Almeida Correia. Trip pricing of one-way station-based carsharing networks with zone and time of day price variations. *Transportation Research Part B: Methodological*, 81:461–482, 11 2015. ISSN 01912615. doi: 10.1016/j.trb.2015.06.003. URL https://linkinghub.elsevier.com/retrieve/pii/S0191261515001265.

[117] Daniel J. Fagnant and Kara M. Kockelman. The travel and environmental implications of shared autonomous vehicles, using agent-based model scenarios. *Transportation Research Part C: Emerging Technologies*, 40:1–13, mar 2014. ISSN 0968090X. doi: 10.1016/j.trc.2013.12.001. URL https://linkinghub.elsevier.com/retrieve/pii/S0968090X13002581.

[118] James M Anderson, Kalra Nidhi, Karlyn D Stanley, Paul Sorensen, Constantine Samaras, and Oluwatobi A Oluwatola. *Autonomous vehicle technology: A guide for policymakers*. Rand Corporation, 2014.

[119] Nikolas Thomopoulos and Moshe Givoni. The autonomous car—a blessing or a curse for the future of low carbon mobility? An exploration of likely vs. desirable outcomes. *European Journal of Futures Research*, 3(1):14, dec 2015. ISSN 2195-4194. doi: 10.1007/s40309-015-0071-z. URL http://link.springer.com/10.1007/s40309-015-0071-z.

[120] Zia Wadud, Don MacKenzie, and Paul Leiby. Help or hindrance? The travel, energy and carbon impacts of highly automated vehicles. *Transportation Research Part A: Policy and Practice*, 86:1–18, apr 2016. ISSN 09658564. doi: 10.1016/j.tra.2015.12.001. URL https://linkinghub.elsevier.com/retrieve/pii/S0965856415002694.

[121] IEA. Energy technology perspectives 2020: clean energy technology guide. URL https://www.iea.org/articles/etp-clean-energy-technology-guide.

[122] M.W. Adler, S. Peer, and T. Sinozic. Autonomous, connected, electric shared vehicles (ACES) and public finance: An explo-

rative analysis. *Transportation Research Interdisciplinary Perspectives*, 2:100038, sep 2019. ISSN 25901982. doi: 10.1016/j.trip.2019.100038. URL https://linkinghub.elsevier.com/retrieve/pii/S2590198219300387.

[123] Graham Currie. Lies, Damned Lies, AVs, Shared Mobility, and Urban Transit Futures. *Journal of Public Transportation*, 21(1):19–30, jan 2018. ISSN 1077-291X. doi: 10.5038/2375-0901.21.1.3. URL http://scholarcommons.usf.edu/jpt/vol21/iss1/3/.

[124] Rafael F.F. Lemme, Edilson F. Arruda, and Laura Bahiense. Optimization model to assess electric vehicles as an alternative for fleet composition in station-based car sharing systems. *Transportation Research Part D: Transport and Environment*, 67:173–196, 2 2019. ISSN 13619209. doi: 10.1016/j.trd.2018.11.008. URL https://linkinghub.elsevier.com/retrieve/pii/S1361920918304656.

[125] Patrick M. Boesch, Francesco Ciari, and Kay W. Axhausen. Autonomous Vehicle Fleet Sizes Required to Serve Different Levels of Demand. *Transportation Research Record: Journal of the Transportation Research Board*, 2542(1):111–119, jan 2016. ISSN 0361-1981. doi: 10.3141/2542-13. URL http://journals.sagepub.com/doi/10.3141/2542-13.

[126] Global Battery Alliance World Economic Forum. A vision for a sustainable battery value chain in 2030.

[127] Nathaniel S. Pearre, Willett Kempton, Randall L. Guensler, and Vetri V. Elango. Electric vehicles: How much range is required for a day's driving? *Transportation Research Part C: Emerging Technologies*, 19(6):1171–1184, dec 2011. ISSN 0968090X. doi: 10.1016/j.trc.2010.12.010. URL https://linkinghub.elsevier.com/retrieve/pii/S0968090X1100012X.

[128] Elizabeth Traut, Chris Hendrickson, Erica Klampfl, Yimin Liu, and Jeremy J. Michalek. Optimal design and allocation of electrified vehicles and dedicated charging infrastructure for minimum life cycle greenhouse gas emissions and cost. *Energy Policy*, 51:524–534, 2012. ISSN 03014215. doi: 10.1016/j.enpol.2012.08.061. URL http://linkinghub.elsevier.com/retrieve/pii/S0301421512007434.

[129] Department for Transport. NTS0705: Travel by household income quintile and main mode or mode: England, 2020. URL https://www.gov.uk/government/statistical-data-sets/nts07-car-ownership-and-access.

[130] John Pucher and John L Renne. Urban-Rural differences in mobility and mode choice: Evidence from the 2001 NHTS. *Bloustein School of Planning and Public Policy, Rutgers University*, pages 1–22, 2004.

[131] Maxime Lenormand, Thomas Louail, Oliva G Cantú-Ros, Miguel Picornell, Ricardo Herranz, Juan Murillo Arias, Marc Barthelemy, Maxi San Miguel, and José J Ramasco. Influence of sociodemographic characteristics on human mobility. *Scientific reports*, 5:10075, 2015.

[132] Department for Transport. NTS9903/NTS9904: Average number of trips / distance travelled by mode, region and rural urban classification: England, 2020. URL https://www.gov.uk/government/statistical-data-sets/nts99-travel-by-region-and-area-type-of-residence.

[133] Henrik Becker, Francesco Ciari, and Kay W. Axhausen. Modeling free-floating car-sharing use in switzerland: A spatial regression and conditional logit approach. *Transportation Research Part C: Emerging Technologies*, 81:286–299, 8 2017. ISSN 0968090X. doi: 10.1016/j.trc.2017.06.008. URL https://linkinghub.elsevier.com/retrieve/pii/S0968090X17301614.

[134] Robert V. Levine and Ara Norenzayan. The pace of life in 31 countries. *Journal of Cross-Cultural Psychology*, 30(2):178–205, 1999. doi: 10.1177/0022022199030002003. URL https://doi.org/10.1177/0022022199030002003.

[135] Nancy M. Salbach, Kelly K. O'Brien, Dina Brooks, Emma Irvin, Rosemary Martino, Pam Takhar, Sylvia Chan, and Jo-Anne Howe. Reference values for standardized tests of walking speed and distance: A systematic review. *Gait & Posture*, 41(2):341 – 360, 2015. ISSN 0966-6362. doi: https://doi.org/10.1016/j.gaitpost.2014.10.002. URL http://www.sciencedirect.com/science/article/pii/S0966636214007280.

[136] Raymond C. Browning, Emily A. Baker, Jessica A. Herron, and Rodger Kram. Effects of obesity and sex on the energetic cost and preferred speed of walking. *Journal of Applied Physiology*, 100(2): 390–398, 2006. doi: 10.1152/japplphysiol.00767.2005. URL https://doi.org/10.1152/japplphysiol.00767.2005. PMID: 16210434.

[137] Joyce M Dargay. Determinants of car ownership in rural and urban areas: a pseudo-panel analysis. *Transportation Research Part E: Logistics and Transportation Review*, 38(5):351 – 366, 2002. ISSN 1366-5545. doi: https://doi.org/10.1016/S1366-5545(01)00019-9. URL http://www.sciencedirect.com/science/article/pii/S1366554501000199.

[138] Mallory Trouve, Gaele Lesteven, and Fabien Leurent. Worldwide investigation of private motorization dynamics at the metropolitan scale. *Transportation Research Procedia*, 48:3413 – 3430, 2020. ISSN 2352-1465. doi: https://doi.org/10.1016/j.trpro.2020.08.113. URL http://www.sciencedirect.com/science/article/pii/S2352146520305299. Recent Advances and Emerging Issues in Transport Research – An Editorial Note for the Selected Proceedings of WCTR 2019 Mumbai.

[139] Aoife Ahern, Gill Weyman, Martin Redelbach, Angelika Schulz, Lars Akkermans, Lorenzo Vannacci, Eleni Anoyrkati, and Anouk Van Grinsven. Analysis of national travel surveys in Europe-OPTIMISM WP2: harmonisation of national travel statistics in Europe. 2013.

[140] Track & Know project, 2020. URL https://trackandknowproject.eu/.

[141] Iddo Riemersma and Peter Mock. Too low to be true? How to measure fuel consumption and CO_2 emissions of plug-in hybrid vehicles, today and in the future. 2017.

[142] Muhammad Amjad, Ayaz Ahmad, Mubashir Husain Rehmani, and Tariq Umer. A review of EVs charging: from the perspective of energy optimization, optimization approaches, and charging techniques. *Transportation Research Part D: Transport and Environment*, 62:386–417, 2018.

[143] Reza Fachrizal, Mahmoud Shepero, Dennis van der Meer, Joakim Munkhammar, and Joakim Widén. Smart charging of electric vehicles considering photovoltaic power production and electricity consumption: A review. *eTransportation*, 4:100056, 2020.

[144] Francisco Javier García Villalobos. *Optimized charging control method for plug-in electric vehicles in LV distribution networks*. PhD thesis, Universidad del País Vasco-Euskal Herriko Unibertsitatea, 2016.

[145] Henrik Lund and Willett Kempton. Integration of renewable energy into the transport and electricity sectors through V2G. *Energy policy*, 36(9):3578–3587, 2008.

[146] Julian Huber, Elisabeth Schaule, Dominik Jung, and Christof Weinhardt. Quo vadis smart charging? A literature review and expert survey on technical potentials and user acceptance of smart charging systems. *World Electric Vehicle Journal*, 10(4):85, 2019.

[147] Wei Wei, Sankaran Ramakrishnan, Zachary A Needell, and Jessika E Trancik. Personal vehicle electrification and charging solutions for high-energy days. *Nature Energy*, 6(1):105–114, 2021.

[148] Xinkai Fu, Danielle N Beatty, Gabrielle G Gaustad, Gerbrand Ceder, Richard Roth, Randolph E Kirchain, Michele Bustamante, Callie Babbitt, and Elsa A Olivetti. Perspectives on cobalt supply through 2030 in the face of changing demand. *Environmental science & technology*, 54(5):2985–2993, 2020.

[149] Christian Thies, Karsten Kieckhäfer, Thomas S Spengler, and Manbir S Sodhi. Assessment of social sustainability hotspots in the supply chain of lithium-ion batteries. *Procedia CIRP*, 80:292–297, 2019.

[150] Transport & Environment. How will electric vehicle transition impact EU jobs?, 2017. URL `https://www.transportenvironment.org/publications/how-will-electric-vehicle-transition-impact-eu-jobs`.

[151] Stefan Hirschberg, Christian Bauer, Brian Cox, Thomas Heck, Johannes Hofer, Warren Schenler, Andrew Simons, Andrea Del Duce,

Hans-Jörg Althaus, Gil Georges, Thilo Krause, Marina Gonzalez Vaya, Francesco Ciari, Rashid Waraich, Boris Jäggi, Alexander Stahel, Andreas Froemelt, and Dominik Saner. Opportunities and challenges for electric mobility: an interdisciplinary assessment of passenger vehicles. 11 2016.

[152] Jens F. Peters, Manuel Baumann, Benedikt Zimmermann, Jessica Braun, and Marcel Weil. The environmental impact of li-ion batteries and the role of key parameters – a review. *Renewable and Sustainable Energy Reviews*, 67:491–506, 2017. ISSN 1364-0321. doi: https://doi.org/10.1016/j.rser.2016.08.039. URL `https://www.sciencedirect.com/science/article/pii/S1364032116304713`.

[153] Ricardo Energy & Environment Directorate-General for Climate Action (European Commission). Determining the environmental impacts of conventional and alternatively fuelled vehicles through LCA.

[154] BloombergNEF. Hitting the EV inflection point.

[155] Transport & Environment. From dirty oil to clean batteries.

[156] John Smart, Warren Powell, and Stephen Schey. Extended range electric vehicle driving and charging behavior observed early in the ev project. In *SAE 2013 World Congress & Exhibition*. SAE International, apr 2013. doi: https://doi.org/10.4271/2013-01-1441. URL `https://doi.org/10.4271/2013-01-1441`.

[157] Office for National Statistics (ONS). 2011 census: Aggregate data. [data collection], 2020. URL `https://www.nomisweb.co.uk/census/2011/key_statistics_uk`. UK Data Service. SN: 7427.

Publications

Journal Publications

- E. Çabukoglu, G. Georges, L. Küng, G. Pareschi, K. Boulouchos, Battery electric propulsion: An option for heavy-duty vehicles? Results from a Swiss case-study, *Transportation Research Part C: Emerging Technologies* 88, 2018, doi: 10.1016/j.trc.2018.01.013

- E. Çabukoglu, G. Georges, L. Küng, G. Pareschi, K. Boulouchos, Fuel cell electric vehicles: An option to decarbonize heavy-duty transport? Results from a Swiss case-study, *Transportation Research Part D: Transport and Environment* 70, 2019, doi: 10.1016/j.trd.2019.03.004

- G. Pareschi, L. Küng, G. Georges, K. Boulouchos, Are travel surveys a good basis for EV models? Validation of simulated charging profiles against empirical data, *Applied Energy* 275, 2020, doi: 10.1016/j.apenergy.2020.115318

- A. Walter, M. Held, G. Pareschi, H. Pengg, R. Madlener, Decarbonizing the European automobile fleet: Impacts of 1.5 degC-compliant climate policies in Germany and Norway, *FCN Working Paper No.* 18, 2020, doi: 10.2139/ssrn.3860164

- O. Weiss, G. Pareschi, G. Georges, K. Boulouchos, The Swiss energy transition: Policies to address the energy trilemma, *Energy Policy* 148 (A), 2021, doi: 10.1016/j.enpol.2020.111926

- M. Mittelviefhaus, G. Pareschi, J. Allen, G. Georges, K. Boulouchos, Optimal investment and scheduling of residential multi-energy systems including electric mobility: A cost-effective approach to climate change mitigation, *Applied Energy* 301, 2021, doi: 10.1016/j.apenergy.2021.117445

- L. Di Natale, L. Funk, M. Rüdisüli, B. Svetozarevic, G. Pareschi, P. Heer, G. Sansavini, The potential of Vehicle-to-Grid to support the energy transition: A case study on Switzerland, *Energies* 14(16), 2021, doi: 10.3390/en14164812

- M. Rüdisüli, C. Bach, C. Bauer, D. Beloin-Saint-Pierre, U. Elber, G. Georges, R. Limpach, G. Pareschi, R. Kannan, S. L. Teske, Prospective life-cycle assessment of greenhouse gas emissions of electricity-based mobility options, *Applied Energy* 306, 2022, doi: 10.1016/j.apenergy.2021.118065

- L. Küng, M. Held, G. Pareschi, M. Bolla, G. Georges, K. Boulouchos, Pathways to contain the Swiss car fleet within the 1.5°C carbon budget: the roles of CO2 emission limits, electric cars and synthetic fuels, *Energy Policy*, Under review

- G. Pareschi, M. Bolla, M. Mittelviefhaus, G. Georges, K. Boulouchos, Seizing the low-hanging benefits of shared electric vehicles, In preparation for submission

- M. Rüdisüli, S. L. Teske, D. Beloin-Saint-Pierre, R. Limpach, G. Pareschi, G. Georges, R. Kannan, C. Bauer, U. Elber, C. Bach, Investigating the impacts of an increased BEV fleet on the electricity generation mix and related GHG emissions in Switzerland and abroad, In preparation for submission

Conference Publications

- G. Pareschi, G. Georges, K. Boulouchos, Assessment of the Marginal Emission Factor associated with Electric Vehicle Charging, *1st E-Mobility Power System Integration Symposium*, 2016, Berlin, Germany, doi: 10.3929/ethz-b-000200058

- L. Küng, G. Georges, G. Pareschi, E. Çabukoglu, K. Boulouchos, Challenges of decarbonizing the Swiss transport system, *17th Swiss Transport Research Conference* (STRC 2017), 2017, Ascona, Switzerland, doi: 10.3929/ethz-b-000199889

- M. Held, L. Küng, E. Çabukoglu, G. Pareschi, G. Georges, K. Boulouchos, Future mobility demand estimation based on sociodemographic

information: A data-driven approach using machine learning algorithms, *18th Swiss Transport Research Conference* (STRC 2018), 2018, Ascona, Switzerland, doi: 10.3929/ethz-b-000266653

- J. Stiasny, T. Zuffrey, G. Pareschi, D. Toffanin, G. Hug, K. Boulouchos, Sensitivity analysis of electric vehicle impact on low-voltage distribution grids, *Electric Power Systems Research, 21st Power Systems Computation Conference* (PSCC 2020), 2020, Porto (virtual), Portugal, doi: 10.1016/j.epsr.2020.106696

- O. Weiss, G. Pareschi, O. Schwery, M. Bolla, G. Georges, K. Boulouchos, Long-term scheduling model of Swiss hydropower, *16th International Conference on the European Energy Market* (EEM), 2019, Ljubljana, Slovenia, doi: 10.1109/EEM.2019.8916260